Geometry & Topology

Volume 27 (2023)

Combinatorial Reeb dynamics on punctured contact 3–manifolds

RUSSELL AVDEK

msp

msp

Geometry & Topology **27**:3 (2023) 953–1082
DOI: 10.2140/gt.2023.27.953
Published: 8 June 2023

Combinatorial Reeb dynamics on punctured contact 3–manifolds

RUSSELL AVDEK

Let $\Lambda^{\pm} = \Lambda^{+} \cup \Lambda^{-} \subset (\mathbb{R}^3, \xi_{\text{std}})$ be a contact surgery diagram determining a closed, connected contact 3–manifold $(S^3_{\Lambda^{\pm}}, \xi_{\Lambda^{\pm}})$ and an open contact manifold $(\mathbb{R}^3_{\Lambda^{\pm}}, \xi_{\Lambda^{\pm}})$. Following work of Bourgeois, Ekholm and Eliashberg, we demonstrate how $\Lambda^{\pm}$ determines a family α_ϵ of contact forms for $(\mathbb{R}^3_{\Lambda^{\pm}}, \xi_{\Lambda^{\pm}})$ whose closed Reeb orbits are in one-to-one correspondence with cyclic words of composable Reeb chords on $\Lambda^{\pm}$. We compute the homology classes and integral Conley–Zehnder indices of these orbits diagrammatically and develop algebraic tools for studying holomorphic curves in surgery cobordisms between the $(\mathbb{R}^3_{\Lambda^{\pm}}, \xi_{\Lambda^{\pm}})$.

These new techniques are used to describe the first known examples of closed, tight contact manifolds with vanishing contact homology: they are contact $1/k$ surgeries along the right-handed, $\text{tb} = 1$ trefoil for $k > 0$, which are known to have nonzero Heegaard Floer contact classes by work of Lisca and Stipsicz.

53D42; 57K33

1 Introduction

The main objects of interest in this paper are *contact 3–manifolds* and their *Legendrian submanifolds*. A *contact form* on an oriented 3–manifold M is a 1–form $\alpha \in \Omega^1(M)$ for which $\alpha \wedge d\alpha > 0$ with respect to the orientation of M. A contact 3–manifold is a pair (M, ξ) consisting of an oriented 3–manifold M together with an oriented 2–dimensional distribution $\xi \subset TM$ which is the kernel of a contact form α satisfying $d\alpha|_\xi > 0$ with respect to the orientation on ξ. We say that α *is a contact form for* (M, ξ). A Legendrian submanifold of (M, ξ) is a link which is tangent to ξ. We'll typically denote Legendrian submanifolds by Λ or Λ^0.

Given a contact 1–form α for some (M, ξ) its *Reeb vector field*, R, is determined by the equations

$$\alpha(R) = 1, \quad d\alpha(R, *) = 0.$$

For the purposes of studying invariants of (M, ξ) and its Legendrian submanifolds defined by counting holomorphic curves — see Eliashberg, Givental and Hofer [23], Etnyre and Ng [26], Hutchings [40] and Seidel [59] — we are interested in finding contact forms on a given (M, ξ) for which R is easy to analyze. Specifically we want to have visibility into the closed orbits of R as well the *chords* of Legendrians $\Lambda^0 \subset (M, \xi)$, that is, the orbits of R parametrized by compact intervals which both begin and end on Λ^0.

Let $(\mathbb{R}^3, \xi_{\text{std}})$ denote the standard contact structure on Euclidean 3–space, where

$$\xi_{\text{std}} = \ker(\alpha_{\text{std}}), \quad \alpha_{\text{std}} = dz - y\, dx,$$

and let (S^3, ξ_{std}) denote the standard contact structure on the unit 3–sphere S^3, where

$$\xi_{\text{std}} = \ker\left(\sum_1^2 x_i\, dy_i - y_i\, dx_i\right).$$

A *contact surgery diagram* is a Legendrian link

$$\Lambda^\pm = \Lambda^+ \cup \Lambda^- \subset (\mathbb{R}^3, \xi_{\text{std}}).$$

Performing contact ± 1 surgery on the components of the $\Lambda^\pm$ as defined by Ding and Geiges [16] produces a contact 3–manifold, which we will denote by $(\mathbb{R}^3_{\Lambda^\pm}, \xi_{\Lambda^\pm})$. By considering $(\mathbb{R}^3, \xi_{\text{std}})$ as being contained in (S^3, ξ_{std}), we can view the surgery diagram $\Lambda^\pm$ as determining a closed contact 3–manifold $(S^3_{\Lambda^\pm}, \xi_{\Lambda^\pm})$, with $(\mathbb{R}^3_{\Lambda^\pm}, \xi_{\Lambda^\pm})$ obtained by removing a point from $(S^3_{\Lambda^\pm}, \xi_{\Lambda^\pm})$. As proved by Ding and Geiges

in [16] — see also Avdek [2] — every closed, connected contact 3–manifold (M, ξ) can be described as $(S^3_{\Lambda^\pm}, \xi_{\Lambda^\pm})$ for some choice of $\Lambda^\pm$.

For the remainder of this introduction we assume basic familiar with contact surgery, Weinstein handle attachment and symplectic field theory (SFT). Further background and references will be provided in Section 2.

1.1 Combinatorial Reeb dynamics on punctured contact 3–manifolds

The primary purpose of this article is to describe a family of particularly well-behaved contact forms α_ϵ for $(\mathbb{R}^3_{\Lambda^\pm}, \xi_{\Lambda^\pm})$ which are determined by the surgery diagram $\Lambda^\pm$. Our intention is to extend the analysis of Reeb dynamics appearing in work of Bourgeois, Ekholm and Eliashberg [7; 18] to allow for contact $+1$ surgeries. In particular, the following theorem states that their "chord-to-orbit correspondence" is applicable to any closed contact 3–manifold:[1]

Theorem 1.1 *Let $\Lambda^\pm$ be a contact surgery diagram presented in the front projection, where each component is equipped with an orientation. Possibly after a Legendrian isotopy of $\Lambda^\pm$ which preserves the front projection up to isotopy, there is*

(1) *a constant ϵ_0,*

(2) *a neighborhood N_{ϵ_0} of $\Lambda^\pm$ in $\mathbb{R}^3$, and*

(3) *a family of contact forms α_ϵ with Reeb vector fields R_ϵ parametrized by $\epsilon < \epsilon_0$ on $(\mathbb{R}^3_{\Lambda^\pm}, \xi_{\Lambda^\pm})$*

such that the following conditions hold:

(1) *For any $\epsilon < \epsilon_0$, performing contact surgery along a neighborhood $N_\epsilon \subset N_{\epsilon_0}$ produces $(\mathbb{R}^3_{\Lambda^\pm}, \xi_{\Lambda^\pm})$ equipped with the contact form α_ϵ.*

(2) *$\alpha_\epsilon = \alpha_{\text{std}}$ on the complement of N_ϵ.*

(3) *For any $\epsilon < \epsilon_0$, there is a one-to-one correspondence between cyclic words of composable ∂_z chords of $\Lambda^\pm$ and closed orbits of R_ϵ (Theorem 5.1).*

(4) *For a given cyclic word of chords w, there exists $\epsilon_w < \epsilon_0$ such that the orbits of R_ϵ corresponding to w are hyperbolic for $\epsilon < \epsilon_w$ (Theorem 5.3).*

(5) *There is pair of sections (X, Y) of $(\mathbb{R}^3_{\Lambda^\pm}, \xi_{\Lambda^\pm})$ determined by $\Lambda^\pm$ and its orientation, providing a symplectic trivialization of the restriction of $(\xi_{\Lambda^\pm}, d\alpha_\epsilon)$ to all closed orbits of R_ϵ. The zero locus $X^{-1}(0) = Y^{-1}(0)$ is a link contained in*

[1] Contact -1 surgery — also known as Legendrian surgery — describes how the convex boundaries of Liouville domains are modified by critical-index Weinstein handle attachment.

$(\mathbb{R}^3 \setminus N_\epsilon) \subset \mathbb{R}^3_{\Lambda^\pm}$ *whose connected components are given by transverse push-offs of the components of* $\Lambda^\pm$ *with nonzero rotation number* (Theorem 6.1).

(6) *The integral Conley–Zehnder indices* $\mathrm{CZ}_{X,Y}$ (Theorem 7.1) *and homology classes* (Theorem 9.1) *of the closed orbits of* R_ϵ *can be computed combinatorially from the surgery diagram.*

By "computed combinatorially", we mean computed via extensions of methods typically used to set up chain complexes for the Legendrian contact homology (LCH) [26] or the Legendrian rational symplectic field theory (*LRSFT*) of Ng [50] of $\Lambda^\pm$. Analogous results are stated for chords of Legendrian links $\Lambda^0 \subset (\mathbb{R}^3_{\Lambda^\pm}, \xi_{\Lambda^\pm})$ throughout the paper, providing a "chord-to-chord" correspondence with diagrammatically computable Maslov indices. The content of Theorem 1.1 is sufficient to compute some algebraic invariants of tight contact structures on the lens space $L(2,1)$ and $S^1 \times S^2$, as shown in Section 12.1.

The dynamics analysis of Theorem 1.1 can be supplemented with a direct limit argument as in Ekholm and Ng [20, Section 4] to obtain a description of the Reeb dynamics on the closed contact manifolds $(S^3_{\Lambda^\pm}, \xi_{\Lambda^\pm})$ associated to a contact surgery diagram, which introduces a pair of embedded elliptic orbits.[2] We will not pursue analysis of closed contact manifolds in this paper, as the open manifolds $(\mathbb{R}^3_{\Lambda^\pm}, \xi_{\Lambda^\pm})$ have particularly friendly geometries, which we'll leverage in applications.

1.2 Constrained topology of holomorphic curves and applications

The secondary purpose of this article is to develop tools for studying holomorphic curves in symplectizations of the $(\mathbb{R}^3_{\Lambda^\pm}, \xi_{\Lambda^\pm})$ and in surgery cobordisms between them. Our intention is to make "hat versions" of holomorphic curve invariants of $(\mathbb{R}^3_{\Lambda^\pm}, \xi_{\Lambda^\pm})$ — as defined by Colin, Ghiggini, Honda and Hutchings [14, Section 7.1] — more computationally accessible. Theorem 1.1 already provides us with rather complete descriptions of the chain complexes underlying such invariants.[3] In particular, we'll be interested in the hat version of contact homology (CH),

$$\widehat{\mathrm{CH}}(S^3_{\Lambda^\pm}, \xi_{\Lambda^\pm}) = \mathrm{CH}(\mathbb{R}^3_{\Lambda^\pm}, \xi_{\Lambda^\pm}).$$

[2] See for example Bourgeois [6, Section 4.1] and Hutchings [40, Example 1.8].

[3] There is some subtlety for $\widehat{\mathrm{ECH}}$: In order to compute relative ECH indices, the links underlying collections of simple Reeb orbits should be known, whereas we will describe the homotopy classes of closed Reeb orbits. Such link embeddings can be computed as solutions to matrix arithmetic problems described in Section 5.6.

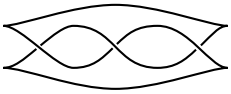

Figure 1: The Legendrian trefoil of Theorem 1.2 shown in the front projection.

Hat versions of other holomorphic curve invariants of $(S^3_{\Lambda^\pm}, \xi_{\Lambda^\pm})$ such as embedded contact homology ($\widehat{\mathrm{ECH}}$) and the *SFT* algebra ($\widehat{SFT}$) are defined analogously.[4]

We demonstrate the utility of our tools in two applications: First we provide a (slightly) new proof of the vanishing of CH of overtwisted contact manifolds (see Eliashberg and Yau [65]) using surgery-theoretic methods (Section 12.3). Second, we prove the following theorem (Section 12.5):

Theorem 1.2 *If $\Lambda^- = \varnothing$ and Λ^+ has a component which is a right-handed trefoil, then*

$$\mathrm{CH}(S^3_{\Lambda^\pm}, \xi_{\Lambda^\pm}) = \widehat{\mathrm{CH}}(S^3_{\Lambda^\pm}, \xi_{\Lambda^\pm}) = 0$$

In particular, contact $1/k$ surgery on the right-handed, $\mathrm{tb} = 1$ trefoil for $k > 0$ produces a closed, tight contact manifold $(S^3_{\Lambda^\pm}, \xi_{\Lambda^\pm})$ with vanishing contact homology. (See Figure 1.)

The development of our tools (Section 11) starts with a variation of the construction of transverse knot filtrations of holomorphic curve invariants from [14, Section 7.2]: Lines in $\mathbb{R}^3$ directed by ∂_z over points $(x, y) \in \mathbb{R}^2 \setminus \pi_{x,y}(N_\epsilon)$ determine infinite-energy holomorphic planes $\mathbb{C}_{x,y}$ in $\mathbb{R} \times \mathbb{R}^3_{\Lambda^\pm}$. The $\mathbb{C}_{x,y}$ form a holomorphic foliation whose existence constrains the topology of curves à la the proofs of uniqueness-of-symplectic-manifold theorems of Eliashberg [22], Gromov [32], Geiges and Zehmisch [30], Hind [34], McDuff [44; 45] and Wendl [61]. Counting intersections $\mathbb{C}_{x,y} \cdot U$ of these planes with finite-energy curves U asymptotic to collections $\gamma^\pm$ of closed R_ϵ orbits yields locally constant, $\mathbb{Z}_{\geq 0}$–valued functions on SFT moduli spaces — topological invariants determined by the relative homology classes

$$[\pi_{\mathbb{R}^3_{\Lambda^\pm}} \circ U] \in H_2(\mathbb{R}^3_{\Lambda^\pm}, \gamma^\pm)$$

of holomorphic curves. Surgery cobordisms may be similarly considered when equipped with special almost-complex structures described in Section 11.2. By tracking these intersections, we can:

(1) Show that certain disks appearing in Ng's combinatorially defined Legendrian *RSFT* [50] determine rigid holomorphic planes in $\mathbb{R} \times \mathbb{R}^3_{\Lambda^\pm}$ (Section 12.2). This

[4] We use *SFT* to denote the *SFT* algebra, while SFT — without italics — refers to Eliashberg, Givental and Hofer's framework for defining holomorphic curve invariants of contact and symplectic manifolds of [23].

follows a Lagrangian-boundary version of Hofer's bubbling argument [35], in which case the $\mathbb{C}_{x,y} \cdot U$ completely dictate the ways in which certain families of holomorphic disks can degenerate into multilevel SFT buildings.

(2) Equip the $\widehat{\mathrm{CH}}$ chain complexes with a new grading, denoted by $\mathcal{I}_\Lambda$, which depends on the surgery diagram (Section 12.4). Variants of this grading may similarly be applied to any holomorphic curve invariant of $(\mathbb{R}^3_{\Lambda^\pm}, \xi_{\Lambda^\pm})$.

In the proof of Theorem 1.2, we show that $+1$ surgery on the $\mathrm{tb} = 1$ trefoil provides a $\mathrm{CZ}_{X,Y} = 2$ closed orbit γ of R_ϵ with $\partial_{\mathrm{CH}}\gamma = \pm 1 \in \mathbb{Q}$. Computations of Conley–Zehnder indices, homology classes, and $\mathcal{I}_\Lambda$ shows that any $\mathrm{ind} = 1$ rational holomorphic curves positively asymptotic to γ must be a plane, and that such planes may be counted using our bubbling argument.

Theorem 1.2 provides the first examples of closed, tight contact manifolds with $\mathrm{CH} = 0$.[5] The tightness of $1/k$ surgeries on the $\mathrm{tb} = 1$ trefoil is provided by computations of Heegaard Floer (HF) contact classes — see Honda, Kazez and Matić [38] and Ozsváth and Szabó [53] — by Lisca and Stipsicz in [43, Section 3]. As the HF contact class contains the same information as the ECH contact class — see Colin, Ghiggini and Honda [13] and Kutluhan, Lee and Taubes [42] — and both ECH and SFT count holomorphic curves of arbitrary topological type — in particular, arbitrary genus — it would be interesting to know if there is some SFT invariant of this contact manifold which is nonvanishing. Broadening the scope of this inquiry, we ask the following:

Question 1.3 *For 3–dimensional contact manifolds, does* $\mathrm{CH}(M, \xi) \neq 0$ *imply that the* $\mathrm{HF} = \mathrm{ECH}$ *contact class of* (M, ξ) *is nonzero? Do there exist tight contact manifolds of dimension greater than three with vanishing contact homology?*

We note that, using the algebraic formalism of [23], the vanishing of contact homology is equivalent to the vanishing of SFT according to Bourgeois and Niederkrüger [9].

Outline of this paper

In Section 2 we outline notation and background information which will be used throughout the rest of the paper. Section 3 is also primarily concerned with notation, associating algebraic data to chords of Legendrian links in $(\mathbb{R}^3, \xi_{\mathrm{std}})$, which will be used to package invariants of chords and closed orbits in the surgered contact manifolds $(\mathbb{R}^3_{\Lambda^\pm}, \xi_{\Lambda^\pm})$.

[5] Due to CH functoriality under Liouville cobordism, Honda's tight contact manifold which becomes overtwisted after contact -1 surgery [37] already provides an example of a contact manifold with convex boundary whose *sutured contact homology* [14] is zero.

Sections 4–9 carry out the computational details of Theorem 1.1 and analogous results for chords of Legendrian links $\Lambda^0 \subset (\mathbb{R}^3_{\Lambda^\pm}, \xi_{\Lambda^\pm})$. In Section 10 we describe handle-attachment cobordisms between the $(\mathbb{R}^3_{\Lambda^\pm}, \xi_{\Lambda^\pm})$ associated to surgeries along their Legendrian knots. The construction of these cobordisms — slight modifications of Ekholm [18] and Weinstein [60] — provides us with model geometry facilitating analysis of holomorphic curves.

Section 11 describes holomorphic curves in symplectizations of and surgery cobordisms between the $(\mathbb{R}^3_{\Lambda^\pm}, \xi_{\Lambda^\pm})$. The algebraic tools described in that section are prerequisite for the applications appearing in Section 12, culminating in the proof of Theorem 1.2.

Content pertaining to Legendrian links $\Lambda^0 \subset (\mathbb{R}^3_{\Lambda^\pm}, \xi_{\Lambda^\pm})$ may be skipped by readers only interested in the applications of Section 12. This material is included to provide a complete picture of relative SFT chain complexes in anticipation of their use in future applications.

Acknowledgments

The author is partly supported by the grant KAW 2016.0198 from the Knut and Alice Wallenberg Foundation. We send our gratitude to Erkao Bao, Guillaume Dreyer, Tobias Ekholm, Ko Honda, Yang Huang and Vera Vértesi for interesting conversations. Special thanks go to Fabio Gironella and András Stipsicz, as well as Georgios Dimitroglou Rizell, for their interest in this project and invitations to give talks in their seminars. Finally, we thank our referees for their thoughtful and detailed commentary.

2 Prerequisites

2.1 General notation

Throughout this paper $\delta_{*,*}$ — with a double subscript — will denote the Kronecker delta and $\lfloor * \rfloor$ will be the floor function $\mathbb{R} \to \mathbb{Z}$. A *collection* will be a set in which elements are allowed to have nontrivial multiplicity. We use set notation for collections. For example $\{1,1,2\}$ is a collection with $\{1,1,2\} \setminus \{1\} = \{1,2\}$ and $\{1,1,2\} \cup \{2,3\} = \{1,1,2,2,3\}$. We'll use often use collections and ordered collection to organize chords and orbits as they may appear in CH, ECH, LCH, etc.

Unless otherwise specified, we use I to denote a connected 1–manifold and, for a positive number ϵ, we write $I_\epsilon = [-\epsilon, \epsilon]$. For $a > 0$, the circle $\mathbb{R}/a\mathbb{Z}$ will be denoted

by S^1_a and, without the subscript, $S^1 = S^1_1$. The unit disk of dimension n and radius C centered about $x \in \mathbb{R}^n$ will be denoted by $\mathbb{D}^n_C(x)$. We'll typically use the simplified notation $\mathbb{D}^n = \mathbb{D}^n_1(0)$ and $\mathbb{D}$ for $\mathbb{D}^2$. The complex projective space will be written $\mathbb{P}^n$.

For a closed manifold M, $\widehat{M}$ will denote the open manifold obtained from M by removing a point or closed disk. When (M,ξ) is a closed contact manifold, $(\widehat{M,\xi})$ will denote (M,ξ) with a point or standard Darboux disk removed. We say that $(\widehat{M,\xi})$ is a *punctured contact manifold*.[6]

For a space M, we denote homology and cohomology groups by $H_*(M)$ and $H^*(M)$, respectively. Integral coefficients will be assumed unless otherwise explicitly stated. When M is a closed manifold, PD will be used to denote the Poincaré duality isomorphism in either direction, $H_i \leftrightarrow H^{\dim(M)-i}$. Abusing notation, we also use PD to denote the associated isomorphisms for punctured manifolds $\widehat{M}$ in degrees $i \neq 0$. By a $\mathbb{Q}$–*homology sphere*, we mean a closed or punctured 3–manifold with finite H_1 (implying that $H_2 = 0$ by the universal coefficients theorem; see [33, Corollary 3.3]).

For a vector bundle E over a manifold M, the space of C^∞ sections will denoted by $\Gamma(E)$. The space of nowhere-zero sections — which may be empty — will be denoted by $\Gamma_{\neq 0}(E)$. Provided that E has finite rank n and trivializations (V_i) and (W_i) of E over some set $U \subset M$, transformations of the form $\sum_{i,j} a_{i,j} W_i \otimes V_j^*$ can be written as matrices, with respect to which we say that (V_i) is the *incoming basis* and (W_i) is the *outgoing basis*. In such situations, provided $a_1, \dots, a_n \in C^\infty(U)$, $\mathrm{Diag}(a_1, \dots, a_n)$ will be the diagonal matrix with a_1 in the top-left corner and J_0 will denote standard complex multiplication where applicable. The Euler class of a finite-dimensional bundle will be written $e(E)$ and Chern classes will be written $c_k(E)$ when the bundle is equipped with a (homotopy class of) complex structure. We will be predominantly interested in the case $E = \xi$ for a 3–dimensional contact manifold (M,ξ), in which case the Euler and first Chern classes coincide: $e(\xi) = c_1(\xi)$.

2.2 Vector fields and almost-complex structures

In this section we review vector fields and almost-complex structures typically encountered in symplectic and contact geometry, primarily for the purpose of establishing conventions which often vary in the literature. We'll use Option 1 of [63]. See that article or [46, Remark 3.3] for further discussion.[7]

[6] In [14], the notation $M(1)$ is used for what we call $\widehat{M}$.

[7] Regarding work we'll be frequently referencing, our signs for symplectic forms on cotangent bundles will be opposite that of [18] and our signs for Hamiltonian vector fields are opposite that of [4; 3; 14].

Let (W,β) be a $2n$–dimensional exact symplectic manifold. That is, W is an oriented $2n$–manifold on which $d\beta$ is symplectic. We call such β a *Liouville form* or *symplectic potential*. If $H\in\mathcal{C}^\infty(W)$ is a smooth function with values in $\mathbb{R}$ or S^1, the associated *Hamiltonian vector field*, denoted by X_H, is the unique solution to the equation

$$d\beta(*,X_H)=dH.$$

Clearly H is constant along the flow-lines of X_H and X_H depends only on $d\beta$ (rather than β). If J is an almost-complex structure for which g_J, defined by

$$g_J(u,v)=d\beta(u,Jv),\quad u,v\in T_p\Sigma,$$

is a J–invariant Riemannian metric, then

$$X_H=J\nabla H,$$

where ∇H is the gradient of H with respect to g_J solving $g_J(\nabla H,*)=dH$. We say that such J is a *compatible* almost-complex structure.

The *Liouville vector field*, denoted by X_β, on W is the unique solution to the equation

$$d\beta(X_\beta,*)=\beta.$$

If W is compact and X_β points outward along the boundary of W, we say that the pair (W,β) is a *Liouville domain*. Given a function $H\in\mathcal{C}^\infty(W)$, the 1–form $\beta_H=\beta+dH$ is also a primitive for $d\beta$ such that

$$X_{\beta_H}=X_\beta+X_H.$$

By our choice of convention, Hamiltonian and Liouville vector fields interact with $d\beta$ via

$$\beta(X_H)=d\beta(X_\beta,X_H)=dH(X_\beta).$$

Given a contact manifold (M,ξ) equipped with a contact form α, action of the chords and closed orbits of its Reeb vector field may be computed as

$$\mathcal{A}(\gamma)=\int_\gamma\alpha.$$

2.3 Contact and symplectic manifolds

Here we review some contact and symplectic manifolds which will appear frequently.

2.3.1 Cotangent bundles Our convention for Liouville forms on the cotangent bundle T^*L of a smooth manifold L will be to use the form $(T^*L,\lambda_{\text{can}})$ with $\lambda_{\text{can}}=p_i\,dq_i$ in

a local coordinate system (q_i) on L. Provided such coordinates on L, we use (p_i, q_i) as local coordinates on T^*L, so that $d\lambda_{\text{can}}$ is symplectic with respect to the induced orientation.

2.3.2 Contactizations Provided an exact symplectic manifold (W, β), we have a contact form $dz+\beta$ on $I\times W$. We will refer to the contact manifold $(I\times W, \ker(dz+\beta))$ and the pair $(\mathbb{R}\times W, dz+\beta)$ both as the *contactization of* (W, β).

It's easy to see that deformations of an exact symplectic manifold give rise to contactomorphic contactizations. For, if $H\in C^\infty(W, \mathbb{R})$, then the contactization of $(W, \beta+dH)$ is equivalent to the contactization of (W, β) by the transformation

$$(t, w)\mapsto (t+H, w).$$

We'll further analyze geometry of contactizations in Sections 10.1 and 11.1. The quintessential example of a contactization is the 1–*jet space* of a closed manifold, which is the contactization of its cotangent bundle.

2.3.3 Symplectizations Provided (M, ξ) and α as above, $(\mathbb{R}\times M, e^t\alpha)$ is an exact symplectic manifold, called the *symplectization* of the pair (M, α). By considering diffeomorphisms of the form $(t, x)\mapsto (t+f(x), x)$ on $\mathbb{R}\times M$ for $f\in C^\infty(M, (0, \infty))$, it is clear that the symplectization is independent of the choice of α for ξ, up to symplectomorphism.

For any constant C, we will likewise refer to $\big([C, \infty)\times M, e^t\alpha\big)$ as the *positive half-infinite symplectization* and $\big((-\infty, C]\times M, e^t, \alpha\big)$ as the *negative half-infinite symplectization* of the pair (M, α). For constants $C<C'$, we will call $([C, C']\times M, e^t\alpha)$ a *finite symplectization* of the pair (M, α).

Here we can compute

$$X_\beta = \partial_t, \quad X_t = e^{-t}R.$$

Hence, there is a one-to-one correspondence between periodic orbits of R and 1–periodic orbits of X_t by associating to each γ in M the loop $(\log \mathcal{A}(\gamma), \gamma)$ in the symplectization.

2.3.4 Liouville cobordisms between closed and punctured contact manifolds Here we review some standard vocabulary regarding symplectic cobordisms, modified to deal with punctured contact manifolds. What are sometimes called "strong symplectic cobordisms" we will simply refer to as *symplectic cobordisms* for notational simplicity.

What are sometimes called "exact symplectic cobordisms" we will refer to as *Liouville cobordisms*. Our reasoning is that there exist symplectic cobordisms which are exact symplectic manifolds but which are not "exact symplectic cobordisms"; see Section 2.4 of [62]. See that paper or [52, Chapter 12] for a review of various notions of fillings and cobordisms with emphasis on low dimensions. We will only be concerned with Liouville cobordisms here.

Let (M, ξ) be a closed contact manifold of dimension $2n+1$ and $p \in M$ a point. We say that a contact form α for ξ defined on $M \setminus \{p\}$ is *standard at infinity* if there exists a ball B_p about $p \in M$, a positive constant C and a diffeomorphism

$$\Phi\colon (B_p \setminus \{p\}) \to (\mathbb{R}^{2n+1} \setminus \mathbb{D}^{2n+1}_C(0))$$

such that $\Phi^*(dz - y_i\, dx_i) = \alpha$ and $|\Phi(\gamma(t))| \to \infty$ for paths $\gamma(t)$ in $B_p \setminus \{p\}$ tending towards p.

A *Liouville cobordism between contact manifolds* (M^+, ξ^+) *and* (M^-, ξ^-) is a compact exact symplectic manifold (W, λ) for which

(1) $\partial W = M^+ - M^-$,

(2) the Liouville vector field X_λ points into W along M^- and out of W along M^+, and

(3) $\lambda|_{TM^\pm}$ is a contact form for $\xi^\pm$.

We call M^+ the *convex boundary of* (W, λ) and M^- the *concave boundary of* (W, λ). We may think of a Liouville domain as cobordism whose concave boundary is the empty set.

A *Liouville cobordism between punctured contact manifolds* $\widehat{(M^+, \xi^+)}$ *and* $\widehat{(M^-, \xi^-)}$ is defined analogously as in the case where the $(M^\pm, \xi^\pm)$ are closed. However, we require that there exists a region

$$I_C \times (\mathbb{R}^{2n+1} \setminus \mathbb{D}^{2n+1}_C(0)) \subset W, \quad \{\pm C\} \times (\mathbb{R}^{2n+1} \setminus \mathbb{D}^{2n+1}_C(0)) \subset M^\pm$$

along which $\lambda = e^t(dz - y_i\, dx_i)$ and such that the $t = \pm C$ slices provide standard at infinity neighborhoods of the punctures of the $M^\pm$.

We won't bother to specify that a Liouville cobordism is between closed or punctured contact manifolds, as it should be clear from the context. In either case, we may define the *completion* of a Liouville cobordism to be the noncompact exact symplectic manifold obtained from a Liouville cobordism by appending a positive half-infinite

symplectization to a collar of its convex boundary and a negative half-infinite symplectization to a collar of its concave boundary. We denote the completion of such a cobordism (W, λ) by $(\overline{W}, \overline{\lambda})$.

2.4 Remarks on SL(2, ℝ)

We briefly review some properties of $\mathrm{SL}(2,\mathbb{R})$ which will be useful for analyzing Reeb dynamics on contact 3–manifolds. By definition, $\mathrm{SL}(2,\mathbb{R})$ coincides with $\mathrm{Symp}(2,\mathbb{R})$ — the space of matrices preserving the standard symplectic form $dx \wedge dy$.

An element $A \in \mathrm{SL}(2,\mathbb{R})$ has characteristic polynomial

$$\det(A - \lambda\,\mathrm{Id}) = \lambda^2 - \mathrm{tr}(A)\lambda + 1, \tag{1}$$

using which eigenvalues of A can be found using the quadratic formula. The *nondegenerate* elements are those for which 1 is not an eigenvalue. A nondegenerate element A falls into one of two classes:

(1) A is called *elliptic* if its eigenvalues lie on the unit circle or, equivalently, $|\mathrm{tr}(A)| < 2$.

(2) A is called *hyperbolic* if its eigenvalues are elements of $\mathbb{R}$ or, equivalently, $|\mathrm{tr}(A)| > 2$.

Hyperbolic elements are further classified as *positive* (*resp. negative*) *hyperbolic* if the eigenvalues are positive (resp. negative) real numbers. The classification of $A \in \mathrm{SL}(2,\mathbb{R})$ as elliptic, positive hyperbolic or negative hyperbolic depends only on the conjugacy class of A.

2.5 Conley–Zehnder indices of Reeb orbits in contact 3–manifolds

Throughout the remaining subsections covering Reeb dynamics and contact homology, we follow the expositions [6] of Bourgeois (which covers all dimensions) and [40, Section 3.2] of Hutchings (which specifically focuses on the 3–manifolds). Let γ be a closed Reeb orbit of a contact manifold (M, ξ) equipped with a contact form α for ξ, whose Reeb vector field will be denoted by R. We assume γ is embedded and comes with a parametrization $\gamma(t)$; write γ^k for its k–fold iterate with $k > 0$.

As the Reeb flow preserves ξ, the Poincaré return map for time $t = \mathcal{A}(\gamma)$ sends $\xi|_{\gamma(0)}$ to itself and — provided a symplectic basis of $(\xi|_{\gamma(0)}, d\alpha)$ — determines a matrix $\mathrm{Ret}_\gamma \in \mathrm{SL}(2,\mathbb{R})$. The orbit γ will be called nondegenerate, elliptic, positive (negative)

hyperbolic if the matrix Ret_γ has the associated property. We say that the contact form α is *nondegenerate* if all of its Reeb orbits are nondegenerate.[8]

Remark 2.1 Having a nondegenerate contact form for which all closed orbits are hyperbolic — as is the case with the contact forms α_ϵ of Theorem 1.1 — is generally desirable as branched covers of trivial cylinders over elliptic orbits can have negative index [41, Section 1]. Likewise, in ECH chain complexes only simple covers of hyperbolic orbits are considered, whereas multiple covers of elliptic orbits cannot be avoided [40]. See also [3; 56], where analysis of holomorphic maps is simplified by considering only hyperbolic orbits.

Suppose that γ is a nondegenerate orbit equipped with a framing $s \in \Gamma_{\neq 0}(\xi|_\gamma)$. By extending s to a symplectic trivialization of the normal bundle $(\xi|_\gamma, d\alpha)$ to γ, we can write the restriction of the linearized flow to $\xi|_\gamma$ as a path $\phi = \phi(t)$ in $\mathrm{SL}(2,\mathbb{R})$. Then we define the *Conley–Zehnder index of the orbit γ with framing s*, denoted by $\mathrm{CZ}_s(\gamma)$, to be the Conley–Zehnder index $\mathrm{CZ}(\phi)$ of the path ϕ.

If γ is hyperbolic, ϕ rotates the eigenspaces of Ret_γ by an angle πn for some $n \in \mathbb{Z}$, in which case

$$\mathrm{CZ}_s(\gamma^k) = kn.$$

Negative hyperbolic orbits have n odd and positive hyperbolic orbits have n even. If γ is elliptic, ϕ rotates the eigenspaces of Ret_γ by some angle $\theta \in \mathbb{R} \setminus 2\pi\mathbb{Z}$ in which case the Conley–Zehnder index is

$$\mathrm{CZ}_s(\gamma^k) = 2\left\lfloor \frac{k\theta}{2\pi} \right\rfloor + 1.$$

Note that CZ_s depends only on the isotopy class of the framing s. If we write $s+n$ for a framing whose isotopy class is given by twisting s by n meridians, then

$$\mathrm{CZ}_{s+n}(\gamma^k) = \mathrm{CZ}_s(\gamma^k) - 2nk. \tag{2}$$

An orbit γ^k is *bad* if the parity of its Conley–Zehnder index disagrees with that of the underlying embedded orbit γ. Orbits which are not bad are *good*. Hence (when $\dim(M) = 3$), the only bad orbits are even covers of negative hyperbolic orbits. See [23, Remarks 1.9.2 and 1.9.6].

[8] In practice, one is typically interested in studying sequences of contact forms α_n with "nice" limiting behavior, namely there exists a sequence $C_n \to \infty$ such that the orbits of α_n of action $\leq C_n$ are nondegenerate. See for example [4; 3; 5; 18]. We take a similar approach in this article.

Note that, as $\mathrm{CZ}_s(\gamma)$ mod 2 is independent of s, so is the property that an orbit is good or bad. We write $\mathrm{CZ}_2(\gamma) \in \mathbb{Z}/2\mathbb{Z}$ for the index modulo 2 which satisfies

$$\operatorname{sgn} \circ \det(\mathrm{Ret}_\gamma - \mathrm{Id}) = (-1)^{\mathrm{CZ}_2 + 1}. \tag{3}$$

The following method of computing the Conley–Zehnder index of a path $\phi(t)$ for $t \in [0,1]$ of symplectic matrices is due to Robbin and Salamon [55]. For a path $\phi\colon [0,1] \to \mathrm{SL}(2,\mathbb{R})$, a point $t \in [0,1]$ is *crossing* if 1 is an eigenvalue of $\phi(t)$. Writing

$$\frac{\partial \phi}{\partial t}(t) = J_0 S(t) \phi(t) \tag{4}$$

for symmetric matrices $S(t)$, we say that a crossing t is *regular* if the quadratic form $\Gamma(t)$ defined as the restriction of $S(t)$ to $\ker(\phi(t) - \mathrm{Id})$ is nondegenerate. For a path ϕ with only regular crossings, we can compute $\mathrm{CZ}(\phi)$ as

$$\mathrm{CZ}(\phi) = \tfrac{1}{2} \operatorname{sgn}(\Gamma(0)) + \sum_{t>0 \text{ crossing}} \operatorname{sgn}(\Gamma(t)). \tag{5}$$

Also of utility for computation is the *loop property* of CZ, which states that, given $k \in \mathbb{Z}$ and a nondegenerate path ϕ, the path $\widetilde{\phi}(t) = e^{i2\pi k t}\phi(t)$ has

$$\mathrm{CZ}(\widetilde{\phi}) = 2k + \mathrm{CZ}(\phi). \tag{6}$$

2.6 Holomorphic curves in symplectizations and the index formula

Now suppose that α is a nondegenerate contact form for some contact 3–manifold (M,ξ) and that J is an almost-complex structure which is *adapted to the symplectization* $(\mathbb{R}\times M, e^t\alpha)$. That is,

(1) J is compatible with $d(e^t\alpha)$,

(2) it is t–invariant and preserves ξ, and

(3) $J\partial_t = R$.

Let

$$\gamma^+ = \{\gamma_1^+, \dots, \gamma_{m^+}^+\} \quad \text{and} \quad \gamma^- = \{\gamma_1^-, \dots, \gamma_{m^-}^-\}$$

be collections of Reeb orbits with γ^+ nonempty and let (Σ, j) be a Riemann surface with marked points $\{p_1^+, \dots, p_{m^+}^+, p_1^-, \dots, p_{m^-}^-\}$. We write Σ' for Σ with its marked

points removed. We say that $(t, U)\colon \Sigma' \to \mathbb{R} \times M$ is *holomorphic* if

$$\overline{\partial}(t, U) = \tfrac{1}{2}(T(t, U) + J \circ T(t, U) \circ j)$$

vanishes. If we wish to specify J and j, we'll say that the map is (J, j)–*holomorphic*. This is equivalent to the conditions

$$dt = U^*\alpha \circ j, \quad J\pi_\alpha \circ TU = \pi_\alpha \circ TU \circ j, \tag{7}$$

where $\pi_\alpha\colon TM \to \xi$ is the projection $V \mapsto V - \alpha(V)R$. We provide a few simple examples.

Example 2.2 (trivial strips, planes and cylinders) Provided a map $\gamma\colon I \to M$ parametrizing a Reeb trajectory for a connected 1–manifold I, $\mathbb{R} \times \operatorname{im}(\gamma) \subset \mathbb{R} \times M$ is an immersion with J–complex tangent planes. Some examples of particular interest:

(1) If I is compact with nonempty boundary parametrizing a chord of R with endpoints on a Legendrian submanifold Λ, we'll call $\mathbb{R} \times \operatorname{im}(\gamma)$ a *trivial strip*.

(2) If $I = \mathbb{R}$ and the map γ is an embedding, we'll say that $\mathbb{R} \times \operatorname{im}(\gamma)$ is a *trivial plane*.

(3) If $I = S^1_a$ parametrizing a Reeb orbit of action a, then we'll say that $\mathbb{R} \times \operatorname{im}(\gamma)$ is a *trivial cylinder*.

Given a holomorphic map $(t, U)\colon (\Sigma, j) \to (\mathbb{R} \times M, J)$, we say that the puncture p_i^+ is *positively asymptotic* to the orbit γ_i^+ if there exists a neighborhood $[C, \infty) \times S^1$ of p_i^+ in Σ with coordinates r and θ for which j is the standard cylindrical complex structure such that $t(r, \theta) \to \infty$ and $U(r, \theta)$ tends to a parametrization of γ_i^+ as $r \to \infty$. Likewise, we say that the puncture p_i^- is *negatively asymptotic* to the orbit γ_i^- if $t(r, \theta) \to -\infty$ and $U(r, \theta)$ tends to a parametrization of $-\gamma_i^+$ as $r \to \infty$. Allowing j and the location of the marked points to vary and then modding out by reparametrization in the domain, we write $\mathcal{M}_{(t,U)}$ for the *moduli space of holomorphic maps* asymptotic to the $\gamma^\pm$ containing the map (t, U).

The *index* of a holomorphic map as above is defined by

$$\operatorname{ind}((t, U)) = \operatorname{CZ}_s(\gamma^+) - \operatorname{CZ}_s(\gamma^-) - \chi(\Sigma') + 2c_s(U) \in \mathbb{Z}, \tag{8}$$

where

$$\operatorname{CZ}_s(\gamma^\pm) = \sum_{i=1}^{m^\pm} \operatorname{CZ}_s(\gamma_i^\pm).$$

The *relative first Chern class* $c_s(U)$ is the signed count of zeros of $U^*\xi$ over Σ' using a section which coincides with s near the punctures. Note that ind is independent of s.

In ideal geometric settings, $\mathcal{M}_{(t,U)}$ is a manifold near the point (t,U) of dimension $\mathrm{ind}((t,U))$.

Remark 2.3 Here we are disregarding asymptotic markers for orbits which are required for a rigorous functional-analytic setup for moduli spaces and curve counts. We refer to [4; 54] for details.

The *energy* of a holomorphic curve is defined by

$$\mathcal{E}(t,U)=\int_{\Sigma'} d\alpha=\sum_1^{m^+}\mathcal{A}(\gamma_i^+)-\sum_1^{m^-}\mathcal{A}(\gamma_i^-).$$

The energy is nonnegative and is zero if and only if (t,U) is a branched cover of a trivial cylinder. Energies of curves will be presumed finite unless otherwise explicitly stated.

2.7 Contact homology and its variants

We now give a brief overview of contact homology and symplectic field theory. As in previous subsections, we focus specifically on the case of contact 3–manifolds.

For each closed Reeb orbit γ with framing s, we define its degree $|\gamma|_s=\mathrm{CZ}_s(\gamma)-1\in\mathbb{Z}$. This degree modulo 2 will be denoted by $|\gamma|$. We write $\mathrm{CC}(\alpha)$ for the supercommutative algebra with unit 1 generated by the good Reeb orbits of α over $\mathbb{Q}$. Here supercommutativity means $\gamma_1\gamma_2=(-1)^{|\gamma_1||\gamma_2|}\gamma_2\gamma_1$. We note that $\mathrm{CC}(\alpha)$ has two canonical gradings:

(1) The *degree grading* given by $|\gamma_1\cdots\gamma_n|:=\sum_1^n|\gamma_i|\in\mathbb{Z}/2\mathbb{Z}$.

(2) The H_1 *grading* given by $[\gamma_1\cdots\gamma_n]:=\sum_1^n[\gamma_i]\in H_1(M)$.

For $i\in\mathbb{Z}/2\mathbb{Z}$ and $h\in H_1(M)$, we will use the notation $\mathrm{CC}_{i,h}$ to denote the relevant graded $\mathbb{Q}$–subspaces. The contact homology differential

$$\partial_{\mathrm{CH}}\colon \mathrm{CC}_{i,h}\to\mathrm{CC}_{i-1,h}$$

is defined by counting $\mathrm{ind}=1$ (possibly perturbed) solutions to $\overline{\partial}(t,U)=0$ with one positive puncture, any number of negative punctures and genus 0. For such curves (t,U) positively asymptotic to some γ^+ and negatively asymptotic to γ_j^- simultaneously framed with some choice of s, equation (8) becomes

$$\mathrm{ind}((t,U))=|\gamma^+|_s-\sum_j|\gamma_j^-|_s+2c_s(U). \tag{9}$$

Each such solution contributes a term to $\partial\gamma^+$ of the form $m(\gamma^+;\gamma_i^-)\gamma_1^-\cdots\gamma_n^-$ with $m(\gamma^+;\gamma_i^-)\in\mathbb{Q}$. If there are no negative punctures, we get a term of the form $m(\gamma^+)1$

and we set $\partial_{\mathrm{CH}} 1 = 0$. The differential is then extended to products of orbits using the graded Leibniz rule

$$\partial_{\mathrm{CH}}(\gamma_1\gamma_2) = (\partial\gamma_1)\gamma_2 + (-1)^{|\gamma_1|}\gamma_1(\partial\gamma_2)$$

and to sums of products linearly.

Definition 2.4 The resulting differential graded algebra $\ker(\partial_{\mathrm{CH}})/\mathrm{im}(\partial_{\mathrm{CH}})$ is defined to be the *contact homology of* (M,ξ), denoted by $\mathrm{CH}(M,\xi)$. As in the case of $\mathrm{CC}(\alpha)$, $\mathrm{CH}(M,\xi)$ also has degree and H_1 gradings. We write $\mathrm{CH}_{i,h}(M,\xi)$ for the subspace of $\mathrm{CH}(M,\xi)$ with degree i and H_1 grading h.

This theory, first proposed by Eliashberg, Givental and Hofer [23], has been proven to be rigorously defined and independent of all choice involved by Bao and Honda [4] and Pardon [54]. We defer to these citations for the specifics of how the coefficients $m(\gamma^+;\gamma_i^-) \in \mathbb{Q}$ are computed and details around any required perturbations of $\overline{\partial}$. For the purposes of this paper, it suffices to know that, for generic J adapted to the symplectization of a contact manifold,

(1) curves which are somewhere injective may be assumed regular,

(2) regularity for these curves may be achieved by perturbations of J in arbitrarily small neighborhoods of the closed orbits of R, and

(3) assuming such regularity, the moduli space of holomorphic planes positively asymptotic to a closed, embedded orbit will be a manifold (rather than an orbifold), so that such ind $= 1$ planes can be counted over $\mathbb{Z}$.

Additional algebraic structures — which require more sophisticated underlying chain complexes — may be constructed as follows:

(1) By counting ind $= 1$, genus 0 holomorphic curves with arbitrary numbers of positive and negative punctures via a differential ∂_{RSFT}, the *rational SFT algebra* (*RSFT*) may be defined.

(2) By counting ind $= 1$ holomorphic curves with arbitrary genus and numbers of positive and negative punctures via a differential ∂_{SFT}, the *SFT algebra* (*SFT*) may be defined.

See [23] for a more complete picture or the exposition [64, Lecture 12] for further details regarding these invariants.[9] For other *RSFT*-like algebraic structures associated

[9] At the time of writing, rigorous definitions of *RSFT* and *SFT* are under construction using a variety of frameworks. We refer to [4; 48; 54] for accounts of the current state of the development of SFT.

to counts of rational curves with multiple positive punctures, see [48], which constructs such invariants and provides an overview of recent additions to the literature.

The lecture notes [6] and Section 1.8 of [54] also contain a rather exhaustive list of additional structures such as grading refinements and twisted coefficient systems for contact homology. We won't address such additional structures in this article, except in the following simple situations:

Proposition 2.5 (canonical $\mathbb{Z}$ gradings) *The $0 \in H_1(M)$ part of $\mathrm{CH}(M,\xi)$ is a subalgebra of CH. Suppose that $\Gamma_{\neq 0}(\xi)$ is nonempty (equivalently, $c_1(\xi) = 0$).*

(1) *The $\mathbb{Z}$–valued degree gradings $|\cdot|_s$ on $\mathrm{CC}(\alpha)$ determine $\mathbb{Z}$–valued gradings on $\mathrm{CH}_{*,0}(M,\xi)$ and are independent of the choice of $s \in \Gamma_{\neq 0}(\xi)$.*

(2) *Moreover, if $H^1(M) = H_2(M) = 0$, then the $\mathbb{Z}$–valued degree gradings $|\cdot|_s$ on $\mathrm{CC}(\alpha)$ determine $\mathbb{Z}$–valued gradings $\mathrm{CH}(M,\xi)$ which are independent of the choice of $s \in \Gamma_{\neq 0}(\xi)$.*

We get canonical $\mathbb{Z}$ gradings on CH when we have a nondegenerate Reeb vector field with only homologically trivial Reeb orbits or when M is a 3–dimensional $\mathbb{Q}$–homology sphere.

Proof The fact that $\mathrm{CH}_{*,0}(M,\xi)$ is a subalgebra of $\mathrm{CH}(M,\xi)$ is clear from the fact that ∂_{CH} preserves H_1 and that $\mathrm{CC}_{*,0}$ is closed under products.

Provided $s \in \Gamma_{\neq 0}(\xi)$, extend s to a trivialization $\xi \to \mathbb{C}$. For our extension, we may use Js for an almost-complex structure J on ξ. In this way, we see that any other nonvanishing section s' defines a map $M \to \mathbb{C}^* \simeq S^1$ and recall that homotopy classes of maps to S^1 are in bijective correspondence with elements of H^1 [33, Theorem 4.57]. Write $[s'-s] \in H^1$ for the cohomological element provided by this correspondence. If γ is a closed orbit of some α for (M,ξ), then $[s'-s]\cdot[\gamma] \in \mathbb{Z}$ equals the difference in meridians between the framings of $\xi|_\gamma$ determined by s and s'. Then $\mathrm{CZ}_s(\gamma) - \mathrm{CZ}_{s'}(\gamma)$ will be determined by this framing difference according to (2).

If $[\gamma] = 0 \in H_1$, then the above tells us $\mathrm{CZ}_s(\gamma) = \mathrm{CZ}_{s'}(\gamma)$, so that the gradings $|\gamma|_s$ on $\mathrm{CC}_{*,0}$ are independent of choice of nonvanishing s. If $H^1(M) = 0$ then s' is necessarily homotopic to s, so that all of the gradings $|\cdot|_s$ are equivalent on $\mathrm{CC}_{*,*}$. As s is nonvanishing, the c_s term in (9) is always 0, meaning that ∂ always lowers the degree $|\cdot|_s$ by exactly 1 and so the $\mathbb{Z}$–valued degree gradings on CC determines a $\mathbb{Z}$ grading on homology.

To complete the proof, we must show that the $\mathbb{Z}$ grading is independent of the choices used to compute CH. Proofs of invariance of CH (see as they appear in [4; 54]) are obtained by considering the symplectization of (M,α) — for some α — equipped with almost-complex structures which are adapted to α at the negative end $(-\infty,-C]\times M$ of the symplectization and adapted to $H\alpha$ at the positive end $[C,\infty)\times M$ for some $C>0$ and $H\in\mathcal{C}^\infty(M,(0,\infty))$. In such a scenario, $T(\mathbb{R}\times M)$ can be split as the direct sum $\operatorname{span}_{\mathbb{R}}(\partial_t, J\partial_t)\oplus\xi$, and we can extend s over $\mathbb{R}\times M$ in the obvious way to frame Reeb orbits at both ends of $\mathbb{R}\times M$. The isomorphism between the contact homologies of the ends of the cobordism is defined by counting $\operatorname{ind}=0$ holomorphic curves in $\mathbb{R}\times M$, which, by the index formula of (9), must preserve the $\mathbb{Z}$ grading. □

The variant of contact homology which will be of the most interest to us is the *hat version*, denoted by $\widehat{\mathrm{CH}}(M,\xi)$ and defined in [14]. To define this theory for (M,ξ), we can equip $\widehat{M}$ with a standard-at-infinity α for $\hat{\xi}=\xi|_{\widehat{M}}$, choose an appropriately convex J on $\hat{\xi}$, and compute CH as above. We describe such J for the $(\mathbb{R}^3_{\Lambda^\pm},\xi_{\Lambda^\pm})$ in Section 11.2.[10]

The following theorem summarizes some properties of $\widehat{\mathrm{CH}}$ laid out in the introduction of [14] (coupled with some well-known results):

Theorem 2.6 *The invariant $\widehat{\mathrm{CH}}(M,\xi)$ satisfies the following properties*:

(1) *For the standard contact 3–sphere (S^3,ξ_{std}), $\widehat{\mathrm{CH}}(S^3,\xi_{\mathrm{std}})=\mathbb{Q}1$.*

(2) *If (M,ξ) is overtwisted, then $\widehat{\mathrm{CH}}(M,\xi)=0$.*

(3) *For a contact-connected sum $(M_1,\xi_1)\#(M_2,\xi_2)$,*

$$\widehat{\mathrm{CH}}((M_1,\xi_1)\#(M_2,\xi_2))\simeq\widehat{\mathrm{CH}}(M_1,\xi_1)\otimes\widehat{\mathrm{CH}}(M_2,\xi_2).$$

(4) *The inclusion $\widehat{(M,\xi)}\to(M,\xi)$ induces an algebra homomorphism*

$$\widehat{\mathrm{CH}}(M,\xi)\to\mathrm{CH}(M,\xi).$$

Consequently, $\mathrm{CH}(M,\xi)\neq0$ implies $\widehat{\mathrm{CH}}(M,\xi)\neq0$.

(5) *A Liouville cobordism (W,λ) with convex boundary $\widehat{(M^+,\xi^+)}$ and concave boundary $\widehat{(M^-,\xi^-)}$ determines an algebra homomorphism*

$$\Phi_{(W,\lambda)}\colon\widehat{\mathrm{CH}}(M^+,\xi^+)\to\widehat{\mathrm{CH}}(M^-,\xi^-).$$

(6) *Consequently, if (M,ξ) admits a Liouville filling, then both $\mathrm{CH}(M,\xi)$ and $\widehat{\mathrm{CH}}(M,\xi)$ are nonzero.*

[10] In [14], less restrictive conditions are placed on α and J to define $\widehat{\mathrm{CH}}$ within the framework of the more general sutured contact homology. We choose more restrictive conditions so as to simplify our exposition and avoid general discussion of sutured contact manifolds and their completions as well as to simplify J–convexity arguments.

Item (5), which will refer to as *Liouville functoriality*, does not explicitly appear in the literature for $\widehat{\mathrm{CH}}$, though it follows from a simple combination of existing arguments and constructions. Liouville functoriality is established for closed contact manifolds in [4; 54]. To extend the results to punctured contact manifolds, one needs to establish SFT compactness [8] of (possibly perturbed) moduli spaces of holomorphic curves positively asymptotic to closed orbits of a standard-at-infinity contact form on $\widehat{(M^+,\xi^+)}$ and negatively asymptotic to closed orbits of a standard-at-infinity form on $\widehat{(M^-,\xi^-)}$ in the completion of (W,λ). To obtain compactness, we may restrict to almost-complex structures J which are t–invariant over the neighborhood of the puncture of the $M^{\pm}$ to ensure that sequences of curves cannot escape the completed cobordism through the horizontal boundary of the symplectization of the puncture. Our definition of Liouville cobordism between punctured contact manifolds and the J of Section 11.2 ensure that these desired hypotheses are in place. Perturbations of $\overline{\partial}$ required to achieve transversality for the counting of curves and gluing of multilevel SFT buildings can be implemented in arbitrarily small neighborhoods of closed Reeb orbits [4, Section 5], so that such perturbations do not interfere with convexity. In this way, the compactness results of [14, Section 5] carry over without issue.

For Theorem 2.6(6), Liouville functoriality tells us that a Liouville filling of a closed contact manifold induces an algebra homomorphism from $\mathrm{CH}(M,\xi)$ to $\mathbb{Q}$ (also known as an augmentation). Therefore, $\mathrm{CH}(M,\xi)\neq 0$, implying $\widehat{\mathrm{CH}}(M,\xi)\neq 0$ by (4).

2.7.1 Relative contact homology We now briefly review SFT invariants of a Legendrian link $\Lambda\subset(M,\xi)$. For the case $(M,\xi)=(\mathbb{R}^3,\xi_{\mathrm{std}})$, we recommend [26], with the general theory laid out in [23, Section 2.8].

Provided a Legendrian link $\Lambda\subset(M,\xi)$ and a contact form α for ξ, consider the space of chords of R which begin and end on Λ. A chord $r=r(t)$ is *nondegenerate* if it satisfies the transversality condition

$$\mathrm{Flow}_R^{\mathcal{A}(r)}(T_{r(0)}\Lambda)\pitchfork T_{r(\mathcal{A}(r))}\Lambda\subset\xi_{r(\mathcal{A}(r))}.$$

We then say that the pair (α,Λ) is *nondegenerate* if all chords for the pair and all closed orbits of R are nondegenerate. Provided nondegeneracy, we consider a $\mathbb{Z}/2\mathbb{Z}$–graded supercommutative algebra $\mathrm{CC}(\alpha,\Lambda)$ generated by the chords of Λ and the good closed orbits of R.[11] As in the nonrelative case, $\mathrm{CC}(\alpha,\Lambda)$ comes with an additional homological grading, given by the relative homology classes of chords and orbits in $H_*(M,\Lambda)$.

[11] We are skipping definition of the gradings of chords in the general case. See [26; 50] for gradings in the case of Legendrians in $(\mathbb{R}^3,\xi_{\mathrm{std}})$.

We may then define a differential

$$\partial_{\mathrm{LCH}}\colon \mathrm{CC}_{i,h}(\alpha,\Lambda)\to \mathrm{CC}_{i-1,h}(\alpha,\Lambda)$$

for $i\in\mathbb{Z}/2\mathbb{Z}$ and $h\in H_1(M,\Lambda)$ as follows: for a chord r, ∂_{LCH} counts $\mathrm{ind}=1$ holomorphic disks in the symplectization of (M,ξ) with

(1) a single boundary puncture positively asymptotic to r,

(2) any number m of boundary punctures negatively asymptotic to chords r_i^- of Λ,

(3) $\partial\mathbb{D}$ with its punctures removed mapped to the Lagrangian cylinder over Λ, and

(4) n interior punctures negatively asymptotic to closed orbits γ_j^-

Each such disk contributes a term of the form $m(r^+;r^-,\gamma^-)r_1^-\cdots r_m^-\gamma_1^-\cdots\gamma_n^-$ to $\partial_{\mathrm{LCH}}r^+$. For a closed orbit γ^+, the differential $\partial_{\mathrm{LCH}}\gamma^+$ coincides with the contact homology differential of γ^+. The differential is then extended to products and sums of products using the Leibniz rule and linearity as in the case of nonrelative contact homology.

Definition 2.7 The resulting differential graded algebra $\ker(\partial_{\mathrm{LCH}})/\mathrm{im}(\partial_{\mathrm{LCH}})$ is defined to be the *Legendrian contact homology* of the triple (M,ξ,Λ), denoted by $\mathrm{LCH}(M,\xi,\Lambda)$. As in the case of CC_Λ, LCH has degree and relative H_1 gradings.

The computation $\partial_{\mathrm{LCH}}^2=0$ and proof of invariance for links in $(\mathbb{R}^3,\xi_{\mathrm{std}})$ — in which case there are no closed Reeb orbits — is carried out in [19], with a proof of the general case sketched in [23]. In the case $\Lambda\subset(\mathbb{R}^3,\xi_{\mathrm{std}})$, a combinatorial version of LCH — originally due to Chekanov [10] — may be computed by counting immersions of disks into the xy–plane with boundary mapped to the Lagrangian projection of Λ, in which case $\partial_{\mathrm{LCH}}^2=0$ may be proved diagrammatically. Additional algebraic structures may derived from the triple (M,ξ,Λ) by considering disks with multiple positive punctures as in [17; 50]. Again, we point to [26] for further references regarding proofs that the combinatorially and analytically defined invariants coincide for $(\mathbb{R}^3,\xi_{\mathrm{std}})$ as well as extensions and generalizations of LCH in both algebraic and geometric directions.

2.8 Legendrian knots and links in $(\mathbb{R}^3,\xi_{\mathrm{std}})$

Legendrian knots and links will be denoted by Λ with sub- and superscripts. Throughout this article, we assume that each component of Λ is equipped with a predetermined orientation. For a Legendrian link Λ in a contact manifold (M,ξ) with contact form α and Reeb vector field R,

$$\mathrm{Flow}_R^\delta(\Lambda)$$

for $\delta > 0$ arbitrarily small will be called the *push-off of* Λ. The Legendrian isotopy class of the pair $(\Lambda, \mathrm{Flow}_R^{\delta}(\Lambda))$ is independent of R and δ. We write λ_ξ for the Legendrian isotopy class of the push-off.

For a Legendrian link Λ in $(\mathbb{R}^3, \xi_{\mathrm{std}})$, the front and Lagrangian projections will be denoted by π_{xz} and π_{xy}, respectively. We will use front projections as our default starting point for analysis of Λ, from which we will transition to the Lagrangian projection — see Section 4.4.

Assuming that Λ has a single connected component, its *classical invariants* are

(1) the Thurston–Bennequin number $\mathrm{tb}(\Lambda)$;

(2) the rotation number, $\mathrm{rot}(\Lambda)$, which depends on an orientation of Λ; and

(3) the smooth topological knot underlying Λ.

In the Lagrangian projection, we may compute $\mathrm{tb}(\Lambda)$ as the writhe and $\mathrm{rot}(\Lambda)$ as the winding number. Geometrically, the Thurston–Bennequin number is defined as the linking number

$$\mathrm{tb}(\Lambda) = \mathrm{lk}(\Lambda, \lambda_\xi),$$

whereas rot is defined as the degree of the Gauss map of $T\Lambda$ in ξ_{std} with respect to a nowhere-vanishing trivialization. If we replace $\mathbb{R}^3$ with any contact $\mathbb{Q}$–homology sphere, then tb is defined for null-homologous Legendrian knots and rot is defined for all Legendrian knots using the framings of Proposition 2.5. See also Definition 6.3.

Classical invariants of a Legendrian knot $\Lambda \subset (\mathbb{R}^3, \xi_{\mathrm{std}})$ are constrained by the *slice-Bennequin bound* of [57]:

$$\tfrac{1}{2}\big(\mathrm{tb}(\Lambda) + |\mathrm{rot}(\Lambda)| + 1\big) \leq g_s(\Lambda) \leq g(\Lambda). \tag{10}$$

Here $g_s(\Lambda)$ is the smooth slice genus of the topological knot underlying Λ and $g(\Lambda)$ is the Seifert genus. See [24, Section 3] for an overview of related results.

Let Λ be a Legendrian knot in a contact manifold (M, ξ). Take a cube $I^3_\epsilon \subset M$ with $\epsilon > 0$ and coordinates x, y and z such that

$$\xi = \ker(\alpha_{\mathrm{std}}), \quad \Lambda \cap I^3_\epsilon = \{y = z = 0\}$$

and ∂_x orients Λ. Then Λ is locally described by Figure 2, left. The *positive and negative stabilizations* of Λ, denoted by $S_+(\Lambda)$ and $S_-(\Lambda)$, are defined as the Legendrian knots determined by modifying Λ in the front projection of I^3_ϵ as described in Figure 2, right. We say that a Legendrian knot Λ is *stabilized* if it is a positive or negative stabilization of some $\Lambda' \subset (M, \xi)$.

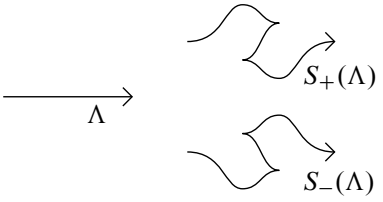

Figure 2: Positive and negative stabilizations of Λ described in the front projection as in [24, Figure 19].

2.9 Contact surgery

Contact surgery — first defined in [16] — provides a way of performing Dehn surgery on a Legendrian link $\Lambda^{\pm}$ so that the surgered manifold carries a contact structure uniquely determined by $\Lambda^{\pm}$ and (M, ξ). We recommend Ozbagci and Stipsicz [52] as a general reference.

We take the coefficients of the components of the sublinks Λ^+ (resp. Λ^-) to be $+1$ (resp. -1). Intuitively speaking, contact -1 (resp. $+1$) surgery removes a neighborhood of a Legendrian knot of the form $I_\epsilon \times I_\epsilon \times S^1$ — the first coordinate being directed by ∂_z — and then glues it back in using a positive (resp. negative) Dehn twist along $\{\epsilon\} \times I_\epsilon \times S^1$. The construction may be formalized using the gluing theory of convex surfaces. A rigorous account of the construction will be carried out in Section 4. For $k \in \mathbb{Z} \setminus \{0\}$ one may analogously perform *contact* $1/k$ *surgery* on a Legendrian knot Λ by applying $-k$ Dehn twists as above. We will take as definition that contact $1/k$ surgery for $k \neq 0$ is given by performing contact $\operatorname{sgn}(k)$ surgery on $|k|$ parallel push-offs of Λ.

We write

$$\Lambda = \Lambda^+ \cup \Lambda^0 \cup \Lambda^- \subset (\mathbb{R}^3, \xi_{\text{std}})$$

to specify a Legendrian link Λ^0 sitting inside of the contact manifold $(\mathbb{R}^3_{\Lambda^\pm}, \xi_{\Lambda^\pm})$. Since the neighborhoods of the components of Λ defining surgery many be chosen to be disjoint from Λ^0, we may consider it to be a Legendrian link in $(\mathbb{R}^3_{\Lambda^\pm}, \xi_{\Lambda^\pm})$ post surgery. The superscript 0 on Λ^0 may be thought of as indicating a trivial $\frac{1}{0} = \infty$ surgery in the usual notation of Kirby calculus.

In Section 10 we will review how contact surgeries may be viewed as the result of handle attachments. We refer the reader to [52] for a review in the low-dimensional case and to [11] for the general case.

Theorem 2.8 *We summarize some known results about contact surgery relevant to this paper*:

(1) *The contact manifold obtained by contact $+1$ surgery on the Legendrian unknot with $\mathrm{tb} = -1$ yields the standard fillable contact structure ξ_{std} on $S^1 \times S^2$.*

(2) *Applying contact -1 surgery on a Legendrian knot in (M, ξ) produces the same contact manifold as is obtained by attaching a Weinstein handle to the convex boundary of the symplectization of (M, ξ).*

(3) *Then performing ± 1 surgery on a Legendrian knot $\Lambda \subset (M, \xi)$ followed by ∓ 1 surgery on a push-off λ_ξ leaves (M, ξ) unchanged.*

(4) *A contact 3–manifold is overtwisted if and only if it can be described as the result of a contact $+1$ surgery along a stabilized Legendrian knot Λ in some (M, ξ).*[12]

(5) *If $\Lambda \subset (\mathbb{R}^3, \xi_{\mathrm{std}})$ satisfies $\mathrm{tb}(\Lambda) = 2g_s(\Lambda) - 1$, then contact $1/k$ surgery on Λ produces a tight contact manifold [43] for any $k \in \mathbb{Z}$.*

(6) *For a Legendrian knot $\Lambda \subset (\mathbb{R}^3, \xi_{\mathrm{std}})$ and an integer $k > 0$, contact $1/k$ surgery on Λ produces a symplectically fillable contact 3–manifold if and only if both $k = 1$ and Λ bounds a Lagrangian disk in the standard symplectic 4–disk [15].*

3 Notation and algebraic data associated to chords

In this section we describe notation and algebraic data associated to chords of Legendrian links which will be used throughout the remainder of the paper. We take $\Lambda \subset (\mathbb{R}^3, \xi_{\mathrm{std}})$ to be a nonempty link with sublinks Λ^+, Λ^- and Λ^0 — any of which may be empty. We write $\Lambda^\pm = \Lambda^+ \cup \Lambda^-$.

Assumptions 3.1 It is assumed throughout that Λ is *chord generic*, meaning that all chords of Λ are nondegenerate and that distinct chords are disjoint as subsets of $\mathbb{R}^3$.

3.1 Surgery coefficients and chords of Λ

It will be convenient to write $\Lambda = \cup \Lambda_i$ with the subscript i indexing the connected components of Λ. Using this notation, we use $c_i \in \{-1, 0, +1\}$ to indicate that $\Lambda_i \subset \Lambda^{c_i}$.

Denote by r_j the Reeb chords of Λ with the contact form $\alpha_{\mathrm{std}} = dz - y\,dx$, which are in one-to-one correspondence with the double points of the Lagrangian projection π_{xy}.

[12] One proof is obtained by proving the "if" statement using [51] and proving "only if" by following the proof of Theorem 12.3. Alternatively, one can apply a handle-slide to [2, Theorem 5.5(2)].

We write $\operatorname{sgn}_j \in \{\pm 1\}$ for the sign of the crossing of Λ in the Lagrangian projection associated with the chord r_j in accordance with the orientation of Λ.

We define l_j^- to be the index i of the Λ_i on which r_j begins and l_j^+ to be the index of the component of Λ on which r_j ends. The *tip* of a chord r_j is the point $q_j^+ \in \Lambda_{l_j^+}$ where the chord ends. The *tail* of r_j is the point $q_j^- \in \Lambda_{l_j^-}$ at which the chord r_j begins. We write the surgery coefficient of the components of Λ corresponding to $l_j^\pm$ as $c_j^\pm$. That is,

$$c_j^\pm = c_{l_j^\pm}.$$

3.2 Words of chords

An ordered pair of chords (r_{j_1}, r_{j_2}) is *composable* if $l_{j_1}^+ = l_{j_2}^-$. A *word of Reeb chords for* Λ is a formal product of chords $w = r_{j_1} \cdots r_{j_n}$ in which each pair $(r_{j_k}, r_{j_{k+1}})$ is composable for $k = 1, \dots, n-1$.

We say that a word of Reeb chords $r_{j_1} \cdots r_{j_n}$ is a *word of chords with boundary on* Λ^0 if r_{j_1} begins on Λ^0 and r_{j_n} ends on Λ^0 and all other endpoints of chords touch components of $\Lambda^+ \cup \Lambda^-$.

A *cyclic word of Reeb chords for* Λ, denoted by $r_{j_1} \cdots r_{j_n}$, is a word of Reeb chords for which (r_{j_n}, r_{j_1}) is composable. Cyclic permutations of cyclic words are considered to be equivalent:

$$r_{j_1} r_{j_2} \cdots r_{j_n} = r_{j_2} \cdots r_{j_n} r_{j_1}.$$

When speaking of cyclic words of Reeb chords on Λ, we will implicitly assume that it is a cyclic word of Reeb chords on $\Lambda^+ \cup \Lambda^-$.

The *word length* of a word w of Reeb chords is the number of individual chords it contains and will be denoted by $\operatorname{wl}(w)$. The actions of each r_j will be denoted by $\mathcal{A}_j$ and the *action* of a word is defined by

$$\mathcal{A}(r_{j_1} \cdots r_{j_n}) = \sum_{k=1}^{n} \mathcal{A}_{j_k}.$$

3.3 Capping paths

Provided a composable pair of chords (r_{j_1}, r_{j_2}), their *capping path* is the unique embedded, oriented segment of $\Lambda_{l_{j_1}^+} = \Lambda_{l_{j_2}^-}$, traveling in the direction of the orientation of Λ from the tip of r_{j_1} to the tail of r_{j_2}. The capping path will be denoted by η_{j_1, j_2}.

The analogously defined path, which travels opposite the orientation of $\Lambda_{l_{j_1}^+}$ will be denoted by $\overline{\eta}_{j_1,j_2}$ and called the *opposite capping path*. We will use ζ_{j_1,j_2} to denote one of either η_{j_1,j_2} or $\overline{\eta}_{j_1,j_2}$. By setting $\overline{\overline{\eta}}_{j_1,j_2} = \eta_{j_1,j_2}$, we can define $\overline{\zeta}_{j_1,j_2}$ in the obvious way.

3.3.1 Rotation angles and numbers Denote by G the Gauss map sending the unit tangent bundle of $\mathbb{R}^2$ to $S^1_{2\pi}$ with

$$G(\cos(t)\partial_x + \sin(t)\partial_y) = t.$$

This determines a map $G_\Lambda : \Lambda \to S^1_{2\pi}$ assigning to each point in Λ the unit tangent vector at that point determined by the orientation on Λ.

For any path $\zeta : [0,1] \to \Lambda$, we can associate an angle $\theta(\zeta) \in \mathbb{R}$ as follows: Composing ζ with G_Λ determines a map

$$\phi = G_\Lambda \circ \zeta : [0,1] \to S^1_{2\pi}.$$

Denoting by $\widetilde{\phi}$ the lift of this map to $\mathbb{R}$, the *rotation angle* of ζ, denoted by $\theta(\zeta)$, is defined by

$$\theta(\zeta) = \widetilde{\phi}(1) - \widetilde{\phi}(0).$$

If $q : S^1 \to \mathbb{R}^3$ is a parametrization of a component Λ_i of Λ, then the rotation angle of the associated path $[0,1] \to \Lambda_i$ is $2\pi \operatorname{rot}(\Lambda_i)$.

The *rotation angle* of a composable pair (r_{j_1}, r_{j_2}), denoted by $\theta_{j_1,j_2} \in \mathbb{R}$, will later help us to compute Conley–Zehnder indices of closed Reeb orbits. It is defined as $\theta_{j_1,j_2} = \theta(\eta_{j_1,j_2})$. We write $\overline{\theta}_{j_1,j_2}$ for the rotation angle computed with the opposite capping path $\overline{\eta}_{j_1,j_2}$, whence

$$\theta_{j_1,j_2} - \overline{\theta}_{j_1,j_2} = 2\pi \operatorname{rot}(\Lambda_{l_{j_1}^+}). \tag{11}$$

The *rotation number of a composable pair of chords* (r_{j_1}, r_{j_2}), denoted by $\operatorname{rot}_{j_1,j_2}$, is defined as

$$\operatorname{rot}_{j_1,j_2} = \left\lfloor \frac{\theta_{j_1,j_2}}{\pi} \right\rfloor \in \mathbb{Z}.$$

3.3.2 Crossing monomials Now we define the *crossing monomials*, which will later facilitate our computations of the homology classes of Reeb orbits of the R_ϵ. Consider a collection of variables μ_i indexed by the connected components Λ_i of Λ.

The *crossing monomial of a chord* r_j, denoted by cr_j, is defined by

$$\operatorname{cr}_j = \tfrac{1}{2}((c_j^- + \operatorname{sgn}_j)\mu_{l_j^-} + (c_j^+ + \operatorname{sgn}_j)\mu_{l_j^+}) \in \bigoplus \mathbb{Z}\mu_i. \tag{12}$$

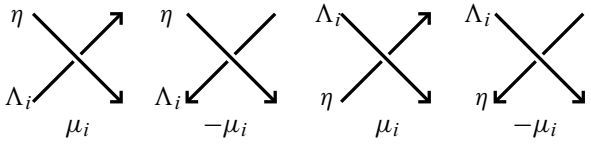

Figure 3: Each subfigure gives a local picture of a crossing of a capping path η with a component of Λ in the Lagrangian projection. Labelings of the strands appears at the left of each subfigure, with the local contribution to the crossing number appearing below. Each subfigure may be rotated by π.

The *crossing monomial of a composable pair of chords* (r_{j_1}, r_{j_2}), denoted by cr_{j_1,j_2}, is defined by

$$\mathrm{cr}_{j_1,j_2} = \sum_{q_{j-}^- \in \mathrm{int}(\eta_{j_1,j_2})} \mathrm{sgn}_{j-} \mu_{l_{j-}^+} + \sum_{q_{j+}^+ \in \mathrm{int}(\eta_{j_1,j_2})} \mathrm{sgn}_{j+} \mu_{l_{j+}^-} \in \bigoplus \mathbb{Z}\mu_i .$$

The contributions are as described in Figure 3.

Remark 3.2 (crossing monomials for connected Λ) When Λ consists of a single connected component, we get a single surgery coefficient c and a single μ. In this case, $\mathrm{cr}_j = (c + \mathrm{sgn}_j)\mu \in 2\mu\mathbb{Z}$ and $\mathrm{cr}_{j_1,j_2} = m\mu$, where m is the number of times the interior capping path η_{j_1,j_2} touches the tips and tails of chords, counted with signs given by the sgn_j.

3.4 Broken closed strings

We temporarily work with an arbitrary contact 3–manifold (M, ξ) containing a Legendrian submanifold Λ. Equip (M, ξ) with a contact form α and write κ_j for the chords of Λ, which will be assumed nondegenerate. Words of chords with boundary on Λ and cyclic words of chords on Λ are defined as above in the obvious fashion.

Let κ_k for $k = 1, \dots, n$ be a sequence of chords on Λ and let $a_k \in \{\pm 1\}$. Let ζ_k be a collection of oriented arcs $\zeta_k : [0, 1] \to \Lambda$ starting at the endpoint (starting point) of κ_k if a_k is positive (negative) and ending at the starting point (endpoint) of κ_{k+1} if a_{k+1} is positive (negative). Assume that the a_k and ζ_{j_k} are such that

$$b = (a_1\kappa_1) * \zeta_1 * \cdots * (a_k\kappa_n) * \zeta_n \tag{13}$$

forms a closed, oriented loop, where $*$ denotes concatenation and $\pm\kappa_k$ is κ_k parametrized with positive (negative) orientation.

Definition 3.3 We call a map b as in (13) a *broken closed string on* Λ. We call the a_k *asymptotic indicators*. We consider broken closed strings which differ by cyclic rotation of indices involved to be equivalent and say that a broken closed string is *parametrized* if a fixed ordering of the indices is in use. We also consider broken closed strings which differ by homotopy of the ζ_k (relative to their endpoints) to be equivalent.

Example 3.4 Let (t, U) be a holomorphic map from a disk with boundary punctures $\{p_j\}$ removed, $\mathbb{D} \setminus \{p_j\}$, to the symplectization of (M, ξ), with boundary punctures asymptotic to chords of Λ. Suppose that

(1) the p_j are indexed according to their counterclockwise ordering along $\partial\mathbb{D}$,

(2) the p_j are a_j–asymptotic to chords κ_j ($a_j = 1$ for positively asymptotic and $a_j = -1$ for negatively asymptotic), and

(3) $U(\partial\mathbb{D} \setminus \{p_j\}) \subset \Lambda$ with ζ_j denoting the restriction of U to the component of $\partial\mathbb{D} \setminus \{p_j\}) \subset \Lambda$ whose oriented boundary is $p_{j+1} - p_j$.

With the data a_j, κ_j and ζ_j specified by (t, U) as above, equation (13) is a broken closed string on Λ. Of particular interest are broken closed strings determined by disks appearing in the *LRSFT* differential for Legendrian links in $(\mathbb{R}^3, \xi_{\text{std}})$ [50].

This may be generalized in the obvious way to holomorphic maps (t, U) whose domain is a compact Riemann surface (Σ, j) decorated with interior punctures (asymptotic to closed Reeb orbits) and boundary punctures (asymptotic to chords). Then any boundary component of Σ determines a broken closed string on Λ.

Definition 3.5 A broken closed string determined by a holomorphic map as in Example 3.4 will be called a *holomorphic boundary component*.

We note that the ζ_k in the definition of a holomorphic boundary component may be constant: for example, if (t, U) is a trivial strip with domain $\mathbb{R} \times I_\epsilon$ for some chord κ, consider

$$b = \kappa * \zeta_1 * (-\kappa) * \zeta_2$$

with ζ_1 being a constant path with value the tip of κ and ζ_2 a constant path with value the tail of κ.

Example 3.6 Suppose that $\Lambda^\pm$ is a contact surgery diagram and let $w = r_{j_1} \cdots r_{j_n}$ be a cyclic word of composable Reeb chords on Λ. There are 2^n parametrized broken closed strings associated to this cyclic word, given by all of the ways that we may

choose orientations for the capping path starting at the tip of each r_{j_k} and ending at the tail of each $r_{j_{k+1}}$:

$$\begin{gathered} r_{j_1} * \eta_{j_1,j_2} * \cdots * r_{j_n} * \eta_{j_n,j_1}, \\ r_{j_1} * \eta_{j_1,j_2} * \cdots * r_{j_n} * \overline{\eta}_{j_n,j_1}, \\ \vdots \\ r_{j_1} * \overline{\eta}_{j_1,j_2} * \cdots * r_{j_n} * \eta_{j_n,j_1}, \\ r_{j_1} * \overline{\eta}_{j_1,j_2} * \cdots * r_{j_n} * \overline{\eta}_{j_n,j_1}. \end{gathered}$$

Definition 3.7 We call each of the broken closed strings described in Example 3.6 an *orbit string* associated to w.

When dealing with orbit strings, the r_j are determined by the indices of the capping paths involved, and so will be omitted from our notation.

Note that a broken closed string on a Legendrian submanifold of dimension n in a contact manifold of dimension $2n+1$ for $n>1$ is uniquely determined by its chords up to homotopy through broken closed strings. We will see in Section 9.3 that a parametrized capping string provides instructions for homotoping a Reeb orbit of $(\mathbb{R}^3_{\Lambda^\pm}, \xi_{\Lambda^\pm})$ into the complement of a neighborhood of $\Lambda^\pm$ in $\mathbb{R}^3$.

3.5 Maslov indices of broken closed strings

Here we define Maslov indices on broken closed strings on Legendrians in contact 3–manifolds, which are relevant to index computation of holomorphic curves. Essentially, we are packaging terminology appearing in the above subsection so as to be cleanly plugged into index computations appearing in [19; 17]. See Section 8.

We assume that $\dim(M)=3$ and that we are working with κ_k, a_k and ζ_k for $k=1,\dots,n$, as described in the previous subsection, determining a broken closed string b whose domain we take to be $\mathrm{dom}(b)=S^1$. We remark on the case $\dim(M)>3$ later in this subsection. Our discussion follows [17, Section 3]. We write $q_k^- \in \Lambda$ for the starting point of each κ_k and q_k^+ for its endpoint.

We assume that ξ is equipped with an adapted almost-complex structure J and suppose that we have a trivialization $s\colon \xi|_{\mathrm{im}(b)} \to \mathbb{C}$ of ξ over the image of a broken closed string b in M which identifies the symplectic structure $d\alpha$ and complex structure J on the target with the standard symplectic and complex structures on $\mathbb{C}$. The trivialization s provides us with an identification

$$b^*\xi \simeq \mathbb{C}\times S^1$$

Denote by $\mathcal{L}(\xi) \to M$ the bundle whose fiber $\mathcal{L}(\xi|_x) \simeq S^1_\pi$ over a point $x \in M$ is the space of unoriented Lagrangian subspaces — that is, unoriented real lines — in $(\xi_x, d\alpha)$.[13] Then s likewise determines an identification

$$b^*\mathcal{L}(\xi) \simeq S^1_\pi \times S^1.$$

Over the subset of S^1 parametrizing the ζ_k, we have a section of this bundle determined by the unoriented Gauss map,

$$t \mapsto T_{b(t)}\Lambda \subset \xi_{b(t)}.$$

Using s, this section determines a map ϕ^G over this subset to S^1_π. We now describe how to extend this section over the subset of S^1 parametrizing the $a_k\kappa_k$.

For each chord κ_k, the time $t \in [0, \mathcal{A}(\kappa_k)]$ flow of R determines a path in $\mathrm{SL}(2,\mathbb{R})$ by writing $\mathrm{Flow}_R^t(\xi_{q_k^-})$ in the standard basis of $\mathbb{R}^2$ determined by s. This likewise determines a section of $\mathcal{L}(\xi)$ over the chord by $\mathrm{Flow}_R^t(T_{q_k^-}\Lambda)$. As we've assumed that κ_k is nondegenerate,

$$\mathrm{Flow}_R^{\mathcal{A}(\kappa_k)}(T_{q_k^-}\Lambda) \neq T_{q_k^+}\Lambda$$

as Lagrangian subspaces of $\xi_{q_k^+}$. In order to assign a Maslov number to b, we must make a correction to obtain a closed loop of Lagrangian subspaces:

(1) If $a_k = 1$, then the orientation of b and the chord coincide. To form a closed loop we join $\mathrm{Flow}_R^{\mathcal{A}(\kappa_k)}(T_{q_k^-}\Lambda)$ to $T_{q_k^+}\Lambda$ by making the smallest possible clockwise rotation to $\mathrm{Flow}_R^{\mathcal{A}(\kappa_k)}(T_{q_k^-}\Lambda)$.

(2) If $a_k = -1$, then the orientation of b and the chord disagree. To form a closed loop of Lagrangian subspaces along b, we start at the endpoint of the chord, follow the negative flow of R, and then join $\mathrm{Flow}_R^{-\mathcal{A}(\kappa_k)}(T_{q_k^+}\Lambda)$ to $T_{q_k^-}\Lambda$ by making the smallest clockwise rotation possible.

Denote by $\phi_{b,s}\colon S^1 \to S^1_\pi$ the map so obtained.

Definition 3.8 We call the degree of the map $\phi_{b,s}$ described above the *Maslov index of the broken closed string b with respect to the framing s*, denoted by $\mathrm{M}_s(b) \in \mathbb{Z}$. It is easy to see that $\mathrm{M}_s(b)$ does not depend on the cyclic ordering of its indices involved, so that it is well defined.

[13] We use the circle of radius π, S^1_π, rather than $S^1_{2\pi}$ due to our ignoring the orientations of the lines involved.

The following easily follows from the construction of M_s:

Proposition 3.9 *Let b be a broken closed string on $\Lambda \subset (M,\xi)$ with a trivialization s of $\xi|_{\mathrm{im}(b)}$. Smooth homotopies of such trivializations s leave $\mathrm{M}_s(b)$ unchanged. The* mod 2 *reduction of $\mathrm{M}_s(b)$ is independent of s, so that we may define $\mathrm{M}_2(b) \in \mathbb{Z}/2\mathbb{Z}$ as an invariant of b.*

Now suppose that $\Gamma_{\neq 0}(\xi)$ is nonempty as in Proposition 2.5, which clearly applies to any $\Lambda \subset (\mathbb{R}^3, \xi_{\mathrm{std}})$:

(1) *If b is homologically trivial in M, then $\mathrm{M}_s(b)$ is independent of $s \in \Gamma_{\neq 0}(\xi)$.*

(2) *If $H_2(M) = H^1(M) = 0$, then $\mathrm{M}_s(b)$ is independent of $s \in \Gamma_{\neq 0}(\xi)$, regardless of the homotopy class of b in M.*

3.6 Generalizations and comparison with existing conventions

3.6.1 Generalized crossing signs and Maslov indices Crossing signs generalize to n–dimensional Legendrian submanifolds inside contact manifolds of dimension $2n+1$ as follows. As above, consider a generic chord κ on an oriented Legendrian submanifold $\Lambda \subset (M,\xi)$ parametrized by an interval $[0,a]$ given by the flow of some R. Then we may define $\mathrm{sgn}(\kappa)$ by

$$\big(\textstyle\bigwedge^n T_{\kappa(a)}\Lambda\big) \wedge \big(\bigwedge^n \mathrm{Flow}_R^a(T_{\kappa(0)}\Lambda)\big) = \mathrm{sgn}(\kappa)\big(\bigwedge^{2n} \xi_{\kappa(a)}\big)$$

as an orientation on $\xi_{\kappa(a)}$. Note that $\mathrm{sgn}(\kappa)$ is independent of the orientation of Λ if and only if Λ is connected. However, the product of sgn over the chords appearing in a broken closed string is always independent of choice of orientation.

We also briefly address generalizations of the Maslov index to higher dimensions. Provided a contact manifold (M,ξ) of dimension $2n+1$, we write $\mathcal{L}(2n) = U(n)/O(n)$ for the space of (unoriented) Lagrangian planes in the standard symplectic vector space and define the bundle

$$\mathcal{L}(2n) \hookrightarrow \mathcal{L}(\xi) \twoheadrightarrow M$$

as above without modification. Provided a trivialization

$$s\colon b^*(\xi) \to \mathbb{C}^n \times S^1,$$

we can view the sections of $b^*\mathcal{L}(\xi)$ as maps from S^1 to $U(n)/O(n)$, in which case $\mathrm{M}_s(b)$ may be defined and computed as the usual Maslov index of loops in the Lagrangian Grassmannian. See for example [46, Theorem 2.35]. The required "clockwise rotation" correction in arbitrary dimensions is described by the paths $\mathrm{f}_j(s)$ appearing in Section 5.9 of [19].

3.6.2 Conventions for capping paths We briefly address how our conventions for capping paths and rotation angles differ from those used to construct gradings in Legendrian contact homology. See for example the exposition [26, Section 3.1]. Assume that $\Lambda \subset (\mathbb{R}^3, \xi_{\text{std}})$ consists of a single component and has a designated basepoint $*$ not coinciding with the tip or tail of any chord.

For a chord r_j, exactly one of $\eta_{j,j}$ or $\overline{\eta}_{j,j}$ will pass through $*$. Denoting by ϕ_j the rotation angle of the path not passing through $*$, the LCH grading is defined — by a slight manipulation of conventional notation — as

$$|r_j| = \left\lfloor \frac{\phi_j}{\pi} \right\rfloor - 1.$$

This is very similar to our computation of rotation numbers except that

(1) knots along which we are performing surgery do not have basepoints,

(2) our capping paths do not necessarily begin and end at endpoints of the same chord,

(3) our capping paths follow the orientation of Λ by default.

We will see that our conventions for computation arise naturally when computing Conley–Zender indices of Reeb orbits of the R_ϵ using the framing construction of Section 6. This convention is also convenient as it will simplify the statements of homology classes of closed Reeb orbits in Section 9.

Our framing construction can be modified so as to naturally lead to computations of rotation angles using basepoints as in LCH. See Remark 6.2. By (11), if $\text{rot}(\Lambda) = 0$ then our computation of rotation angles coincide when the endpoints of a capping path lie over the same chord:

$$\theta_{j,j} = \overline{\theta}_{j,j} = \phi_j.$$

3.6.3 Conventions for broken closed strings In [50, Definition 3.1], broken closed strings have discontinuities at Reeb chords, whereas our broken closed strings are continuous maps. We have chosen to define broken closed strings to include the data of the chords in question, so as reduce ambiguity when discussing chords on Legendrians contained in surgered contact manifolds $(\mathbb{R}^3_{\Lambda^\pm}, \xi_{\Lambda^\pm})$.

4 Model geometry for Legendrian links and contact surgery

In this section we construct neighborhoods of Legendrian links and then perform contact surgery on $\Lambda^\pm$ using these neighborhoods to describe the contact manifolds $(\mathbb{R}^3_{\Lambda^\pm}, \xi_{\Lambda^\pm})$ and the contact forms α_ϵ.

Our strategy is to develop highly specialized models for the objects involved in contact surgery, determining Reeb vector fields on surgered contact manifolds which are linear in a way which will be made precise in Section 5.1. The main benefits of this approach are that the proofs of the following will be considerably simplified:

(1) The chord-to-orbit (Theorem 5.1) and chord-to-chord (Theorem 5.10) correspondences.

(2) The Conley-Zehnder index (Theorem 7.1) and Maslov index (Theorem 7.2) computations.

We will also be able to determine the embeddings of simple closed orbits in surgered manifolds as fixed points of explicitly defined affine endomorphisms of $\mathbb{R}^2$ (Section 5.6). While we don't pursue computation in this paper, we anticipate this being of utility in future applications.

The primary disadvantage to our contact forms being so specialized is that surgery cobordisms between the $(\mathbb{R}^3_{\Lambda^\pm}, \xi_{\Lambda^\pm})$ will be less explicitly defined and will require greater effort in their construction (Section 10). Furthermore, we will be imposing restrictions on the Lagrangian projections of Legendrian links in the style of [49], so that our analysis — which is applicable to all Legendrian *isotopy classes* $\Lambda^\pm$ — will not be applicable to all chord-generic Legendrian links in $(\mathbb{R}^3, \xi_{\text{std}})$.

Remark 4.1 Our approach to contact surgery is quite similar to that of Foulon and Hasselblatt [29], who defined surgery using a model Dehn twist as in our Section 4.6.

In [7; 18], Bourgeois, Ekholm and Eliashberg describe surgeries as the result of critical-index Weinstein handle attachments and then study the resulting Reeb dynamics. This contrasts with our approach in that we will first describe our contact forms α_ϵ and then build specialized Weinstein handles that have the α_ϵ as the restriction of their Liouville form to their contact boundaries.

The approaches to contact surgery here and [29; 7; 18] all have at least one feature in common: shrinking the size of the surgery locus is used to control Reeb dynamics.

4.1 Almost-complex structures, metrics and the Gauss map

We will want our Legendrians and their neighborhoods to interact nicely with an almost-complex structure J_0 and a metric $g_{\mathbb{R}^3}$, which we now describe.

Define vector fields $X, Y \in \Gamma(\xi_{\text{std}})$ by lifting the derivatives of the usual coordinates:

$$X = \partial_x + y\partial_z, \quad Y = \partial_y.$$

We define a complex structure J_0 on ξ_{std} as the lift of the usual complex structure on $\mathbb{R}^2 = \mathbb{C}$:

$$J_0 X = Y, \quad J_0 Y = -X. \tag{14}$$

This determines an almost-complex structure, which we'll also call J_0, adapted to the symplectization $(\mathbb{R} \times \mathbb{R}^3, e^t \alpha_{\text{std}})$, defined by

$$J_0 \partial_t = \partial_z, \quad J_0 \partial_z = -\partial_t.$$

This almost-complex structure determines a J_0–invariant metric $g_{\mathbb{R}^3}$ on $\mathbb{R}^3$, defined by

$$g_{\mathbb{R}^3}(u, v) = \alpha(u)\alpha(v) + d\alpha(\pi_\alpha u, J_0 \pi_\alpha v), \quad \pi_\alpha(u) = u - \alpha(u)\partial_z \in \xi_{\text{std}}.$$

The metric yields a simple formula for the lengths of vectors in ξ_{std}:

$$Z = aX + bY \in \xi_{\text{std}} \implies |Z| = \sqrt{a^2 + b^2}. \tag{15}$$

4.2 Good position and Lagrangian resolution

Definition 4.2 We say that a Legendrian link $\Lambda \subset \mathbb{R}^3$ is in *good position* if it is chord generic and, for each double point $(x_0, y_0) \in \mathbb{R}^2$ of its Lagrangian projection $\pi_{xy}(\Lambda)$, there exists a neighborhood within which

(1) the over-crossing arc admits a parametrization satisfying

$$(x, y)(q) = (x_0 + q, y_0 - q),$$

and

(2) the under-crossing arc admits a parametrization satisfying

$$(x, y)(q) = (x_0 + q, y_0 + q).$$

Good position guarantees that the Gauss map of a parametrization of Λ evaluates to $\frac{3}{4}\pi$ or $\frac{7}{4}\pi$ near an over-crossing and to $\frac{1}{4}\pi$ or $\frac{5}{4}\pi$ near an under-crossing.[14] Likewise, the condition ensures that capping paths of composable pairs of chords satisfy

$$\theta_{j_1, j_2} \bmod 2\pi \in \left\{\tfrac{1}{2}\pi, \tfrac{3}{2}\pi\right\}.$$

[14] In [7], it is presumed that the tangent map of Reeb flow along a chord r sends $T_{r(0)}\Lambda \subset \xi$ to the subspace $J T_{r(a)}\Lambda$, which is achieved by an appropriate choice of almost-complex structure on the contact hyperplane of the manifold containing Λ. In our case, this is achieved by assuming that Λ is in good position. We will see in the proof of Theorem 7.1 that our analysis is contingent upon this assumption. Similarly precise perturbations of Legendrian submanifolds near endpoints of chords appear in [19] for the purpose of guaranteeing transversality of moduli spaces used to compute differentials for the contact homology of Legendrians in $(\mathbb{R}^{2n+1}, \xi_{\text{std}})$.

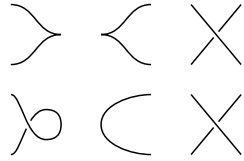

Figure 4: The first row of subfigures shows segments of a Legendrian link appearing in the front projection. Directly below each subfigure is how it appears in the Lagrangian resolution.

Proposition 4.3 *Provided a front projection of a Legendrian link Λ, we may perform a Legendrian isotopy so that the following properties are satisfied*:

(1) *Λ is in good position.*

(2) *The Lagrangian diagram is obtained by resolving singularities of the front as depicted in Figure 4.*

(3) *The arc length of each connected component of Λ with respect to $g_{\mathbb{R}^3}$ is 1.*

Proof The proof proceeds in three steps. The first step establishes the first two desired properties of Λ. This step is essentially the proof of Proposition 2.2 from [49] and so we will omit the details. The only modification required to ensure a link is in good position after Legendrian isotopy is to control $\partial z/\partial x$ of a parametrization of Λ near the right-pointing cusps and what are called "exceptional segments" in that proof. In particular, $\partial z/\partial x$ can be made quadratic with highest-order coefficient $\frac{1}{2}$ $\left(\text{resp. } -\frac{1}{2}\right)$ on neighborhoods of the positive (resp. negative) endpoints of chords.

In our second step, we modify Λ so that the arc length of each component is arbitrarily small while maintaining our desired conditions on the Lagrangian projection. For $\rho > 0$, consider the linear transformation ϕ_ρ of $\mathbb{R}^3$, defined by $\phi_\rho(x, y, z) = (\rho x, \rho y, \rho^2 z)$. Then $\phi_\rho^* \alpha_{\text{std}} = \rho^2 \alpha_{\text{std}}$, so that each ϕ_ρ is a contact transformation. The map ϕ_ρ also has the following useful properties:

(1) It preserves the angles of vectors in ξ_{std}.

(2) If Λ_i is a Legendrian curve with arc length ℓ, then $\phi_\rho(\Lambda_i)$ has arc length $\rho\ell$.

Take the family of Legendrians $\phi_{e^{-T}}(\Lambda)$ for $T \in [0, T_0]$ with T_0 large enough that each connected component of $\phi_{e^{-T_0}}(\Lambda)$ will have arc length ≤ 1. This interpolation between Λ and $\phi_{e^{-T_0}}(\Lambda)$ determines a 1–parameter family of Legendrian submanifolds and so may be realized by a Legendrian isotopy.

In the case that Λ connected, we choose T_0 so that the arc length is exactly equal to 1 after the isotopy and conclude the proof. When Λ is disconnected, a final, third step is

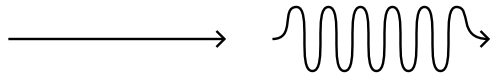

Figure 5: Locally modifying a Legendrian in the Lagrangian projection by a rapidly oscillating function $\tilde{y}$ to increase its arc length.

required. In this step we increase the arc lengths of the connected components of Λ so that they are all 1 while preserving good position and the smooth isotopy type of the Lagrangian projection.

We demonstrate how to increase arc lengths so as to achieve the desired result. Consider a segment of Λ_i along which the x–derivative is nonzero, parametrized via the x variable by $x \mapsto (x, y(x), z(x))$ with $x \in [-\delta, \delta]$ for an arbitrarily small positive constant δ. We assume that the Lagrangian projection of the segment does not touch any double points. Let $\tilde{y} \in \mathcal{C}^\infty([-\delta, \delta])$ be a function with compact support contained in $(-\delta, \delta)$ and for which $\int_{-\delta}^{\delta} \tilde{y}\, dx = 0$. Consider perturbations $\Lambda_{i,T}$ of Λ_i parametrized by $T \in [0, 1]$ which modify Λ_i along our segment to take the form

$$x \mapsto \left(x, y + T\tilde{y}, z + T\int_{-\delta}^{x} \tilde{y}\, dx\right).$$

The vanishing of the integral of $\tilde{y}$ ensures that the z–values at the endpoints of the segment are unaffected by the perturbation. By making $\sup \tilde{y}$ small and $\int |\partial\tilde{y}/\partial x|\, dx$ very large, we can ensure that, for $T \in [0, 1]$, our perturbations introduce no new double points in the Lagrangian projection and that $\Lambda_{i,T}$ has arc length as large as we like, say 2 when $T = 1$. See Figure 5. Hence, for some $T_0 \in [0, 1]$, the arc length of Λ_{i,T_0} will be exactly 1.

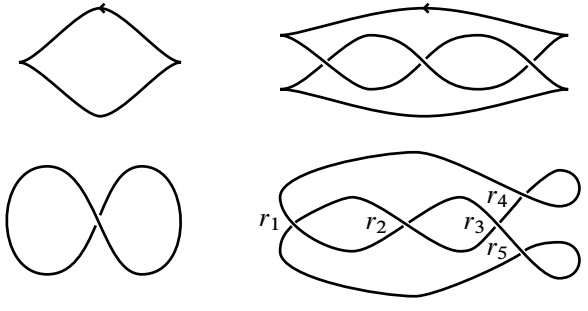

Figure 6: The left column shows Legendrian $\mathrm{tb} = -1$ unknot in the front and Lagrangian projections. A right-handed trefoil knot with $\mathrm{tb} = 1$ and $\mathrm{rot} = 0$ is shown in the front and Legendrian projections on the right. The Reeb chords of the Lagrangian projection of the trefoil are labeled r_i.

Apply such perturbations to each connected component of Λ so that no new double points are created and neighborhoods of double points are unaffected. Each perturbation is realizable by a Legendrian isotopy. Thus, we have obtained a Legendrian isotopy of Λ having all of the desired properties. □

Provided Λ as a front projection diagram, we call the Lagrangian projection of (an isotopic copy of) Λ obtained as in the above proposition the *Lagrangian resolution* of the front diagram. Figure 6 displays Lagrangian resolutions of an unknot and a trefoil. Following [49], we say that a front projection of a Legendrian link Λ is *nice* if there exists some $x_0 \in \mathbb{R}$ for which all right-pointing cusps have x–value x_0. It's not difficult to see that any Λ can be isotoped to have a nice front projection.

4.3 Conventions for link diagrams

We will not concern ourselves with specific requirements of good position or arc length when drawing Legendrian links in the Lagrangian projection and consider such a diagram to be valid if it recovers the Lagrangian projection of a Legendrian link after an isotopy of the xy–plane. In particular, we will not take care to ensure that angles at crossings are precise or that the components of $\mathbb{R}^2 \setminus \pi_{xy}(\Lambda)$ satisfy the area requirements of [24, Section 2].

Throughout, Legendrian knots with surgery coefficient $+1$ will be colored blue and knots with surgery coefficient -1 will be colored red. If the coefficient of a knot is not already determined or the knot corresponds to a component of Λ^0, it will be colored black.

4.4 Standard neighborhoods

Before stating the properties we will want our neighborhoods of Λ to have, we will create model neighborhoods near under- and over-crossings of chords. The neighborhood construction is completed in Proposition 4.5.

4.4.1 Model neighborhoods near endpoints of chords Here we describe a construction of a neighborhood of Λ along the arcs described in Definition 4.2. We can reparametrize the arcs to have unit speed, so that they take the form

$$q \mapsto \left(x_0 + \tfrac{1}{\sqrt{2}}q,\, y_0 - \tfrac{1}{\sqrt{2}}q,\, z_0 + \tfrac{1}{\sqrt{2}}y_0 q - \tfrac{1}{4}q^2\right)$$

near an over-crossing and

$$q \mapsto \left(x_0 + \tfrac{1}{\sqrt{2}}q,\, y_0 + \tfrac{1}{\sqrt{2}}q,\, z_0 + \tfrac{1}{\sqrt{2}}y_0 q + \tfrac{1}{4}q^2\right)$$

along an under-crossing. For $\epsilon > 0$ sufficiently small, we extend these embeddings to embeddings of $I_\epsilon \times I_\epsilon \times I_{2\epsilon}$ into $\mathbb{R}^3$ using coordinates (z, p, q). Near an over-crossing, this embedding takes the form

$$\begin{aligned}(16)\quad &\Phi^+_{x_0,y_0,z_0}(z,p,q)\\ &= \big(x_0 - \tfrac{1}{\sqrt{2}}p + \tfrac{1}{\sqrt{2}}q,\, y_0 - \tfrac{1}{\sqrt{2}}p - \tfrac{1}{\sqrt{2}}q,\, z_0 + z + y_0\tfrac{1}{\sqrt{2}}q - p + \tfrac{1}{4}p^2 + \tfrac{1}{2}pq - \tfrac{1}{4}q^2\big).\end{aligned}$$

Near an under-crossing arc, this takes the form

$$\begin{aligned}(17)\quad &\Phi^-_{x_0,y_0,z_0}(z,p,q)\\ &= \big(x_0 + \tfrac{1}{\sqrt{2}}p + \tfrac{1}{\sqrt{2}}q,\, y_0 - \tfrac{1}{\sqrt{2}}p + \tfrac{1}{\sqrt{2}}q,\, z_0 + z + y_0\tfrac{1}{\sqrt{2}}p + q - \tfrac{1}{4}p^2 + \tfrac{1}{2}pq + \tfrac{1}{4}q^2\big).\end{aligned}$$

Properties 4.4 *The following properties are satisfied by the* $\Phi^\pm_{x_0,y_0,z_0}$:

(1) $\Phi^\pm_{x_0,y_0,z_0}(0,0,q)$ *provides a parametrization of* Λ *with unit speed.*

(2) $(\Phi^\pm_{x_0,y_0,z_0})^*\alpha_{\text{std}} = dz + p\,dq$.

(3) *With respect to the basis* $P = \partial_p$ *and* $Q = \partial_q - p\partial_z$, *we have* $J_0 = \left(\begin{smallmatrix} 0 & -1 \\ 1 & 0 \end{smallmatrix}\right)$.

(4) $\pi_{xy} \circ \Phi^\pm_{x_0,y_0,z_0}$ *is an affine map.*

(5) *The images of* $\pi_{xy} \circ \Phi^\pm_{x_0,y_0,z_0}$ *overlap in squares of the form* $I_\epsilon \times I_\epsilon$ *near a crossing* (see Figure 9).

4.4.2 Neighborhood construction We now assume that Λ satisfies the conclusions of Proposition 4.3.

Proposition 4.5 *For* ϵ_0 *sufficiently small, there exists a neighborhood* $N_{\epsilon_0,i}$ *of each* Λ_i *parametrized by an embedding*

$$\Phi_i : I_{\epsilon_0} \times I_{\epsilon_0} \times S^1 \to \mathbb{R}^3$$

with coordinates (z, p, q) *such that the following conditions are satisfied*:

(1) $\Phi_i^*\alpha_{\text{std}} = dz + p\,dq$.

(2) *The* $N_{\epsilon_0,i}$ *are disjoint.*

(3) $\Phi_i(0,0,q)$ *provides a unit-speed parametrization of* Λ_i.

(4) J_0 *is* z*–invariant in* $N_{\epsilon_0,i}$ *and, with respect to the basis* $P = \partial_p$ *and* $Q = \partial_q - p\partial_z$, *it satisfies*

$$\Phi_i^* J_0 = \begin{pmatrix} 0 & -1 \\ 1 & 0 \end{pmatrix} + \mathcal{O}(p).$$

(5) *Near the endpoints* $(x_j, y_j, z_j^{\pm})$ *with* $z_j^+ > z_j^-$ *of each chord* r_j *of touching* Λ, *we can find a matrix of the form* $M = \mathrm{Diag}(1,1,1)$ *or* $\mathrm{Diag}(1,-1,-1)$ *such that*

$$\Phi_i(z,p,q) = \Phi^{\pm}_{x_j,y_j,z_j^{\pm}} \circ M(z,p,q-q_j^{\pm}),$$

where the $\Phi_{x_j,y_j,z_j^{\pm}}$ *are as in Properties 4.4.*

Proof Presuming that Λ_i is parametrized with a variable q with respect to which it has unit speed, we pick an arbitrarily small positive constant ϵ_1 and define a map $I_{\epsilon_1} \times S^1 \to \mathbb{R}^3$ as

$$\phi_1 \colon (p,q) \mapsto \exp_{\Lambda_i(q)}\left(-pJ_0\frac{\partial \Lambda_i}{\partial q}(q) + h_1(p,q)\right),$$

where $h_1 \in C^\infty(I_{\epsilon_1} \times S^1, \mathbb{R}^3)$ vanishes up to second order in p and is chosen so that it produces the map

$$(p,q) \mapsto \Phi^{\pm}_{x_j,y_j,z_j^{\pm}} \circ M(0,p,q-q_j^{\pm})$$

near the endpoints of the chords of Λ as in the statement of the proposition. Here exp is the exponential map with respect to the metric $g_{\mathbb{R}^3}$ and the matrix M is as in the statement of the proposition.

Since the tangent map of the exponential map is the identity along the zero section,

$$T\exp_{\Lambda_i(q)} = \mathrm{Id} \colon T_{\Lambda_i(q)}\mathbb{R}^3 \to T_{\Lambda_i(q)}\mathbb{R}^3$$

and h_1 is $\mathcal{O}(p^2)$, we have

$$\left.\frac{\partial \phi_1}{\partial p}\right|_{p=0} = -J_0\frac{\partial \Lambda_i}{\partial q} + \left.\frac{\partial h_1}{\partial p}\right|_{p=0} = -J_0\frac{\partial \Lambda_i}{\partial q} = -J_0 e^{J_0 G_i} X = -e^{J_0 G_i(q)} Y,$$

$$\left.\frac{\partial \phi_1}{\partial q}\right|_{p=0} = \frac{\partial}{\partial q}\exp_{\Lambda_i(q)}(0) = \frac{\partial \Lambda_i}{\partial q} = e^{J_0 G_i} X.$$

Therefore, the tangent map for ϕ_1 can be expressed along $\{p=0\}$ as a matrix

$$T\phi_1|_{p=0} = -J_0 e^{J_0 G_i(q)} \tag{18}$$

with incoming basis (P, Q) and outgoing basis (X, Y). This map will be an embedding when restricted to some $I_{\epsilon_1} \times S^1$ for ϵ_1 sufficiently small.

From (18), we compute $\phi_1^* \, d\alpha_{\mathrm{std}} = dp \wedge dq$ along $\{p=0\}$. More generally, we can write $\phi_1^* \, d\alpha_{\mathrm{std}} = F \, dp \wedge dq$ for some smooth function F satisfying $F|_{\{p=0\}} = 1$. Hence, F will be strictly positive on some tubular neighborhood of $\{p=0\} \subset I_{\epsilon_1} \times S^1$, so that $\phi_1^* \, d\alpha_{\mathrm{std}}$ will be symplectic on some $I_{\epsilon_2} \times S^1$ for ϵ_2 sufficiently small.

Applying a fiberwise Taylor expansion to $\phi_1^*\alpha_{\text{std}}$ along the annulus $I_{\epsilon_2}\times S^1$, we write

$$\phi_1^*\alpha_{\text{std}} = (f_0 + pf_1 + p^2 f_2 + f_{\text{hot}})\,dp + (g_0 + pg_1 + p^2 g_2 + g_{\text{hot}})\,dq,$$

where

(1) f_{hot} and g_{hot} are functions of p and q which are $\mathcal{O}(p^3)$, and

(2) $f_0,\dots,g_2$ are functions of q.

As Λ_i is Legendrian and J_0 preserves the contact structure, we must have $f_0 = g_0 = 0$. Then, computing

$$\phi_1^*\,d\alpha_{\text{std}} = d\phi_1^*\alpha_{\text{std}} = \left(g_1 + p\left(2g_2 - \frac{\partial f_1}{\partial q}\right) - p^2\frac{\partial f_2}{\partial q} + \frac{\partial g_{\text{hot}}}{\partial p} - \frac{\partial f_{\text{hot}}}{\partial q}\right) dp\wedge dp,$$

we must have $g_1 = 1$, so that

$$\phi_1^*\alpha_{\text{std}} = (pf_1 + p^2 f_2 + f_{\text{hot}})\,dp + (p + p^2 g_2 + g_{\text{hot}})\,dq.$$

We can eliminate the f_1 term in this equation with a perturbation in the z direction. With $h_2 = \frac{1}{2}p^2 f_1$, we have $dh_2 = pf_1\,dp + \frac{1}{2}p^2\partial f_1/\partial q\,dq$. Hence,

$$\phi_2(p,q) = \phi_1(p,q) - (0,0,h_2(p,q)),$$

admits an expansion of the form

$$\phi_2^*\alpha_{\text{std}} = (p^2 f_2 + f_{\text{hot}})\,dp + (p + p^2 g_2 + g_{\text{hot}})\,dq.$$

To ensure that this map is an embedding, we restrict its domain to $I_{\epsilon_3}\times S^1$ for some sufficiently small $\epsilon_3 \le \epsilon_2$. We note that the f_2 and g_2 here may differ from those in the Taylor expansion of $\phi_1^*\alpha_{\text{std}}$.

Now we'll apply a Moser argument as in [46, Section 3.2] to modify ϕ_2 by precomposing it with an isotopy to produce a map ϕ_3 so that $\phi_3^*\,d\alpha_{\text{std}} = dp\wedge dq$. Due to the facts that the annulus is not closed and that we'll require the result to be an codimension 1 embedding, we cannot simply quote [46, Section 3.2].

Writing $\phi_2^*\alpha_{\text{std}} = p\,dq + \sigma$ and, solving for a vector field X_σ satisfying

$$dp\wedge dq(*, X_\sigma) = \sigma,$$

we see that σ and X_σ have coefficient functions, vanishing up to second order,

$$\sigma = \mathcal{O}(p^2)\,dp + \mathcal{O}(p^2)\,dq, \quad X_\sigma = \mathcal{O}(p^2)\partial_p + \mathcal{O}(p^2)\partial_q.$$

Writing $\text{Flow}^t_{X_\sigma}$ for the time t flow of X_σ, choose $\epsilon_4 \le \epsilon_3$ so that $\text{Flow}^t_{X_\sigma}(I_{\epsilon_4}\times S^1) \subset I_{\epsilon_3}\times S^1$ for all $t\in[0,1]$ and define

$$\phi_3(p,q) = \phi_2 \circ \text{Flow}^1_{X_\sigma}(p,q)\colon I_{\epsilon_4}\times S^1 \to \mathbb{R}^3.$$

The Moser argument shows that $\phi_3^* d\alpha_{\text{std}} = dp \wedge dq$, as desired. Moreover our conditions on X_σ imply that $\text{Flow}^1_{X_\sigma}$ must agree with the identity mapping up to third order along $\{p = 0\}$. Hence, we can continue to write $\phi_3^*\alpha_{\text{std}} = p\,dq + \sigma$ for some σ which vanishes up to second order in p. Using $\phi_3^* d\alpha_{\text{std}} = dp \wedge dq$, we know that σ is closed, and, since it mush vanish along $\{p = 0\}$, we conclude that it is exact. Hence, $\phi_3^*\alpha_{\text{std}} = p\,dq + dh_4$ for some $h_4 \in C^\infty(I_{\epsilon_3} \times S^1, \mathbb{R})$. Possibly restricting to some $I_{\epsilon_4} \times S^1$, we define

$$\phi_4(p, q) = \phi_3(p, q) - (0, 0, h_4),$$

so that ϕ_4 is an embedding, whence $\phi_4^*\alpha_{\text{std}} = p\,dq$. Now define

$$\Phi_i(z, p, q) = \phi_4(p, q) + (0, 0, z).$$

Restricting to some $I_{\epsilon_0} \times I_{\epsilon_0} \times S^1$ for ϵ_0 sufficiently small, we can ensure that $\bigsqcup \Phi_i$ is an embedding. By construction of the Φ_i, we have

$$\Phi_i^*\alpha_{\text{std}} = dz + p\,dq.$$

Regarding the formula for J_0 in the basis (P, Q), note that this is satisfied for the map ϕ_1 and that subsequent perturbations — ϕ_2, ϕ_3 and ϕ_4 — preserve (P, Q) up to second order in p. The z–invariance of J_0 is clear from the definition of the Φ_i and z–invariance of the almost-complex structure on ξ_{std}.

For the last condition stated in the proposition, we note that ϕ_1 produces the desired result by definition of the function h_1. As all other required conditions are satisfied by ϕ_1, where the last condition is required to be satisfied as per Properties 4.4. The perturbations of ϕ_1 carried out in the remainder of the proof are trivial where this condition is required to be satisfied. Indeed, near the endpoints of chords h_2 (used to define ϕ_2), σ (used to define ϕ_3) and h_4 (used to define ϕ_4) all vanish. □

Assumptions 4.6 We assume throughout the remainder of this article that the Legendrian link Λ is in good position and has unit arc length with respect to $g_{\mathbb{R}^3}$, and write

$$N_\epsilon = \bigcup_i N_{\epsilon,i}$$

for a neighborhood of Λ as described in the above proposition with $\epsilon \le \epsilon_0$. We call the set $\{z = 0\} \subset N_{\epsilon,i}$ the *ribbon* of Λ_i. From the above proof, we may assume that the image of the projection of the ribbon of Λ_i to the xy–plane coincides with the image of the projection of $N_{\epsilon,i}$.

4.5 Transverse push-offs

The boundary of the ribbon of a component Λ_i of Λ consists of two knots

$$T^+_{i,\epsilon} = \{z = 0, p = \epsilon\} \quad T^-_{i,\epsilon} = \{z = 0, p = -\epsilon\}. \tag{19}$$

Definition 4.7 With ϵ fixed, the knots $T^+_{i,\epsilon}$ and $T^-_{i,\epsilon}$ will be called the *positive and negative transverse push-offs* of Λ_i. We orient both of these knots so that $\partial_q > 0$ in the coordinate system on $N_{\epsilon,i}$.

The positive (negative) transverse push-off is positively (negatively) transverse to ξ_Λ. Because these knots live on the boundary of $N_{\epsilon,i}$, we may consider them as living within either $(\mathbb{R}^3_{\Lambda^\pm}, \xi_{\Lambda^\pm})$ or $(\mathbb{R}^3, \xi_{\text{std}})$.

4.6 Model Dehn twists

In this and the following subsection we describe contact forms on $\mathbb{R}^3_{\Lambda^\pm}$ which will facilitate analysis on Reeb orbits after contact ± 1 surgery. We begin by providing an explicit model for a Dehn twist and then describe the gluing map used to define contact ± 1 surgery explicitly.

Provided a smooth function $f : \mathbb{R} \to S^1$, we define $\tau_f \in \text{Diff}^+(\mathbb{R} \times S^1)$ by

$$\tau_f(p, q) = (p, q + f(p))$$

and note that $\tau_{-f} = \tau_f^{-1}$. We'll call the map τ_f a *positive* (*resp. negative*) *Dehn twist by* f if:

(1) The derivative of f has compact support in $\mathbb{R}$.

(2) $\int_{\mathbb{R}} \partial f/\partial p \, dp = -1$ (resp. $+1$).

A positive (resp. negative) Dehn twist by f is a positive (resp. negative) Dehn twist in the usual sense of the expression. We compute

$$\tau_f^* p \, dq = p \, dq + p \frac{\partial f}{\partial p} \, dp, \quad \tau_f^*(dp \wedge dq) = dp \wedge dq, \tag{20}$$

so that τ_f is always a symplectomorphism with respect to $dp \wedge dq$ but does not preserve $p \, dq$ unless f is constant. For any f and $\epsilon > 0$, we write

$$f_\epsilon(p) = f\left(\frac{p}{\epsilon}\right).$$

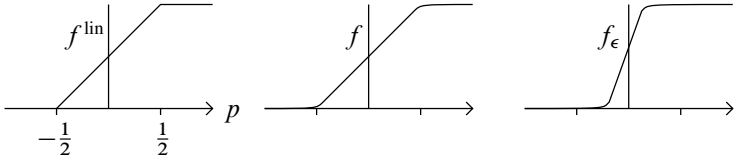

Figure 7: The functions f^{lin}, f and f_ϵ.

Assumptions 4.8 Throughout the remainder of this paper, f will denote a function for which τ_f is a negative Dehn twist whose derivative $\partial f/\partial p$ is

(1) nonnegative,

(2) an even function of p,

(3) supported on $I_1 = [-1, 1]$, and

(4) bounded in absolute value pointwise by 1.

We think of f as being a smooth approximation to a piecewise-linear function

$$f^{\mathrm{lin}}(p) = \begin{cases} 0 & \text{if } p \in \left(-\infty, -\frac{1}{2}\right], \\ p + \frac{1}{2} & \text{if } p \in I_{1/2}, \\ 1 & \text{if } p \in \left[\frac{1}{2}, \infty\right). \end{cases} \tag{21}$$

See Figure 7.

The following proposition gathers some properties of the deviation of twists by f_ϵ from preserving $p\,dq$, as described in (20):

Proposition 4.9 *Suppose that f satisfies Assumptions 4.8 and, for $\epsilon \in (0, 1)$, define*

$$H_\epsilon(p) = \int_{-\infty}^{p} P \frac{\partial f_\epsilon}{\partial p}(P)\, dP.$$

Then H is well defined, zero on the complement of I_ϵ, symmetric and satisfies $-\epsilon \le H_\epsilon \le 0$ pointwise.

Proof The first two statements are clear from the compact support and symmetry of the derivative of f. Then, using the fact that $\partial f_\epsilon/\partial p$ is supported on I_ϵ, we have

$$|H_\epsilon(p)| = \frac{1}{\epsilon}\left|\int_{-\epsilon}^{p} P \frac{\partial f}{\partial p}\left(\frac{P}{\epsilon}\right) dP\right| \le \frac{1}{\epsilon} \sup_p \left|\frac{\partial f}{\partial p}\right| \int_{-\epsilon}^{\epsilon} |P|\, dP = \epsilon \sup_p \left|\frac{\partial f}{\partial p}\right| \le \epsilon.$$

For $p \le 0$, $H_\epsilon(p)$ is an integral of a nonpositive function and so must be nonpositive. Then, for $p \ge 0$,

$$H_\epsilon(p) = H_\epsilon(0) + \int_0^p P \frac{\partial f_\epsilon}{\partial p}(P)\, dP = H_\epsilon(0) - \int_{-p}^0 P \frac{\partial f_\epsilon}{\partial p}(P)\, dP = H_\epsilon(-p)$$

by the symmetry of the derivative of f. □

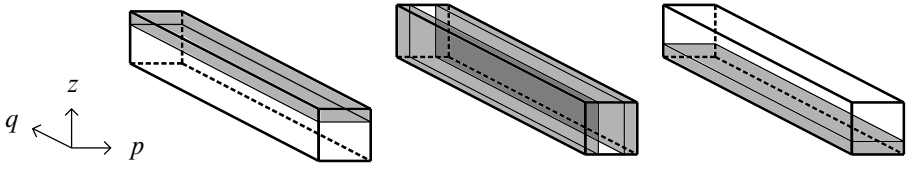

Figure 8: From left to right: the top, side and bottom pieces of our neighborhood are shaded.

4.7 Gluing maps

Now we define the gluing maps to define contact surgery on Λ and contact forms α_ϵ on the surgered manifold $\mathbb{R}^3_{\Lambda\pm}$.

Let ϵ_0 be a sufficiently small as described in Proposition 4.5 and choose $\epsilon \in (0, \epsilon_0)$. We decompose a neighborhood of each $\partial N_{\epsilon,i}$ into top, side and bottom pieces as shown in Figure 8:

(1) $T_{\delta,\epsilon} = \{z \geq \epsilon - \delta\}$.

(2) $S_{\delta,\epsilon} = \{|p| \geq \epsilon - \delta\}$.

(3) $B_{\delta,\epsilon} = \{z \leq -\epsilon + \delta\}$.

To perform contact surgery along Λ_i with surgery coefficient c_i, we define a map $\phi_{c_i,f,\epsilon,\delta}$ in coordinates (z, p, q) by

$$\phi_{c,f,\epsilon,\delta}(z,p,q) \sim \begin{cases} (z - c_i H_\epsilon(p), p, q + c f_\epsilon(p)) & \text{along } T_{\delta,\epsilon}, \\ (z,p,q) & \text{along } S_{\delta,\epsilon} \cup B_{\delta,\epsilon}, \end{cases} \tag{22}$$

where H_ϵ is as described in Proposition 4.9. Due to the properties of f_ϵ and H_ϵ described in the previous section, we have that $\phi_{c,f,\epsilon,\delta}$ agrees on the overlaps of the top, bottom and sides of $N_{\epsilon,i}$ for δ sufficiently small. Therefore, the map determines a smooth gluing.

The tangent map of the gluing map is given by

$$T\phi_{c_i,f,\epsilon,\delta} = \partial_z \otimes \left(dz - c_i\, p \frac{\partial f_\epsilon}{\partial p}\, dp \right) + \partial_p \otimes dp + \partial_q \otimes \left(dq + c_i \frac{\partial f_\epsilon}{\partial p}\, dp \right) \tag{23}$$

along $T_{\delta,\epsilon}$ and $T\phi_{c_i,f,\epsilon,\delta} = \mathrm{Id}$ along $S_{\delta,\epsilon} \cup B_{\delta,\epsilon}$, so that

$$\phi^*_{c_i,f,\epsilon,\delta}(dz + p\, dq) = dz + p\, dq.$$

The gluing map therefore determines a contact form $\alpha_{c_i,f,\epsilon,\delta}$ on the manifold $\mathbb{R}^3_{\Lambda_i}$ obtained by performing the surgery and hence a contact structure $\xi_{\Lambda\pm} = \ker(\alpha_{c_i,f,\epsilon,\delta})$

on this manifold. Shrinking δ amounts to a restriction of the domain of the map and so does not affect the associated contact manifold.

Definition 4.10 For $\epsilon \in (0, \epsilon_0)$, we write α_ϵ for the contact form on $\mathbb{R}^3_{\Lambda^\pm}$ determined by performing surgery using the gluings $\phi_{c_i, f, \epsilon, \delta}$ as described in (22) to each connected component $N_{\epsilon,i}$ of N_ϵ. The Reeb vector field of α_ϵ will be denoted by R_ϵ.

5 Chord-to-orbit and chord-to-chord correspondences

In this section we study the dynamics of the Reeb vector fields R_ϵ for the contact forms α_ϵ for $(\mathbb{R}^3_{\Lambda^\pm}, \xi_{\Lambda^\pm})$ as described in Definition 4.10. Our results are summarized by the following:

Theorem 5.1 *There exist one-to-one correspondences between*:

(1) *Closed orbits of R_ϵ in $(\mathbb{R}^3_{\Lambda^\pm}, \xi_{\Lambda^\pm})$ and cyclic words of chords on $\Lambda^\pm \subset (\mathbb{R}^3, \xi_{\text{std}})$.*

(2) *Chords of R_ϵ with boundary on $\Lambda^0 \subset (\mathbb{R}^3_{\Lambda^\pm}, \xi_{\Lambda^\pm})$ and words of chords with boundary on $\Lambda^0 \subset (\mathbb{R}^3, \xi_{\text{std}})$.*

A description of the correspondences will be given below.

Definition 5.2 Via the above theorem, we use the notation

$$(r_{j_1} \cdots r_{j_n})$$

to denote either a closed orbit of R_ϵ or a chord of $\Lambda^0 \subset (\mathbb{R}^3_{\Lambda^\pm}, \xi_{\Lambda^\pm})$ whose underlying word is $r_{j_1} \cdots r_{j_n}$.

After establishing Theorem 5.1, we estimate the actions of chords and closed orbits in $(\mathbb{R}^3_{\Lambda^\pm}, \xi_{\Lambda^\pm})$ in Section 5.5. Then, in Section 5.6, we describe equations whose solutions determine the embeddings of closed Reeb orbits and allow exact calculation of their actions. While we do not provide a closed form solutions to these equations, their analysis provides the following:

Theorem 5.3 *For each $n > 0$, there exists ϵ_n such that, for all $\epsilon \le \epsilon_n$, all orbits γ of word length $\le n$ are hyperbolic with*

$$\mathrm{CZ}_2(\gamma) = \sum_{k=1}^{n} (\mathrm{rot}_{j_k, j_{k+1}} + \delta_{1, c^+_{j_k}}) \in \mathbb{Z}/2\mathbb{Z}.$$

Moreover, if either $\Lambda^+ = \varnothing$ or $\Lambda^- = \varnothing$, then all closed orbits of R_ϵ are hyperbolic for all $\epsilon < \min\{\frac{1}{2}, \epsilon_0\}$.

Throughout this section, γ will denote a closed orbit of R_ϵ and κ will denote a chord of $\Lambda^0 \subset (\mathbb{R}^3_{\Lambda^\pm}, \xi_{\Lambda^\pm})$.

5.1 Overlapping rectangles

In order to state our chord-to-orbit and chord-to-chord correspondences, we need to introduce the objects which will define them: embedded squares in $(\mathbb{R}^3_{\Lambda^\pm}, \xi_{\Lambda^\pm})$ which record the positions of Reeb orbits as they propagate through the manifold. Along the way, we slightly refine the specifications of the function f in our surgery construction so as to reduce our analysis of dynamics of R_ϵ to analysis of affine linear transformations.

With ϵ — the constant which governs the size of N_ϵ — sufficiently small, the projection of N_ϵ to the xy–plane will have overlaps only at rectangles centered about double points of the Lagrangian projection of Λ. There is a unique rectangle $\mathcal{D}_j \subset \mathbb{R}^2$ for each chord r_j. As per Assumptions 4.6 and Properties 4.4, each $\mathcal{D}_j$ is the image of a map of the form

$$(p, q) \mapsto (x_0 + p - q, y_0 + p + q)$$

for $(p, q) \in I_{\epsilon_1} \times I_{\epsilon_2}$ for some $\epsilon_i \in (0, \infty)$ with $(x_0, y_0) \in \mathbb{R}^2$ being the coordinates of the double point of Λ in the xy–plane corresponding to r_j.

We write $\mathcal{D}_j^{\text{ex}}$ for the lift of this disk to the top of the N_{ϵ, l_j^-} and $\mathcal{D}_j^{\text{en}}$ for the lift to the bottom of N_{ϵ, l_j^+}. The superscripts are indicative of the fact that closed orbits of R_ϵ enter N_ϵ through the $\mathcal{D}_j^{\text{en}}$ and exit N_ϵ through the $\mathcal{D}_j^{\text{ex}}$. See Lemma 5.6.

Again using Assumptions 4.6 and Properties 4.4, we have that each $\mathcal{D}_j^{\text{en}}$ and $\mathcal{D}_j^{\text{ex}}$ can be described as

$$\{z = \pm\epsilon, q \in [q_j^\pm - \delta, q_j^\pm + \delta]\} \tag{24}$$

for some $\delta \in (0, \infty)$ with respect to the coordinates (z, p, q) provided by Proposition 4.5 on the "outside" of the surgery handle.

If we flow $\mathcal{D}_j^{\text{en}}$ through the surgery handle in which it is contained, we will see it pass through the top $\{z = \epsilon\}$ in a set $\mathcal{D}_j^\tau$, which, when projected onto the (p, q) coordinates, is of the form

$$\mathcal{D}_j^\tau = \tau_{f_\epsilon}^{c_j^+}(\{q \in [q_0 - \delta, q_0 + \delta]\})$$

for some $q_0 \in S^1$ and $\delta > 0$. This set will intersect the each $\mathcal{D}_{j'}^{\text{ex}}$ for $j' \neq j$ in a connected set diffeomorphic to a square. These intersections are depicted as the dark gray regions in Figure 9, right.

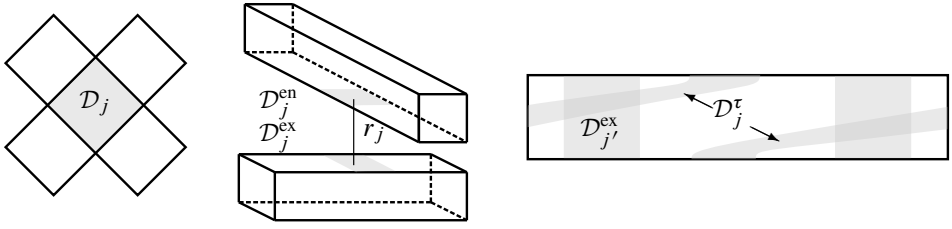

Figure 9: On the left, we see the xy–projection of the ribbon of Λ overlapping at a rectangle $\mathcal{D}_j$. In the middle — with a slightly offset point of view — we see the $\mathcal{D}_j^*$ touching the endpoints of a chord r_j. Here the boxes represent portions of N_ϵ. On the right, we see τ_{f_ϵ} applied to one rectangle intersecting other rectangles. In this portion of the diagram, ∂_p points upward and ∂_q points to the left.

Assumptions 5.4 For a fixed ϵ, we refine our choice of f in Assumptions 4.8 so that it is affine with derivative equal to 1 on some $I_{1-\delta} \subset I_1$, with δ chosen sufficiently small that each $\mathcal{D}_j^\tau \cap \mathcal{D}_{j'}^{\text{ex}}$ with $j \neq j'$ is determined by a pair of linear inequalities

$$\mathcal{D}_j^\tau \cap \mathcal{D}_{j'}^{\text{ex}} = \{q \in [q_0 - \delta_1, q_0 + \delta_1],\, a + bq \in [\delta_2, \delta_3]\}$$

for constants a, b, δ_1, δ_2 and δ_3.

Properties 5.5 *Under Assumptions 5.4, we have that, at any point $(p,q) \in \mathcal{D}_j^{\text{en}}$ for which $\tau_{f_\epsilon}(p,q) \in \mathcal{D}_{j'}^{\text{ex}}$,*

$$\frac{\partial f_\epsilon}{\partial p}(p) = \frac{1}{\epsilon}, \quad H_\epsilon(p) = H_\epsilon(0) + \frac{p^2}{2\epsilon},$$

where $i = l_j^+$. At such points we can write $\tau_{f_\epsilon}^{c_i}$ as

$$(p,q) \mapsto \left(p, q + \frac{1}{2} + \frac{c_i\, p}{\epsilon}\right).$$

5.2 Cyclic words from Reeb orbits

Here we prove the easy part of the of the (cyclic words) $\leftrightarrow$ (closed orbits) correspondence, showing that each γ uniquely determines a cyclic word of chords on $\Lambda^+ \cup \Lambda^-$.

Lemma 5.6 *Any closed orbit γ of R_ϵ must pass through N_ϵ. Every time γ enters N_ϵ, it must pass through some $\mathcal{D}_j^{\text{en}}$, and, every time it exits N_ϵ, it must pass through some $\mathcal{D}_j^{\text{ex}}$.*

Proof The Reeb vector field R_ϵ agrees with ∂_z on the complement of N_ϵ and flows $\mathcal{D}_j^{\text{ex}}$ into $\mathcal{D}_j^{\text{en}}$. The orbit γ must pass through N_ϵ as otherwise $z(\gamma)$ would take on

arbitrarily large values, implying that γ is not closed. If when passing through some component $N_{\epsilon,i}$ of the surgery handles γ exits the top of $N_{\epsilon,i}$ in the complement of the $\mathcal{D}_j^{\mathrm{ex}}$, then, again, $z(\gamma)$ would tend to ∞ as we follow the trajectory of the orbit. Likewise, if γ enters some $N_{\epsilon,i}$ in the complement of the $\mathcal{D}_j^{\mathrm{en}}$, then, following the orbit backwards in time, we see that $z(\gamma)$ is unbounded from below. □

Then γ must intersect some nonempty finite collection of the $\mathcal{D}_j^{\mathrm{ex}}$. Let $j_1, \dots, j_n$ be the indices of the $\mathcal{D}_j^{\mathrm{ex}}$ through which γ passes, ordered in accordance with a parametrization of γ.

Definition 5.7 We define the *cyclic word map* as

$$\mathrm{cw}(\gamma) = r_{j_1} \cdots r_{j_n}$$

and write $\mathrm{wl}(\gamma)$ for the word length of $\mathrm{cw}(\gamma)$.

5.3 Reeb orbits from cyclic words

In this section we describe how a cyclic word of composable Reeb chords uniquely determines an closed orbit of R_ϵ. Let $r_{j_1} \cdots r_{j_n}$ be a cyclic word and consider the squares $\mathcal{D}_{j_k}^*$, $* = \mathrm{en}, \mathrm{ex}, \tau$ as described in the previous subsection.

Theorem 5.8 *For $\epsilon \leq \epsilon_0$ and each word $w = r_{j_1} \cdots r_{j_n}$, there is a unique closed Reeb orbit γ_w of R_ϵ for which $\mathrm{cw}(\gamma_w) = w$.*

Our logic follows directly from arguments in [7, Section 6.1] — carried out in detail in [18] — which are simplified by our reduction of dynamics to that of affine transformations in Section 5.1.

Proof The proof follows from an analysis of $\mathrm{Flow}_{R_\epsilon}^t$ applied to the disk $\mathcal{D}_{j_1}^{\mathrm{ex}}$. Recall that this disk is contained in the "top" of a surgery handle $N_{\epsilon,l_{j_1}^-}$.

Write $S_1 = \mathcal{D}_{j_1}^{\mathrm{ex}}$ and let $G_1 = \mathrm{Id}_{S_1}$. Consider the following iterative process, for which Figure 10 serves as a visual aid:

(1) **Flow through the handle complement** There is a function $t(p,q)$ solving for the minimal $t > 0$ such that $\mathrm{Flow}_{R_\epsilon}^{t(p,q)}$ applied to $(p,q) \in S_1$ is an element of the square $\mathcal{D}_{j_1}^{\mathrm{en}}$ directly above S_1. Write $F_1^{\mathrm{co}}(p,q) = \mathrm{Flow}_{R_\epsilon}^{t(p,q)}(p,q)$, whose image is the square S_1', which is contained in the bottom of $N_{\epsilon,l_{j_1}^+}$. By the results of Section 5.1, $S_1' = \mathcal{D}_{j_1}^{\mathrm{en}}$. Briefly, F_1^{co} is the flow of our square $\mathcal{D}_{j_1}^{\mathrm{en}}$ through the handle complement.

(2) **Flow through the handle** Similarly define a function F_1^h which flows $S_1' \subset \{z = -\epsilon\} \subset N_{\epsilon,l_{j_1}^+}$ up to the top, $\{z = \epsilon\}$, of the surgery handle. The square $F^h(S_1')$

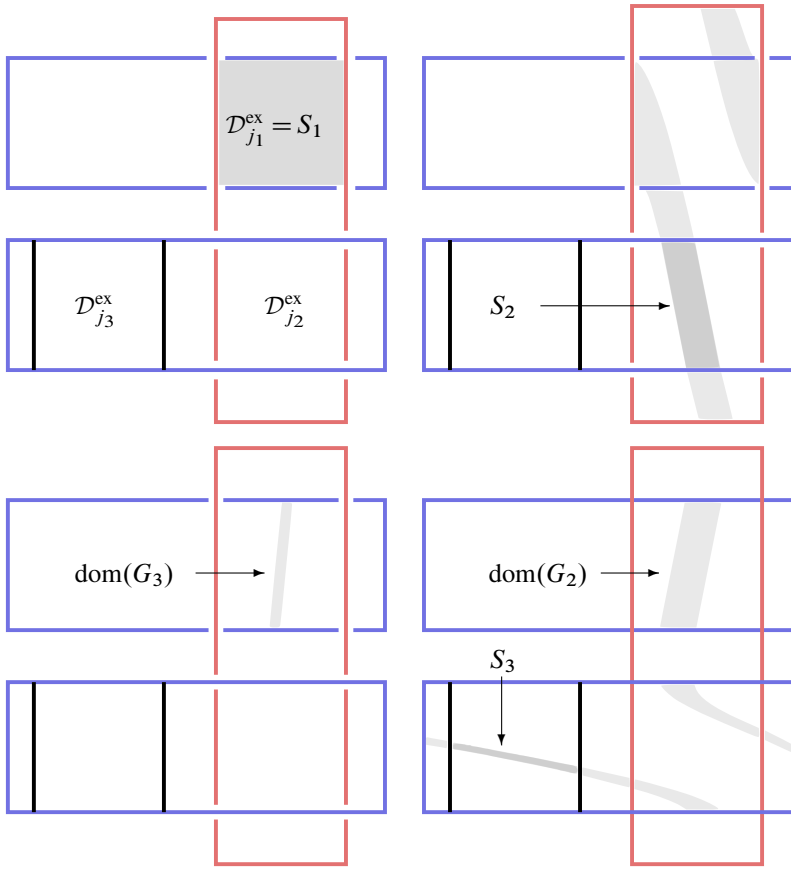

Figure 10: Following the subfigures clockwise we see the sets S_k and $\mathrm{dom}(G_k)$ drawn schematically. The S_k are shaded dark gray. Each rectangle represents the ribbon of some component of Λ cut at some value of q, layered over each other as indicated by the crossings so that the value of z increases as we traverse each subfigure clockwise. Within each rectangle, the sides of shorter (resp. longer) length are directed by p (resp. q). In the top-right we see $F_1^h \circ F_1^{\mathrm{co}}(S_1)$ as a subset of the top of $N_{\epsilon,l^+_{j_1}} = N_{\epsilon,l^-_{j_2}}$. Taking the intersection of this set with $\mathcal{D}^{\mathrm{ex}}_{j_2}$ determines S_2.

will appear in the coordinates (z, p, q) on the "outside" of the surgery handle as the application of a (positive or negative) Dehn twist to S_1'. That is, in the notation of Section 5.1, $F_1^h(S_1') = \mathcal{D}^{\tau}_{j_2}$ is the flow through the handle.

(3) **Trim** We write $S_2 = F_1^h(S_1') \cap \mathcal{D}^{\mathrm{ex}}_{j_2}$ for the intersection of $F_1^h(S_1')$ with the next square in the sequence $\mathcal{D}^{\mathrm{ex}}_{j_k}$ determined by w. Then S_2 is contained in the top of $N_{\epsilon,l^-_{j_2}}$.

We get a diffeomorphism G_2 from $\mathrm{dom}(G_2) = (F_1^h \circ F_1^{\mathrm{co}})^{-1}(S_2) \subset S_1$ to $\mathrm{im}(G_2) = S_2$ by $G_2 = F_1^h \circ F_1^{\mathrm{co}}$.

(4) **Repeat** We now inductively repeat the process by applying it to $S_k \subset \mathcal{D}^{\mathrm{ex}}_{j_k}$. We analogously define F_k^{co} and F_k^h with domain S_k then apply $F_k^h \circ F_k^{\mathrm{co}}$ to flow S_k up through the next handle in the sequence $N_{\epsilon,l^+_{j_k}}$ whose image we trim to define S_{k+1}. This determines a diffeomorphism

$$G_{k+1} = F_k^h \circ F_k^{\mathrm{co}} \circ \cdots \circ F_1^h \circ F_1^{\mathrm{co}} \colon (\mathrm{dom}(G_{k+1}) \subset S_1) \to (S_{k+1} \subset \mathcal{D}^{\mathrm{ex}}_{j_{k+1}}).$$

Making use of the results in Section 5.1, we have the following observations:

(1) Each F_k^{co} — considered with the domain $\mathcal{D}^{\mathrm{ex}}_{j_k}$ in which S_k is contained — is an affine transformation with respect to the (p,q) coordinates of the components of N_ϵ. Each F_k^{co} sends $\mathcal{D}^{\mathrm{ex}}_{j_k}$ diffeomorphically to $\mathcal{D}^{\mathrm{en}}_{j_k}$ and is a symplectomorphism with respect to $d\alpha_\epsilon$.

(2) Each F_k^h — considered with the domain $\mathcal{D}^{\mathrm{en}}_{j_k}$ — is nonlinear, as can by seen by looking at where p is extremal. It is also a symplectomorphism with respect to $d\alpha_{\mathrm{std}}$. The restriction of F_k^h to $(F_k^h)^{-1}(\mathcal{D}^{\mathrm{ex}}_j)$ for each j is an affine transformation by Properties 4.4.

(3) We see by induction that S_k is a connected, nonempty quadrilateral determined by a nondegenerate pair of linear inequalities, one of which is of the form $q \in [q_0 - \delta, q_0 + \delta]$.

(4) Combining the above with the fact that a composition of affine transformations is an affine transformation, $\mathrm{dom}(G_k)$ is a quadrilateral determined by a pair of linear inequalities, one of which is the trivial $p \in [-\epsilon, \epsilon]$.

(5) Each trimming step monotonically decreases the area with respect to $d\alpha_\epsilon$ and, for each k, we have $\mathrm{dom}(G_{k+1}) \subsetneq \mathrm{dom}(G_k)$:

$$0 < \int_{S_{k+1}} d\alpha_\epsilon < \int_{S_k} d\alpha_\epsilon, \quad 0 < \int_{\mathrm{dom}(G_{k+1})} d\alpha_\epsilon < \int_{\mathrm{dom}(G_k)} d\alpha_\epsilon.$$

Now observe that $\mathrm{dom}(G_n)$ stretches across $\mathcal{D}^{\mathrm{ex}}_{j_1}$ in the p direction and that S_n stretches across $\mathcal{D}^{\mathrm{ex}}_{j_1}$ in the q direction. Since both sets are convex, $U_1 = \mathrm{dom}(G_n) \cap S_n$ must be nonempty and convex. We likewise define U_k as the intersection of S_{nk} with $\mathrm{dom}(G_{nk})$ for all $k > 0$. See Figure 11.

The U_k satisfy $U_{k+1} \subsetneq U_k$ and we claim that $\mathrm{area}(U_k) \to 0$ as $k \to \infty$. To see this, recall that f_ϵ is linear on $p \in [-\epsilon(1-\delta), \epsilon(1-\delta)]$, where $\delta \in (0,1)$ is as described in Assumptions 5.4. By the conditions which characterize δ, for each $k \geq 0$ the set of points in S_k which reach S_{k+1} via the map $F_k^h \circ F_k^{\mathrm{co}}$ must be contained in the set

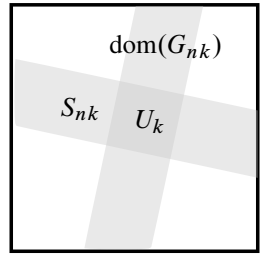

Figure 11: Overlaps of the sets S_{nk} and $\mathrm{dom}(G_{nk})$ within in the set $S_1 = \mathcal{D}^{\mathrm{ex}}_{j_1}$.

$S^{\mathrm{lin}}_k = \{p \in [-\epsilon(1-\delta), \epsilon(1-\delta)]\} \cap S_k$. By the fact that S^k is a rectangle stretching across the p coordinate of the annulus, $\mathrm{area}(S^{\mathrm{lin}}_k) = (1-\delta)\,\mathrm{area}(S_k)$. By the definition of S^{lin}_k and the fact that $F^h_k \circ F^{\mathrm{co}}_k$ is symplectic, $\mathrm{area}(S_{k+1}) \leq \mathrm{area}(S^{\mathrm{lin}}_k)$. Inductively, we conclude $\mathrm{area}(S_k) \leq (1-\delta)^{k-1}\,\mathrm{area}(S_1)$. Since U_k is contained in S_{nk}, our claim is established.

By our construction, any Reeb orbit with word w^k must intersect $\mathcal{D}^{\mathrm{ex}}_{j_1}$ at a point in $\mathrm{dom}(G_{nk})$ which is sent to itself via G_{nk}. Hence, such a point of intersection must lie in U_k. By considering multiple covers of the orbit γ_w — whose existence we seek to establish — we see that, if such a point of intersection lies in U_1, then it must lie in U_k for all $k > 0$. We therefore define

$$U_\infty = \bigcap_1^\infty U_k \subset \mathcal{D}^{\mathrm{ex}}_{j_1},$$

which, by our previous analysis, consists of a single point.

To complete our proof, it suffices to show that $G_{nk}(U_\infty) = U_\infty$ for all $k > 0$. This amounts to unwinding the definitions established in the proof so far. If we write $k = k_1 + k_2$ for any pair of natural numbers k_1 and k_2, then we must have

$$G_{nk_1}(\mathrm{dom}(G_{nk})) \subset \mathrm{dom}(G_{nk_2})$$

as otherwise $G_{nk_2} \circ G_{nk_1}(\mathrm{dom}(G_{nk}))$ would not be contained in $\mathcal{D}^{\mathrm{ex}}_{j_1}$. On the other hand, $\mathrm{dom}(G_{nk}) \subsetneq \mathrm{dom}(G_{nk_1})$ implies that

$$G_{nk_1}(\mathrm{dom}(G_{nk})) \subsetneq S_{nk_1}.$$

Combining the above two equations, we conclude that

$$U_\infty = \bigcap_1^\infty (S_{nk} \cap \mathrm{dom}(G_{nk})) = \left(\bigcap_1^\infty S_{nk}\right) \cap \left(\bigcap_1^\infty \mathrm{dom}(G_{nk})\right)$$

satisfies $G_{nk}(U_\infty) = U_\infty$. □

5.4 Reeb chords of Λ^0 after surgery

In this section, we describe open-string versions of our results for closed Reeb orbits, establishing the chord-to-chord correspondence of Theorem 5.10.

Definition 5.9 Suppose that a chord κ of $\Lambda^0 \subset (\mathbb{R}^3_{\Lambda^\pm}, \xi_{\Lambda^\pm})$ passes through a sequence of the $\mathcal{D}^*_j$ of the form

$$\mathcal{D}^{\text{en}}_{j_1}, \mathcal{D}^{\text{ex}}_{j_2}, \mathcal{D}^{\text{en}}_{j_2}, \dots, \mathcal{D}^{\text{ex}}_{j_{n-1}}, \mathcal{D}^{\text{en}}_{j_{n-1}}, \mathcal{D}^{\text{ex}}_{j_n}.$$

Then we write $\mathrm{w}(\kappa) = r_{j_1} \cdots r_{j_n}$. We call the association $\kappa \mapsto \mathrm{w}(\kappa)$ the *word map*.

Theorem 5.10 *For each $\epsilon < \epsilon_0$, the word map* w *determines a one-to-one correspondence between words of chords with boundary on $\Lambda^0 \subset (\mathbb{R}^3, \xi_{\text{std}})$ and Reeb chords of $\Lambda^0 \subset (\mathbb{R}^3_{\Lambda^\pm}, \xi_{\Lambda^\pm})$ determined by the contact form α_ϵ. For each such word w, the associated chord κ_w is nondegenerate for all $\epsilon < \epsilon_0$.*

The chords with word length 1 are those which exist for $\Lambda^0 \subset \mathbb{R}^3$ prior to surgery, while the rest of the chords in Theorem 5.10 are created after the performance of surgery along $\Lambda^\pm$.

Proof The proof is analogous to the proof of Theorem 5.8, although considerably simpler.

Let $w = r_{j_1} \cdots r_{j_n}$ be a word of chords on Λ^0 with word length $n > 1$. By (16), flowing Λ^0 up to N_ϵ along a chord sends Λ^0 to a strand in N_ϵ of the form $q = q_0$, which we call A_1'. Flow this arc up to the top of N_ϵ and take its intersection with $\mathcal{D}^{\text{ex}}_{j_2}$ to obtain an arc we'll call A_1. Define arcs A_k for $k > 1$ as follows:

(1) **Flow through the handle complement** Flow $A_{k-1} \subset \mathcal{D}^{\text{ex}}_{j_k}$ up to $\mathcal{D}^{\text{en}}_{j_k}$ using the map F^{co}_k as in the proof of Theorem 5.8.

(2) **Flow through the handle** Now we apply the map F^h_k as defined in Theorem 5.8 to flow $F^{\text{co}}_k(A_{k-1})$ up to the top of N_ϵ.

(3) **Trim** Define $A_k = F^h_k \circ F^{\text{co}}_k(A_{k-1}) \cap \mathcal{D}^{\text{ex}}_{j_k}$.

(4) **Repeat** Repeat the above steps until we obtain an arc $A_n \subset \mathcal{D}^{\text{ex}}_{j_n}$.

Again, following the logic of the proof of Theorem 5.8 using the linearity conditions of Section 5.1, each $A_k \subset \mathcal{D}^{\text{ex}}_{j_k}$ is a line segment which wraps across $\mathcal{D}^{\text{ex}}_{j_k}$ in the q direction. In other words, each admits a parametrization of the form

$$A_k = \{(aq + b, q) : q \in [q_0 - \delta, q_0 + \delta]\}$$

for some constants $a \neq 0, b, q_0, \delta$. Since flowing Λ^0 downward to $\mathcal{D}^{\mathrm{ex}}_{j_n}$ along the chord r_{j_n} is a set of the form $q = q_0$, the intersection of this set with A_k consists of a single point. Since A_k wraps across $\mathcal{D}^{\mathrm{ex}}_{j_n}$ in the q direction, this intersection is transverse. By construction, the collection of such intersections are in one-to-one correspondence with the collection of chords of $\Lambda^0 \subset (\mathbb{R}^3_{\Lambda^\pm}, \xi_{\Lambda^\pm})$.

For words of length 1, the restriction of R_ϵ to the complement of the surgery handles is ∂_z, so that words of length 1 correspond exactly to the chords of Λ^0 present prior to surgery. □

5.5 Action estimates

To obtain refined estimates of the actions of the chords and orbits of R_ϵ we'll need the following lemmas. The first lemma tells us how much time it takes to flow from the top of N_ϵ to the bottom in a neighborhood of a chord r_j.

Lemma 5.11 *Let r_j be some chord of $\Lambda \subset (\mathbb{R}^3, \xi_{\mathrm{std}})$ with action $\mathcal{A}(r_j)$ and parametrize the disk $\mathcal{D}^{\mathrm{ex}}_j \subset \partial N_\epsilon$ with coordinates (p, q) as in (17). Then, for each $(p, q) \in \mathcal{D}^{\mathrm{en}}_j$, there exists a minimal-length chord from $\mathcal{D}^{\mathrm{ex}}_j$ to $\mathcal{D}^{\mathrm{en}}_j$ starting at (P, Q) with action*

$$t = \mathcal{A}(r_j) - 2\epsilon - pq.$$

Proof This is a straightforward calculation, so we omit the details. For a given j, write $(p^{\mathrm{ex}}, q^{\mathrm{ex}})$ and $(p^{\mathrm{en}}, q^{\mathrm{en}})$ for the coordinates on $\mathcal{D}^{\mathrm{ex}}_j$ and $\mathcal{D}^{\mathrm{en}}_j$ provided by (17) and (16), respectively. Then $p^{\mathrm{en}} = -q^{\mathrm{ex}}$ and $q^{\mathrm{en}} = p^{\mathrm{ex}}$. Plug these into the equations provided to compute the differences in the z coordinates and consider the fact that $R_\epsilon = \partial_z$ on $\mathbb{R}^3 \setminus N_\epsilon$. □

Our second lemma tells how much time it takes for an orbit to flow through one of the surgery handles.

Lemma 5.12 *For some j, again consider coordinates (p, q) on $\mathcal{D}^{\mathrm{ex}}_j \subset \partial N_\epsilon$ as provided by (17). Then the time it takes a point in $\mathcal{D}^{\mathrm{en}}_j$ to reach this point via the flow of R_ϵ is*

$$t = 2\epsilon + c_i H_\epsilon(p).$$

This becomes obvious if we look at the graph of the "top" part of the gluing map of (22). See Figure 12. By comparing Proposition 4.9 with the definition of the gluing map in (22), actions increase slightly as we pass through a surgery handle with coefficient -1 and decrease slightly as we pass through a surgery handle with coefficient $+1$.

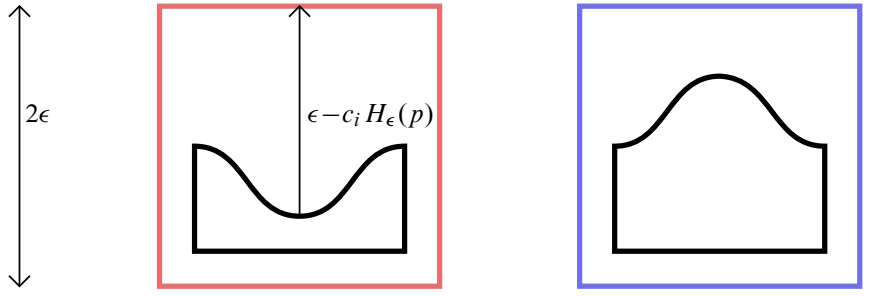

Figure 12: The squares represent $\{q = q_0\} \subset N_{\epsilon,i}$ slices of the N_ϵ at components $N_{\epsilon,i}$ with surgery coefficient $c_i = -1$ (left) and $c_i = 1$ (right). The black arcs represent the boundaries of the gluing region, as it intersects each slice.

Proposition 5.13 *For all closed Reeb orbits γ of R_ϵ, we have*

$$|\mathcal{A}(\gamma) - \mathcal{A}(\mathrm{cw}(\gamma))| < 3\epsilon\, \mathrm{wl}(\gamma).$$

For each chord r of R_ϵ with boundary on $\Lambda^0 \subset (\mathbb{R}^3_{\Lambda^\pm}, \xi_{\Lambda^\pm})$, we have

$$|\mathcal{A}(r) - \mathcal{A}(\mathrm{w}(\gamma))| < 3\epsilon\, \mathrm{wl}(r).$$

This is obvious from Lemmas 5.11 and 5.12 together with Proposition 4.9.

5.6 Calculating orbit embeddings

Let $\gamma = (r_{j_1} \cdots r_{j_n})$ be a closed orbit of some R_ϵ. Let (p_k, q_k) be coordinates on the squares $\mathcal{D}^{\mathrm{ex}}_{j_k}$ described by (16). Suppose that, in these coordinates, γ passes through the points (P_k, Q_k). If γ is simply covered and we compute the exact values of the (P_k, Q_k), then we can see the knot formed by γ inside of $\mathbb{R}^3_{\Lambda^\pm}$ and be able to compute the action $\mathcal{A}(\gamma)$ exactly. In this section, we describe how these (P_k, Q_k) can be calculated. The analysis here will be the starting point for the computation of Conley–Zehnder indices.

In the above notation, we can describe (P_1, Q_1) as a fixed point of an affine transformation

$$A + b\colon \mathbb{R}^2 \to \mathbb{R}^2, \quad A \in \mathrm{SL}(2, \mathbb{R}),\ b \in \mathbb{R}^2,$$

as follows.

Starting at (a subset of) $\mathcal{D}^{\mathrm{ex}}_{j_k}$, apply $\mathrm{Flow}_{R_\epsilon}$ to pass through the handle complement to $\mathcal{D}^{\mathrm{en}}_{j_k}$ and then through the surgery handle $N_{\epsilon,l^+_{j_k}}$ to $\mathcal{D}^{\mathrm{ex}}_{j_{k+1}}$. As we are only interested in the set of points in $\mathcal{D}^{\mathrm{ex}}_{j_k}$ along which the $\tau_{\pm f_\epsilon}$ are linear, we can write this as a map

$A_k + b_k$ with $A_k \in \mathrm{SL}(2,\mathbb{R})$. The $b_k \in \mathbb{R}^2$ term is required by (16) centering the q coordinate about the endpoint of the Reeb chord r_{k+1}.

Hence, we may write

$$\begin{aligned} A + b &= (A_n + b_n) \circ \cdots \circ (A_1 + b_1) \\ &= (A_n \cdots A_1) + (A_n \cdots A_2) b_1 + \cdots + A_n b_{n-1} + b_n \end{aligned} \tag{25}$$

with (P_1, Q_1) being the fixed point of this map. By linearity of the equations involved and our prior knowledge (Theorem 5.8) that there exists a unique fixed point, we may as well consider the $A_k + b_k$ to be transformations of $\mathbb{R}^2$. We can then solve for $u_1 = (P_1, Q_1)$ as

$$u_1 = (\mathrm{Id} - A)^{-1} b = (\mathrm{Id} - A_n \cdots A_1)^{-1} (A_n \cdots A_2 b_1 + \cdots + A_n b_{n-1} + b_n).$$

Provided u_1, we can then find the $u_k = (P_k, Q_k)$ by applying the $(A_k + b_k)$:

$$u_{k+1} = A_k u_k + b_k = (A_k + b_k) \cdots (A_1 + b_1) u_1.$$

Proposition 5.14 *In the above notation,*

$$\begin{aligned} (-1)^{\mathrm{rot}_{j_k, j_{k+1}}} A_k &= \begin{pmatrix} 0 & -1 \\ 1 & -c_{j_k}/\epsilon \end{pmatrix} = J_0 \begin{pmatrix} 1 & -c_{j_k}/\epsilon \\ 0 & 1 \end{pmatrix}, \\ (-1)^{\mathrm{rot}_{j_k, j_{k+1}}} b_k &= \begin{pmatrix} 0 \\ \frac{1}{2} - d_{j_k, j_{k+1}} \end{pmatrix} = J_0 \begin{pmatrix} \frac{1}{2} - d_{j_k, j_{k+1}} \\ 0 \end{pmatrix}, \end{aligned}$$

where $d_{j_k, j_{k+1}}$ is the minimal length of a capping path for the pair $(r_j, r_{j_{k+1}})$ projected to the xy–plane using the standard Euclidean metric on $\mathbb{R}^2$.

Proof We can determine $A_k + b_k$ as a composition of the following elementary mappings:

(1) The change of coordinates from $\mathcal{D}^{\mathrm{ex}}_{j_k}$ to $\mathcal{D}^{\mathrm{en}}_{j_k}$, which we see when flowing points (p, q) through the handle complement,

$$(p, q) \mapsto (-q, p).$$

(2) The flow from $\mathcal{D}^{\mathrm{en}}_{j_k}$ to the top of $N_{\epsilon, l^+_{j_k}}$, which, according to Properties 5.5, is given by

$$(p, q) \mapsto \left(p, q + \frac{1}{2} + \frac{c^+_{j_k}}{\epsilon} p \right).$$

(3) A shift in the q coordinate such that $(0, 0)$ is identified with the tail of $r_{j_{k+1}}$. Here $d^{\mathrm{in}}_{k,k+1}$ is the magnitude of this shift when Λ_{j_k} is parametrized with Φ_{i+},

as in Proposition 4.5,

$$(p,q)\mapsto(p,q-d^{\text{in}}_{k,k+1}).$$

(4) A mapping of the coordinates on the top of $N_{\epsilon,l^+_{j_k}}$ to $\mathcal{D}^{\text{ex}}_{k+1}$,

$$(p,q)\mapsto(-1)^{\text{rot}_{j_k,j_{k+1}}}(p,q).$$

The result of composing the above maps produces

$$(p,q)\mapsto(-1)^{\text{rot}_{j_k,j_{k+1}}}\left(-q,\,p+\frac{1}{2}-d^{\text{in}}_{k,k+1}-\frac{c^+_{j_k}}{\epsilon}q\right). \qquad \square$$

5.7 Hyperbolicity and the $\mathbb{Z}/2\mathbb{Z}$ index

For a given closed orbit $\gamma=(r_{j_1}\cdots r_{j_n})$, we can use the above formula to write its Poincaré return map as $\text{Ret}_\gamma=A_n\cdots A_1$, where the A_k are given by (25). By using the calculation of the A_k in Proposition 5.14, we have an explicit representation of Ret_γ as

$$\begin{aligned}(-1)^{\text{rot}}\,\text{Ret}_\gamma&=\prod_{K=1}^{n}J_0\begin{pmatrix}1&-c^+_{j_{n+1-K}}\epsilon^{-1}\\0&1\end{pmatrix}\\&=J_0\begin{pmatrix}1&-c^+_{j_n}\epsilon^{-1}\\0&1\end{pmatrix}\cdots J_0\begin{pmatrix}1&-c^+_{j_1}\epsilon^{-1}\\0&1\end{pmatrix}\\&=J_0^n+\sum_{K=1}^{n}\left(\sum_{k\in I_K}\left(\prod_{i=1}^{K}-c^+_{j_{k_i}}\right)M_k\right)\epsilon^{-K},\qquad(26)\\ \text{rot}&=\sum_{K=1}^{n}\text{rot}_{j_K,j_{K+1}},\\M_k&=J_0^{n-k_K}\,\text{Diag}(0,1)J_0^{k_K-k_{K-1}-1}\cdots J_0^{k_2-k_1-1}\,\text{Diag}(0,1)J_0^{k_1-1},\\I_K&=\{k=(k_1,\dots,k_K):1\le k_1<\cdots<k_K\le n\}.\end{aligned}$$

The equality in the third line involving the M_k easily follows from an induction on n.

Observe that I_n consists of a single element $(1,\dots,n)$, so that the $K=n$ term in the above formula is

$$\epsilon^{-n}\left(\prod_{k=1}^{n}-c^+_{j_k}\right)\text{Diag}(0,1)=\epsilon^{-n}(-1)^{\#(c^+_{j_k}=1)}\,\text{Diag}(0,1). \qquad (27)$$

Thus, for a fixed word, $\text{tr}(\text{Ret}_\gamma)$ can be expressed as a polynomial in ϵ^{-1} whose highest-order term is given by the above expression.

Proof of Theorem 5.3 For ϵ_w sufficiently small, the ϵ^{-n} term in the polynomials for $\mathrm{tr}(\mathrm{Ret}_\gamma)$ determines their sign for all $\epsilon < \epsilon_w$ and words of length $\leq n$ as there are only finitely many cyclic words less than a given length. Possibly making ϵ_w smaller, we can guarantee that the absolute values of the traces are bounded below by 2. To compute CZ_2, we apply (1) and (3), noting that $\det(\mathrm{Ret} - \mathrm{Id}) = 2 - \mathrm{tr}(\mathrm{Ret})$.

If one of Λ^+ or Λ^- is empty, then each orbit of word length n has return map

$$\mathrm{Ret}_\gamma = \pm M_a^n, \quad M_a = \begin{pmatrix} 0 & -1 \\ 1 & a \end{pmatrix}, \quad a = \pm\epsilon^{-1}.$$

If $\epsilon < \frac{1}{2}$, then M_a is hyperbolic and so is conjugate to $\mathrm{Diag}(\lambda, \lambda^{-1})$ with

$$\lambda = \tfrac{1}{2}(a + \sqrt{a^2 - 4}), \quad \lambda^{-1} = \tfrac{1}{2}(a - \sqrt{a^2 - 4}),$$

implying that Ret_γ is conjugate to $\pm\,\mathrm{Diag}(\lambda^n, \lambda^{-n})$. In this case, it's clear that $|\mathrm{tr}(\mathrm{Ret}_\gamma)| > 2$ independent of n, implying that all closed orbits of R_ϵ are hyperbolic for $\epsilon < \frac{1}{2}$. □

6 The semiglobal framing (X, Y)

Having computed the $\mathbb{Z}/2\mathbb{Z}$ Conley–Zehnder indices of the closed Reeb orbits of R_ϵ, we now seek to compute $\mathbb{Z}$–valued indices with respect to a framing as well as Maslov indices of broken closed strings on $\Lambda^0 \subset (\mathbb{R}^3_{\Lambda^\pm}, \xi_{\Lambda^\pm})$.

In this section we describe sections of $\xi_{\Lambda^\pm}$, which we will later use to compute these indices. This will allow us to draw a cycle representing $\mathrm{PD}(c_1(\xi_{\Lambda^\pm})) = \mathrm{PD}(e(\xi_{\Lambda^\pm}))$ as a link in the Lagrangian projection: See Figure 13 for an example. The results of this section are summarized as follows:

Theorem 6.1 *For each $\epsilon < \epsilon_0$ there are sections $X, Y \in \Gamma(\xi_\Lambda)$ such that the following conditions hold*:

(1) $(X, Y) = (\partial_x + y\partial_z, \partial_y)$ *on* $\mathbb{R}^3_{\Lambda^\pm} \setminus N_\epsilon \simeq \mathbb{R}^3 \setminus N_\epsilon$.

(2) (X, Y) *is a symplectic basis of* $(\xi_{\Lambda^\pm}, d\alpha_\epsilon)$ *at each point contained in a closed Reeb orbit of* R_ϵ.

(3) $X^{-1}(0) = Y^{-1}(0)$ *is a union of connected components of* $\bigcup_i T_i^{c_i}$, *where the* $T_i^\pm$ *are the transverse push-offs of the* Λ_i *as described in Definition 4.7.*

Using the (X, Y), the first Chern class of $\xi_{\Lambda^\pm}$ may be computed as

$$\mathrm{PD}(c_1(\xi_{\Lambda^\pm})) = \sum_{\Lambda_i \subset \Lambda^\pm} -c_i \,\mathrm{rot}(\Lambda_i)[T_i^{c_i}] = \sum_{\Lambda_i \subset \Lambda^\pm} \mathrm{rot}(\Lambda_i)\mu_i \in H_1(\mathbb{R}^3_{\Lambda^\pm}).$$

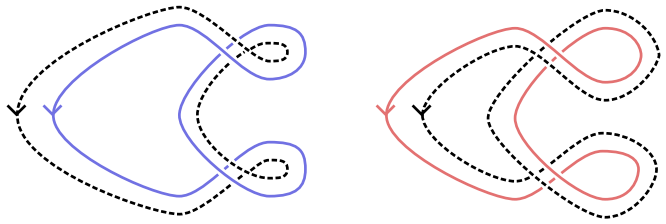

Figure 13: Here we consider contact ± 1 surgery on the Legendrian unknot with $\mathrm{rot}(\Lambda) = 1$. In each case, Theorem 6.1 provides a framing of ξ_Λ on the complement of a transverse push-off of Λ which travels along the right-hand side of Λ when the surgery coefficient is $+1$ and along the left side of Λ when the coefficient is -1. These push-offs are depicted as the dashed, black circles.

The classes μ_i are given by a standard presentation of $H_1(\mathbb{R}^3_{\Lambda^\pm})$ determined by the surgery diagram, which we will describe in Section 9.

Theorem 6.1 may be compared with [31, Proposition 2.3], where a similar result is stated for Chern classes integrated over 2–cycles in Stein surfaces, and with [27, Section 3], where Chern classes are computed when performing surgery along Legendrians lying in pages of open book decompositions.

For notational simplicity, we assume throughout this section that $\Lambda^\pm$ has a single connected component unless otherwise stated. Accordingly, we temporarily drop the indices i appearing in the notation of Section 3. The surgery coefficient of this knot will be denoted by c.

Our framing is constructed in three steps:

(1) We start with a framing of ξ_{std} over the complement of N_ϵ and express it in terms of our local coordinate system (z, p, q) along the boundary of our surgery handles.

(2) Next, we describe an explicit extension of this framing throughout most of the handle. We will need this explicit description to compute Conley–Zehnder and Maslov indices in Section 7.

(3) Finally, we describe the zero locus of this extension.

6.1 Change of bases between trivializations

Consider the following pairs of sections of ξ_{std} and $\xi_{\Lambda^\pm}$, which form symplectic bases:

$$\{X = \partial_x + y\partial_x,\ Y = \partial_y\},\quad \{P_{\text{in}} = \partial_p,\ Q_{\text{in}} = \partial_q - p\partial_z\},\quad \{P_{\text{out}} = \partial_p,\ Q_{\text{out}} = \partial_q - p\partial_z\}.$$

These come from

(1) the coordinate systems (x, y, z) on $\mathbb{R}^3$,

(2) the coordinates (z, p, q) on N_ϵ viewed "from the outside" of the surgery handle prior to surgery, and

(3) (z, p, q) on N_ϵ viewed "from the inside" of the surgery handle after surgery,

respectively. After performing surgery, the pairs (X, Y) and $(P_{\text{in}}, Q_{\text{in}})$ are well defined on the complement of a neighborhood of the form $N_{\epsilon'}$ for some $\epsilon' < \epsilon$. Our strategy will be to apply a series of change-of-basis transformations to extend the framing (X, Y) of $\xi_{\Lambda^\pm}$ throughout the surgery handle in so far as cohomological obstruction — $c_1(\xi_{\Lambda^\pm})$ — will allow.

First we describe change of bases from $(P_{\text{in}}, Q_{\text{in}})$ to $(P_{\text{out}}, Q_{\text{out}})$. Following (23), the restriction of the tangent map of the gluing map $\phi_{c,f,\epsilon,\delta}$ — defined in (22) — to $\xi_{\Lambda^\pm}$ can be written as

$$T\phi_{c,f,\epsilon,\delta}(z, p, q)|_\xi = \begin{pmatrix} 1 & 0 \\ c\,\partial f_\epsilon/\partial p(p) & 1 \end{pmatrix} \tag{28}$$

along $T_{\delta,\epsilon}$ and as $\mathrm{Diag}(1, 1)$ along $B_{\delta,\epsilon} \cup S_{\delta,\epsilon}$. Here the incoming basis is $(P_{\text{in}}, Q_{\text{in}})$, the outgoing basis is $(P_{\text{out}}, Q_{\text{out}})$, and coordinates (z, p, q) correspond to the coordinate system inside of the surgery handle.

Now we describe change of bases from $(P_{\text{out}}, Q_{\text{out}})$ to (X, Y). To this end, let G be the Gauss map for a parametrization of Λ as described in Section 4.4. Using the construction of N_ϵ in Proposition 4.5, we can write the change of basis at a point (p, q, z) as

$$E(p, q)e^{J_0(G(q)-\pi/2)}, \tag{29}$$

where $E = \mathrm{Diag}(1, 1) + \mathcal{O}(p)$. Here the incoming basis is $(P_{\text{out}}, Q_{\text{out}})$, the outcoming basis is (X, Y), and coordinates (z, p, q) correspond to the coordinate system on "the outside" — the complement of the surgery handle in N_ϵ.

By composing the changes of bases described above in (28) and (29) and then inverting, we can write (X, Y) in the basis $(P_{\text{in}}, Q_{\text{in}})$ on a neighborhood of ∂N_ϵ as follows: Along $B_{\delta,\epsilon} \cup S_{\delta,\epsilon}$ the change of basis is given by

$$e^{J_0(\pi/2-G(q))}E^{-1}(p, q). \tag{30}$$

Along $T_{\delta,\epsilon}$ the transition map is

$$\begin{pmatrix} 1 & 0 \\ -c\,\partial f_\epsilon/\partial p(p) & 1 \end{pmatrix} e^{J_0(\pi/2-G(q+cf_\epsilon(p)))}E^{-1}(p, q + cf_\epsilon(p)). \tag{31}$$

Here the incoming basis is (X, Y), the outcoming basis is $(P_{\text{in}}, Q_{\text{in}})$, and coordinates (z, p, q) correspond to the coordinate system inside of the surgery handle. Then, where they are defined, equations (30) and (31) provide X and Y as a linear combination of P_{in} and Q_{in} by multiplying the above expressions on the left by $\binom{1}{0}$ and $\binom{0}{1}$, respectively.

6.2 Framing extension up to obstruction

We use the above equations to extend the framing (X, Y) of $\xi_{\Lambda^\pm}$ inside of the surgery handle. To this end, let $\delta > 0$ be an arbitrarily small constant and consider a smooth function $\nu\colon I_\epsilon \to [0, 1]$ with the following properties:

(1) $\nu(-\epsilon) = 0$ and $\nu(\epsilon) = 1$.

(2) All of its derivatives vanish outside of $I_{\epsilon-\delta}$.

When $c = 1$, we use (30) and (31) to extend the definitions of (X, Y) over the set $\{p < \epsilon - \delta\} \subset N_\epsilon$ using the family of matrices

$$\begin{pmatrix} 1 & 0 \\ -\partial f_\epsilon/\partial p(\zeta^+) & 1 \end{pmatrix} e^{J_0(\pi/2 - G(\eta^+))} E^{-1}(\zeta^+, \eta^+), \tag{32}$$

where

$$\zeta^+(z, p) = p\nu(z) - \epsilon(1 - \nu(z)), \quad \eta^+(z, p, q) = q + f_\epsilon(\zeta^+(z, p)).$$

Note that $\zeta^+ = -\epsilon$ along $\{z = -\epsilon\} \cup \{p = -\epsilon\}$ and that $\zeta^+ = p$ along $z = \epsilon$. By these properties and the properties of f_ϵ and its derivatives in Section 4.7, we have that this family of matrices agrees with (30) along $B_{\delta,\epsilon}$ and with (31) along $T_{\delta,\epsilon}$.

Likewise, when $c = -1$, we extend the definitions of (X, Y) over $\{p > -\epsilon + \delta\} \subset N_\epsilon$, using the family of matrices which provide (X, Y) in the basis $(P_{\text{in}}, Q_{\text{in}})$,

$$\begin{pmatrix} 1 & 0 \\ \partial f_\epsilon/\partial p(\zeta^-) & 1 \end{pmatrix} e^{J_0(\pi/2 - iG(\eta^-))} E^{-1}(\zeta^-, \eta^-), \tag{33}$$

where

$$\zeta^-(z, p) = p\nu(z) + \epsilon(1 - \nu(z)), \quad \eta^-(z, p, q) = q - f_\epsilon(\zeta^-(z, p)).$$

Note that $\zeta^- = \epsilon$ along $\{z = -\epsilon\} \cup \{p = \epsilon\}$ and that $\zeta^- = p$ along $z = \epsilon$. As in the $c = 1$ case, this family of matrices agrees with (30) along $B_{\delta,\epsilon} \cup S_{\delta,\epsilon}$ and with (31) along $T_{\delta,\epsilon}$.

The extension of the fields (X, Y) through the surgery handle N_ϵ is illustrated in Figure 14.

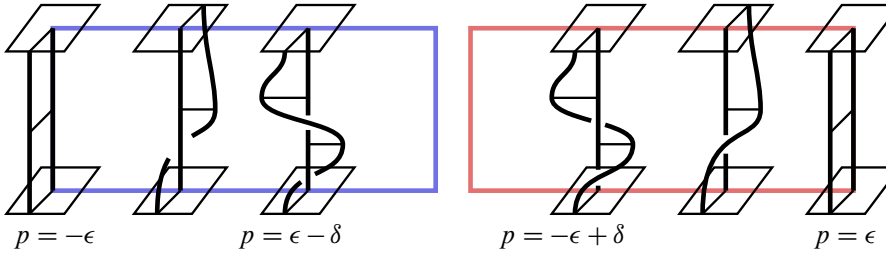

Figure 14: On the left we have the extension of the framing (X, Y) through the surgery handle over a square of the form $\{q = q_0,\, p < \epsilon - \delta\}$ in N_ϵ when $c = 1$ and $\mathrm{rot}(\Lambda) = 1$. On the right is the case $c = -1$, $\mathrm{rot}(\Lambda) = 1$. Here ∂_p points to the right, ∂_q points in to the page, and ∂_z points upwards. Along the bottom of the square, the framing is constant. At each p, the framing twists with respect to the trivialization $(\partial_p, \partial_q - p\partial_z)$ according to the twisting of Gauss map along the path in Λ from q_0 to $q_0 + f_\epsilon(p)$. For $c = 1$, moving from left to right, we eventually get to $p_0 = \epsilon - \delta$ such that $f_\epsilon(p) = 1$ for $p > p_0$.

6.3 Obstruction to global definition of (X, Y)

The Chern class $c_1(\xi_{\Lambda^\pm})$ agrees with the Euler class of $\xi_{\Lambda^\pm}$ and so can be represented as the zero locus of a generic section $s \in \Gamma(\xi_{\Lambda^\pm})$. In attempting to extend the definition of (X, Y) over the squares $S^+_{q_0,\epsilon,\delta} := \{q = q_0, \epsilon - \delta \le p \le \epsilon\}$ when $c = 1$ and $S^+_{q_0,\epsilon,\delta} := \{q = q_0, -\epsilon \le p \le -\epsilon + \delta\}$ when $c = -1$, we may complete the proof of Theorem 6.1.

Proof of Theorem 6.1 We attempt to extend X throughout the entirety of the handle, assuming that δ is small enough so that f_ϵ is constant on each component of $[-\epsilon, -\epsilon + \delta) \cup (\epsilon - \delta, \epsilon]$. For the case of $+1$ contact surgery we study (32). We orient $S^+_{q_0,\epsilon,\delta}$ so that ∂_q points positively through it. Parametrize the oriented boundary of each $S^+_{q_0,\epsilon,\delta}$ with a piecewise-smooth curve $\gamma = \gamma(t)$ so that

$$\frac{\partial \gamma}{\partial t} = \begin{cases} \partial_z & \text{if } p = \epsilon - \delta, \\ \partial_p & \text{if } z = \epsilon, \\ -\partial_z & \text{if } p = \epsilon, \\ -\partial_p & \text{if } z = \epsilon. \end{cases}$$

Applying the vector $\left(\begin{smallmatrix} 1 \\ 0 \end{smallmatrix}\right)$ to the left of (31) gives us the section X as a linear combination of P_{in} and Q_{in} along γ. By throwing away the shearing and rescaling terms in (32), this section is homotopic through nonvanishing sections of $\xi_{\Lambda^\pm}$ to a section of the form

$$t \mapsto \begin{cases} e^{-J_0 G(q_0 + f_\epsilon(t\epsilon))} & \text{for } p = \epsilon - \delta, t \in [-1, 1], \\ e^{-J_0 G(q_0 + f_\epsilon(\epsilon))} & \text{on } \{z = -\epsilon\} \cup \{p = \epsilon\} \cup \{z = \epsilon\}. \end{cases} \tag{34}$$

This is homotopic to

$$t \mapsto e^{\text{const}-2\pi i t\, \text{rot}(\Lambda)}, \quad t \in [0,1].$$

Therefore, a generic extension of X over each $S^+_{q_0,\epsilon,\delta}$ will have $-\text{rot}(\Lambda)$ zeros counted with multiplicity. Taking a generic extension of X over $\{p > \epsilon - \delta\}$ will then be an oriented link which transversely intersects each square with multiplicity $\text{rot}(\Lambda)$. Pushing this zero locus through the side $p = \epsilon$ of the surgery handle provides $\text{PD}(c_1(\xi_{\Lambda^\pm})) = -\text{rot}(\Lambda)\lambda_\xi$.

The case $c = -1$ is similar; we only check signs. Consider a parametrization of the boundary of the square $S^-_{q_0,\epsilon,\delta}$ with a loop γ satisfying

$$\frac{\partial \gamma}{\partial t} = \begin{cases} -\partial_z & \text{if } p = -\epsilon + \delta, \\ -\partial_p & \text{if } z = -\epsilon, \\ \partial_z & \text{if } p = -\epsilon, \\ \partial_p & \text{if } z = \epsilon. \end{cases}$$

Then, following (33), the analog of (34) for the $c = -1$ case is

$$t \mapsto \begin{cases} e^{-J_0 G(q_0 - f_\epsilon(t\epsilon))} & \text{for } p = -\epsilon + \delta, t \in [-1,1], \\ e^{-J_0 G(q_0 - f_\epsilon(\epsilon))} & \text{on } \{z = \epsilon\} \cup \{p = -\epsilon\} \cup \{z = -\epsilon\}, \end{cases}$$

so that the zero locus of the extension of the vector field X throughout the handle is homologous to $\text{rot}(\Lambda)\lambda_\xi$. □

Remark 6.2 We sketch how the framing (X, Y) can be modified so that its zero locus is contained in a union of meridians of the Λ_i. Take a meridian μ_i of Λ_i and handle-slide it through N_ϵ to obtain a longitude $-c_i \lambda_i$, which we may take to be $-c_i T^{c_i}$.

This homotopy, say parametrized by $[0,1]$ may be chosen so that the surface S it sweeps out is an embedded cylindrical cobordism parametrized by an annulus $[0,1] \times S^1$. Then we can find a family (X_t, Y_t) of sections of ξ_Λ whose zero loci are contained in $\{t\} \subset S^1$, so that (X_1, Y_1) will vanish along some union of the Λ_i, as desired.

If γ is a Reeb orbit of R_ϵ, then, according to (2), we can compute CZ_{X_1,Y_1} from $\text{CZ}_{X,Y}$ by counting the number of intersections of γ with S, which measures the meridional framing difference.

6.4 Rotation numbers and Chern classes in arbitrary contact 3–manifolds

We briefly state how the above can be generalized to understand how c_1 changes after contact surgery on an arbitrary contact manifold (M, ξ). A section $s \in \Gamma(\xi)$ determines a homotopy class of oriented trivialization of ξ on the complement of $s^{-1}(0)$ by considering $\xi_x = \text{span}_{\mathbb{R}}(s_x, Js_x)$ for an almost-complex structure J on ξ

compatible with $d\alpha$ for a contact form α for ξ and $x \in M \setminus s^{-1}(0)$. Suppose that s is transverse to the zero section and nonvanishing along a neighborhood N_ϵ of Λ. Write η_s for the oriented link

$$T_s = s^{-1}(0) \subset (M \setminus N_\epsilon) = (M_\Lambda \setminus N_\epsilon).$$

Definition 6.3 The *rotation number* $\mathrm{rot}_s(\Lambda)$ is the winding number of ∂_q in ξ_Λ determined by the trivialization of $\xi|_\Lambda$ provided by s.

Note that changing the orientation of Λ multiplies the rotation number by -1 and that rot_s agrees with the standard definition of the rotation number for oriented Legendrians in $(\mathbb{R}^3, \xi_{\mathrm{std}})$ if we take $s \in \Gamma_{\neq 0}(\xi_{\mathrm{std}})$. More generally, the rotation number of Legendrian knot Λ is canonically defined whenever ξ admits a nonvanishing section and at least one of $H^1(M) = 0$ or $[\Lambda^0] = 0 \in H_1(M)$ holds as in Proposition 2.5.

We note that Definition 6.3 may be applied to Legendrian knots in $(\mathbb{R}^3_{\Lambda^\pm}, \xi_{\Lambda^\pm})$ even when these hypotheses are not satisfied: if such a knot Λ^0 is contained in $\mathbb{R}^3 \setminus N_\epsilon = \mathbb{R}^3_{\Lambda^\pm} \setminus N_\epsilon$, then $\mathrm{rot}_{X,Y}(\Lambda^0)$ may be computed using the typical methods for Legendrian knots in $(\mathbb{R}^3, \xi_{\mathrm{std}})$ as described in Section 2.8. This follows immediately from the first condition listed in Theorem 6.1.

Proposition 6.4 *Following the notation in the preceding discussion and writing λ_ξ for a longitude of Λ determined by ξ, and μ for a meridian of Λ, the Chern class $c_1(\xi_\Lambda)$ for the contact manifold (M_Λ, ξ_Λ) obtained by performing contact ± 1 surgery on $\Lambda \subset M$ is determined by the formula*

$$\mathrm{PD}(c_1(\xi_\Lambda)) = [T_s] \mp \mathrm{rot}_s(\Lambda)\lambda_\xi = [T_s] \pm \mathrm{rot}_s(\Lambda)\mu \in H_1(M_\Lambda).$$

This can be proved using the same strategy as Theorem 6.1, replacing X with s.

7 Conley–Zehnder and Maslov index computations

The goal of this section is to compute the integral Conley–Zehnder indices of closed orbits of the R_ϵ and the Maslov indices of broken closed strings on $\Lambda^0 \subset (\mathbb{R}^3_{\Lambda^\pm}, \xi_{\Lambda^\pm})$ using the framing (X, Y) defined in Section 6.

Theorem 7.1 *For each $n > 0$, there exists ϵ_0 such that, for all $\epsilon \leq \epsilon_0$, all orbits γ of word length $\leq n$ are hyperbolic with*

$$\mathrm{CZ}_{X,Y}(\gamma) = \sum_{k=1}^{n} (\mathrm{rot}_{j_k, j_{k+1}} + \delta_{1, c^+_{j_k}}) \in \mathbb{Z}.$$

Theorem 7.2 *Let b be a broken closed string on $\Lambda^0 \subset (\mathbb{R}^3_{\Lambda^\pm}, \xi_{\Lambda^\pm})$ of the form*

$$b = \zeta_1 * (a_1\kappa_1) * \cdots \zeta_n * (a_n\kappa_n),$$

where each ζ_k is a path in Λ^0 and each κ_k is a chord of Λ^0 with respect to R_ϵ. By Theorem 5.10, we can write

$$\kappa_k = (r_{k_1} \cdots r_{k_{n_k}})$$

for some word of chords with boundary on $\Lambda^0 \subset (\mathbb{R}^3, \xi_{\text{std}})$. In this notation,

$$\mathrm{M}_{X,Y}(b) = \sum_1^n \left(\frac{\theta(\zeta_k)}{\pi} - \frac{1}{2} + a_k m_{X,Y}(\kappa_k) \right),$$
$$m_{X,Y}(\kappa_k) = \sum_{l=1}^{n_k - 1} (\mathrm{rot}_{j_{k_l}, j_{k_l+1}} + \delta^+_{1,c_{k_l}}).$$

Proving the above theorems requires further analysis of (32) and (33). The analysis will provide an expression of the linearized flow of R_ϵ as a path of matrices in $\mathrm{SL}(2,\mathbb{R})$ with entries in $\mathbb{R}[\epsilon^{-1}]$ determined by $\mathrm{cw}(\gamma)$. Analysis of the highest-order terms of these polynomials gave us the proof of Theorem 5.3. Analysis of the second-highest-order terms of these polynomials will yield a formula for integral Conley–Zehnder indices, $\mathrm{CZ}_{X,Y}$.

7.1 Matrix model for the linearized flow

With respect to the coordinate system (z, p, q) inside of the surgery handles $R_\epsilon = \partial_z$. Hence computing the restriction of the linearized to flow to $\xi_{\Lambda^\pm}$ from the bottom ($z = -\epsilon$) to a point above it ($z > -\epsilon$) in the surgery handle with respect to (X, Y) amounts to writing $(X, Y)_{-\epsilon,p,q}$ in the basis $(X, Y)_{z,p,q}$. We write $F_i(z, p, q) \in \mathrm{SL}(2,\mathbb{R})$ for this path of matrices associated to points (z, p, q) in the component of N_ϵ associated to Λ_i.

By composing (30) with equations (32) — in the case of $+1$ surgery — and (33) — in the case of -1 surgery — we have

$$F_i(z,p,q) = E(\zeta^{c_i}, \eta^{c_i}) e^{J_0 G_i(\eta^{c_i})} \begin{pmatrix} 1 & -c_i\, \partial f_\epsilon / \partial p(\zeta^{c_i}) \\ 0 & 1 \end{pmatrix} e^{-J_0 G_i(q)} E^{-1}(p,q) \tag{35}$$
$$= e^{J_0 G_i(\eta^{c_i})} \begin{pmatrix} 1 & -c_i\, \partial f_\epsilon / \partial p(\zeta^{c_i}) \\ 0 & 1 \end{pmatrix} e^{-J_0 G(q)} (\mathrm{Id} + \mathcal{O}(p)).$$

We have preemptively simplified the expression with some basic arithmetic. Here G_i is the Gauss map associated to the component Λ_i of Λ. The following collection of assumptions will allow us to further simplify the above expression:

Assumptions 7.3 We refine our previous constructions as follows: At any point through which a closed Reeb orbit passes, the sections X and Y of $\xi_{\Lambda^\pm}$ described in Section 6.2 are defined according to the formula contained within that section. This can be achieved by setting the constant δ to be sufficiently small.

Some consequences of the above assumptions coupled with Assumptions 5.4 are:

(1) Equation (35) is valid for any point contained in a closed Reeb orbit.

(2) The expression $-c_i\,\partial f_\epsilon/\partial p(\zeta^{c_i})$ in that formula simplifies to $-c_i\epsilon^{-1}$ for any point lying in a closed Reeb orbit.

Combining these consequences with a conjugation, we have that F_i in a neighborhood of a Reeb segment which exits $N_{\epsilon,i}$ near $l^+_{j_1}$ and exits near $l^-_{j_2}$ for composable Reeb chords r_{j_i} and r_{j_2} is homotopic — relative endpoints — to a path of the form

$$\mathcal{F}_{j_1,j_2}(t) = e^{J_0 t\theta_{j_1,j_2}} \begin{pmatrix} 1 & -tc^+_{j_1}\epsilon^{-1} \\ 0 & 1 \end{pmatrix} (\mathrm{Id} + \mathcal{O}(\epsilon)) \in \mathrm{SL}(2,\mathbb{R}), \quad t \in [0,1], \tag{36}$$

where we use the basis $e^{i\pi/4}(X, Y)$.

Using (36), we can write the restriction of Poincaré return map to ξ of a closed Reeb orbit γ of α_ϵ with $\mathrm{cw}(\gamma) = r_{j_1}\cdots r_{j_n}$ as

$$\mathrm{Ret}_\gamma = \mathcal{F}_{j_n,j_1}(1)\mathcal{F}_{j_{n-1},j_n}(1)\cdots\mathcal{F}_{j_1,j_2}(1) \tag{37}$$

by composing the flow maps as an orbit passes through the various surgery handles. If the word consists of a single chord, then we have $\mathrm{Ret} = \mathcal{F}_{j_1,j_1}(1)$. Note that, while our expression for Ret depends on a particular representation of the associated cyclic word, its conjugacy class in $\mathrm{SL}(2,\mathbb{R})$ does not.

7.2 Integral Conley–Zehnder indices

In this subsection we prove Theorem 7.1 via induction on the word length n of γ. The proof is computational, making use of the Robbin–Salamon characterization of the Conley–Zehnder index described in (5).

7.2.1 The case $n = 1$ We begin with the case $n = 1$, analyzing (36). A slight modification of the proof of the following lemma along with further analysis of (26) will provide the general case. For the sake of notational simplicity, we temporarily drop the subscripts required to describe words of length greater than 1.

Lemma 7.4 *Theorem 7.1 is valid for Reeb orbits of word length* 1.

Proof We homotop the path $\mathcal{F}$ so that it is parametrized with the interval $[0, 3]$, taking the form

$$\mathcal{F}(t) = e^{J_0 t_1 \theta} \begin{pmatrix} 1 & -t_2 c\epsilon^{-1} \\ 0 & 1 \end{pmatrix} E(t_3), \quad E(0) = \mathrm{Id}, \quad E(1) = \mathrm{Id} + \mathcal{O}(\epsilon),$$

$$t_k = \begin{cases} 0 & \text{if } t \leq k-1, \\ t-k+1 & \text{if } t \in (k-1, k), \\ 1 & \text{if } t \geq k. \end{cases} \tag{38}$$

With this parametrization we are performing the rotation first so that the path is nondegenerate at $\mathcal{F}(0) = \mathrm{Id}$. A standard computation shows that, along the interval $[0, 1]$, the contributions to $\mathrm{CZ}_{X,Y}$ are given by $2\lfloor \theta/2\pi \rfloor + 1$. Then, along $t \in [1, 2]$, we have

$$\mathcal{F}(t) = (-1)^{\mathrm{rot}} \begin{pmatrix} 0 & -1 \\ 1 & -t_2 c\epsilon^{-1} \end{pmatrix}$$

By the $\mathrm{SL}(2, \mathbb{R})$ trace formula of (1), $t \in [1, 2]$ will be crossing exactly when

$$\mathrm{tr}(\mathcal{F}(t)) = (-1)^{1+\mathrm{rot}} t_2 c = 2.$$

Therefore, we find a crossing in the interval — and a single one at that — if and only if $c = (-1)^{1+\mathrm{rot}}$. At such a crossing, if it exists, the matrix $S(t)$ of (4) is $S(t) = \mathrm{Diag}(t_2 c\epsilon^{-1}, 0)$. So the contribution to $\mathrm{CZ}_{X,Y}$ can be computed as $\frac{1}{2}(c - (-1)^{\mathrm{rot}})$.

Adding up the contributions along $t \in [0, 2]$, we have

$$\begin{aligned} \mathrm{CZ} &= 2\left\lfloor \frac{\theta}{2\pi} \right\rfloor + 1 + \tfrac{1}{2}(c - (-1)^{\delta}) = 2\left\lfloor \frac{\theta}{2\pi} \right\rfloor + \tfrac{1}{2}(1 - (-1)^{\mathrm{rot}}) + \tfrac{1}{2}(c+1) \\ &= \mathrm{rot} + \delta_{1,c}. \end{aligned}$$

Along the interval $[2, 3]$, the addition of the E term to the formula contributes a term to the trace which is bounded by a constant which is independent of ϵ. Thus, this interval is devoid of crossings for ϵ small. □

7.2.2 The case $n > 1$ Now we prove the induction step in our index computation. We suppose that the Reeb orbit in question has word length $n + 1 > 1$ and is parametrized with an interval $[0, n + 1]$. Then we can compute the Conley–Zehnder index using the

path of symplectic matrices

$$\phi(t) = \mathcal{F}_{j_n,j_{n+1}}(t_{n+1}) \cdots \mathcal{F}_{j_{n+1},j_1}(t_1), \quad t_k = \begin{cases} 0 & \text{if } t \le k-1, \\ t-k+1 & \text{if } t \in (k-1,k), \\ 1 & \text{if } t \ge k, \end{cases}$$

by combining (36) and (37). As in the proof of Lemma 7.4, we can drop the E terms in the equations, count the contributions to CZ coming from the rotation and shearing matrices, then reintroduce the E terms, noting that they do not contribute to CZ due to the large absolute values of traces. Consequently, we ignore these E terms during computation. With this simplification, ϕ takes the form, when $t \in [n, n+1]$,

$$\phi(t) = \widetilde{\phi}(t_{n+1}) \operatorname{Ret}_n, \tag{39}$$

where

$$\begin{aligned} \widetilde{\phi}(t_{n+1}) &= e^{i t_n \theta_{j_{n+1},j_1}} \begin{pmatrix} 1 & -t_{n+1} c^+_{j_{n+1}} \epsilon^{-1} \\ 0 & 1 \end{pmatrix}, \\ \operatorname{Ret}_n &= \mathcal{F}_{j_{n-1},j_n}(1) \cdots \mathcal{F}_{j_{n+1},j_1}(1) \\ &= (-1)^{\mathrm{rot}_n} \Bigg(J^n + \sum_{K=1}^{n} \Bigg(\sum_{k \in I_K} \Bigg(\prod_{i=1}^{K} -c^+_{j_{k_i}} \Bigg) M_k \Bigg) \epsilon^{-K} \Bigg), \\ \mathrm{rot}_n &= \sum_{0}^{n-1} \mathrm{rot}_{j_k,j_{k+1}}, \end{aligned}$$

over the subinterval $[n, n+1]$. Here indices are cyclic, so that $\mathrm{rot}_{j_0,j_1} = \mathrm{rot}_{j_{n+1},j_1}$. The M_k are as in (26).

By Theorem 5.3, the trace of Ret_n has absolute value of order ϵ^{-n}. Therefore, $n, n+1 \in [0, n+1]$ are not crossing for ϵ small. The ϵ^{-n} term in Ret_n is given by (27). The ϵ^{1-n} term is also easily computable. Noting that $\operatorname{Diag}(0,a) J \operatorname{Diag}(0,b) = 0$ for $a, b \in \mathbb{R}$, the only k for which M_k is nonzero with $k \in I_n$ are $(1, \dots, n-1)$ and $(2, \dots, n)$. Thus, the ϵ^{1-n} terms in Ret_n are

$$\Bigg(\prod_{1}^{n-1} -c^+_{j_{k_i}} \Bigg) \operatorname{Diag}(0,1) J + \Bigg(\prod_{2}^{n} -c^+_{j_{k_i}} \Bigg) J \operatorname{Diag}(0,1) = \begin{pmatrix} 0 & -\prod_2^n -c^+_{j_{k_i}} \\ \prod_1^{n-1} -c^+_{j_{k_i}} & 0 \end{pmatrix}.$$

Combining this with (27), we have

$$\begin{aligned} \operatorname{Ret}_n &= (-1)^{\mathrm{rot}_n} \begin{pmatrix} 0 & -\epsilon^{-n+1} \prod_2^n -c^+_{j_{k_i}} \\ \epsilon^{-n+1} \prod_1^{n-1} -c^+_{j_{k_i}} & \epsilon^{-n} \prod_1^n -c^+_{j_{k_i}} \end{pmatrix} + \mathcal{O}(\epsilon^{2-n}) \\ &= (-1)^{\mathrm{rot}_n} \epsilon^{-n+1} \Bigg(\prod_{1}^{n} -c^+_{j_{k_i}} \Bigg) \begin{pmatrix} 0 & c^+_{j_{k_1}} \\ -c^+_{j_{k_n}} & \epsilon^{-1} \end{pmatrix} + \mathcal{O}(\epsilon^{2-n}). \end{aligned} \tag{40}$$

Lemma 7.5 *For ϵ sufficiently small, the contribution to $\mathrm{CZ}_{X,Y}$ along the interval $[n, n+1]$ in (39) is*

$$\mathrm{rot}_{j_n, j_{n+1}} + \delta_{1, c^+_{j_{n+1}}}.$$

Proof We begin by making some temporary notational simplifications and further subdivide the interval $[n, n+1]$ along which the map $\widetilde{\phi}$ is changing and Ret_n is constant. We are referring here to (39) and use notation from that equation throughout the proof. We write

$$\sigma = (-1)^{\mathrm{rot}_n}\left(\prod_1^n -c^+_{j_{k_i}}\right) \in \{\pm 1\},$$

$$c_1 = c^+_{j_1}, \quad c_n = c^+_{j_n}, \quad c_{n+1} = c^+_{j_{n+1}},$$

$$\mathrm{rot} = \mathrm{rot}_{j_n, j_{n+1}}, \quad \mathrm{rot}_2 = \mathrm{rot} \mod 2 \in \mathbb{Z}/2\mathbb{Z},$$

$$\theta_{j_n, j_{n+1}} = \pi\big(2k + \delta_{1,\mathrm{rot}_2} + \tfrac{1}{2}\big), \quad k = \left\lfloor \frac{\theta_{j_n, j_{n+1}}}{2\pi} \right\rfloor \in \mathbb{Z}.$$

By combining the above notation with (40), we can write $\phi(t) = \widetilde{\phi}(t_n)\,\mathrm{Ret}_n$, where

$$\widetilde{\phi}(t_{n+1}) = e^{J_0 t_{n+1} \theta_{j_n, j_{n+1}}} \begin{pmatrix} 1 & -t_{n+1} c_{n+1} \epsilon^{-1} \\ 0 & 1 \end{pmatrix},$$

$$\mathrm{Ret}_n = \sigma \epsilon^{1-n} \begin{pmatrix} 0 & c_1 \\ -c_n & \epsilon^{-1} \end{pmatrix} + \mathcal{O}(\epsilon^{2-n}).$$

Along the subset $t \in [n, n+1]$, we homotop $\widetilde{\phi}$ to take the form

$$\widetilde{\phi}(t_{n+1}) = e^{J_0 \theta} \begin{pmatrix} 1 & -s_2 c_{n+1} \epsilon^{-1} \\ 0 & 1 \end{pmatrix}, \quad \theta = \pi\big(s_1 \cdot \tfrac{1}{4} + s_3\big(\delta_{1,\mathrm{rot}_2} + \tfrac{1}{4}\big) + s_4 \cdot 2k\big),$$

where s_i are functions of t taking values in $[0, 1]$ as described in Figure 15, so that $\theta = \theta_{j_n, j_{n+1}}$ when $s_1 = \cdots = s_4 = 1$. In words, we will be applying a rotation by $\frac{1}{4}\pi$, a shear, a rotation by $\pi\big(\delta_{1,\mathrm{rot}_2} + \frac{1}{4}\big)$, and then finally a rotation by $2\pi k$. Taking the arguments of all trigonometric functions to be θ,

$$\begin{aligned} \phi &= \begin{pmatrix} \cos & -\sin \\ \sin & \cos \end{pmatrix} \begin{pmatrix} 1 & -s_2 c_{n+1} \epsilon^{-1} \\ 0 & 1 \end{pmatrix} \left(\sigma \epsilon^{1-n} \begin{pmatrix} 0 & c_1 \\ -c_n & \epsilon^{-1} \end{pmatrix} + \mathcal{O}(\epsilon^{2-n}) \right) \\ &= \sigma \epsilon^{-n} \begin{pmatrix} s_2 c_n c_{n+1} \cos & -s_2 c_{n+1} \epsilon^{-1} \cos - \sin \\ s_2 c_n c_{n+1} \sin & -s_2 c_{n+1} \epsilon^{-1} \sin + \cos \end{pmatrix} + \mathcal{O}(\epsilon^{1-n}), \\ \mathrm{tr}(\phi) &= \sigma \epsilon^{-n} (s_2 c_n c_{n+1} \cos - s_2 c_{n+1} \epsilon^{-1} \sin + \cos) + \mathcal{O}(\epsilon^{1-n}). \end{aligned}$$

Along our first subinterval parametrized by s_1, we have $s_2 = s_3 = s_4 = 0$ with θ increasing from 0 to $\frac{1}{4}\pi$. Here $\mathrm{tr}(\phi) = \sigma \epsilon^{-n} \cos + \mathcal{O}(\epsilon^{1-n})$ has large absolute value

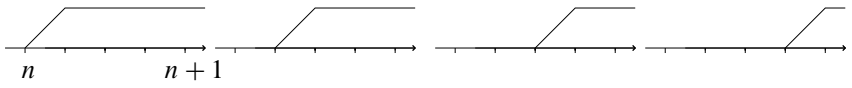

Figure 15: From left to right are graphs of the functions $s_1(t), \dots, s_4(t)$.

when ϵ is small. Hence, for ϵ small, there are no crossings over the s_1 subinterval and so there are no contributions to the Conley–Zehnder index.

Along the subinterval parametrized by s_2, we have $\theta = \frac{1}{4}\pi$, so that $\cos(\theta) = \sin(\theta) = \frac{1}{\sqrt{2}}$. Hence,

$$\operatorname{tr}(\phi) = \tfrac{1}{\sqrt{2}}\sigma\epsilon^{-n}(s_2c_nc_{n+1} - s_2c_{n+1}\epsilon^{-1} + 1) + \mathcal{O}(\epsilon^{1-n}). \tag{41}$$

At both the $s_2 = 0$ and $s_2 = 1$ endpoints of the interval, $\operatorname{tr}(\phi)$ will have large absolute value of orders ϵ^{-n} and ϵ^{-1-n}, respectively, so that ϕ cannot be crossing at either of these endpoints. Over the interior of the subinterval, we see that there is a single crossing if $c_{n+1} = 1$ and no crossings if $c_{n+1} = -1$.

If $c_{n+1} = 1$, then at the unique crossing we compute the crossing form

$$S = -J_0\frac{\partial\phi}{\partial s_2}\phi^{-1} = \frac{1}{2\epsilon}\begin{pmatrix} 1 & -1 \\ -1 & 1 \end{pmatrix}, \quad \begin{pmatrix} a & b \end{pmatrix} S \begin{pmatrix} a \\ b \end{pmatrix} = \frac{1}{2\epsilon}(a-b)^2.$$

The quadratic form determined by S vanishes exactly along the line $\mathbb{R}\binom{1}{1}$. Therefore, to see that the unique crossing along the s_2 subinterval is nondegenerate, we only need to check that $\phi\binom{1}{1} \neq 0$ at the crossing. Plugging $c_{n+1} = 1$ into (41), at the crossing we must have

$$s_2(c_n - \epsilon^{-1}) + 1 = \mathcal{O}(\epsilon)$$

in order to eliminate the ϵ^{-n} and ϵ^{-n-1} terms. Therefore, at the crossing,

$$\phi\begin{pmatrix} 1 \\ 1 \end{pmatrix} = \tfrac{1}{\sqrt{2}}\sigma\epsilon^{-n}\begin{pmatrix} s_2(c_n - \epsilon^{-1}) - 1 \\ s_2(c_n - \epsilon^{-1}) + 1 \end{pmatrix} + \mathcal{O}(\epsilon^{1-n}) = \tfrac{1}{\sqrt{2}}\sigma\epsilon^{-n}\begin{pmatrix} -2 \\ 0 \end{pmatrix} + \mathcal{O}(\epsilon^{1-n})$$

is nonzero for ϵ small. We conclude that, at the crossing, $\ker(\phi - \mathrm{Id})$ must be 1–dimensional and the restriction of S to $\ker(\phi - \mathrm{Id})$ must be positive. Hence, the s_2 subinterval contributes $\delta_{c_{n+1},1}$ to the Conley–Zehnder index.

Now we study the s_3 subinterval along which $s_2 = 1$ and $\theta \in \left[\frac{1}{4}\pi, \pi\left(\delta_{1,\mathrm{rot}_2} + \frac{1}{2}\right)\right]$. Along this subinterval,

$$\operatorname{tr}(\phi) = \sigma\epsilon^{-n}(c_nc_{n+1}\cos - c_{n+1}\epsilon^{-1}\sin + \cos) + \mathcal{O}(\epsilon^{1-n}).$$

If $\delta_{1,\mathrm{rot}_2} = 0$ and ϵ is very small, then, as θ increases from $\frac{1}{4}\pi$ to $\frac{1}{2}\pi$, the sin term dominates, $\mathrm{tr}(\phi)$ maintains a large absolute value, and there are no crossings.

If $\delta_{1,\mathrm{rot}_2} = 1$, then we have a single crossing at which the crossing form is determined by the matrix

$$S = -J_0 \frac{\partial \phi}{\partial s_2} \phi^{-1} = \tfrac{3}{4}\pi \,\mathrm{Id}.$$

Because the crossing form is positive definite, the contribution to the Conley–Zehnder index is the dimension of $\ker(\phi - \mathrm{Id})$ — either 1 or 2. At the crossing, sin is $\mathcal{O}(\epsilon)$, implying that $\theta \to \pi$ (and so $\cos(\theta) \to -1$) as $\epsilon \to 0$. Therefore, at the crossing,

$$\begin{aligned}(\phi - \mathrm{Id}) \begin{pmatrix} 0 \\ 1 \end{pmatrix} &= \sigma \epsilon^{-n} \begin{pmatrix} -c_{n+1}\epsilon^{-1} \cos - \sin \\ -c_{n+1}\epsilon^{-1} \sin + \cos \end{pmatrix} + \mathcal{O}(\epsilon^{1-n}) \\ &= \sigma \epsilon^{-1-n} \begin{pmatrix} -c_{n+1} \cos \\ 0 \end{pmatrix} + \mathcal{O}(\epsilon^{-n}) \neq 0,\end{aligned}$$

implying that $\dim \ker(\phi - \mathrm{Id}) = 1$. We conclude that the contribution to CZ along the s_3 interval is $\delta_{1,\mathrm{rot}_2}$.

For the s_4 subinterval, we appeal to the loop property of CZ described in (6) to see a contribution of $2k$. Combining the contributions over the four s_i subintervals, we get

$$2k + \delta_{\mathrm{rot}_2,1} + \delta_{c_{n+1},1} = \mathrm{rot}_{j_n, j_{n+1}} + \delta_{c^+_{j_{n+1}},1},$$

by reverting to our original notation, thereby completing the proof. □

The combination of the above lemmas completes our induction, thereby proving Theorem 7.1.

7.3 Integral Maslov indices

The proof of Theorem 7.2 follows from the same methods of calculation as Theorem 7.1.

Proof of Theorem 7.2 According to Definition 3.8, we need to measure the rotation of $\mathrm{Flow}^t_{R_\epsilon}(T_{q^-_{k_1}} \Lambda^0)$ along each chord $(r_{k_1} \cdots r_{k_{n_k}})$ with respect to the framing (X, Y). For chords κ_k of word length 1, the flow is trivial, so we restrict attention to chords of word length > 1. The required analysis can be carried out via analysis of (36); we recall that this describes the restriction of the linearized flow of R_ϵ to $\xi_{\Lambda^\pm}$ through a component N_{ϵ,j_1} of N_ϵ starting at a point near the tip of one chord r_{j_1} up to a point near the tail of another chord r_{j_2}.

We study the rotation along a single $\kappa = (r_{j_1} \cdots r_{j_n})$: The matrix expression $\mathcal{F}_{j_1,j_2}(t)$ in (36) applies to the basis

$$e^{i\pi/4}(X, Y) \simeq (\partial_q - p\partial_z, -\partial_p),$$

beginning on the bottom, $\{z = -\epsilon\}$, of the surgery handle N_{ϵ,j_1}. For $j_1 = k_1$ and $j_2 = k_2$, the strand of Λ^0 touching the starting point of the chord r_{j_1} is such that $T\Lambda^0 = \mathbb{R}\binom{0}{1}$. Therefore, we need to see how $\mathcal{F}_{j_1,j_2}(t)$ rotates this subspace for $t \in [0, 1]$. As in the proof of Theorem 7.1, we can modify the path so as to apply the shearing first, and then the rotation.

For the shearing, we study the family of real lines in $\mathbb{R}^2$ given by

$$\mathbb{R}\begin{pmatrix} 1 & -tc^+_{j_1}\epsilon^{-1} \\ 0 & 1 \end{pmatrix}(\mathrm{Id} + \mathcal{O}(\epsilon))\begin{pmatrix} 0 \\ 1 \end{pmatrix}, \quad t \in [0, 1].$$

The end result is a line of the form $\mathbb{R}\left(\binom{1}{0} + \mathcal{O}(\epsilon)\right)$ obtained by rotating $\mathbb{R}\binom{0}{1}$ by an angle of

$$c^+_{j_1} \cdot \tfrac{1}{2}\pi + \mathcal{O}(\epsilon). \tag{42}$$

Then, applying the rotation through angles $t\theta_{j_1,j_2}$ as in (36), we rotate this subspace by

$$\theta_{j_1,j_2} = \pi \,\mathrm{rot}_{j_1,j_2} + \tfrac{1}{2}\pi, \tag{43}$$

which we recall from Section 3 is the rotation angle of the capping path $\eta_{i,j}$ associated to the pair of composable chords (r_{j_1}, r_{j_2}).

Continuing the flow by applying the remaining $\mathcal{F}_{k_l,k_{l+1}}$ for $l = 2, \ldots, n_k - 1$ provides us a total rotation angle of

$$\pi\left(\sum_{l=1}^{n_k-1} \mathrm{rot}_{k_l,k_{l+1}} + \tfrac{1}{2} + \tfrac{1}{2}c^+_{k_l}\right) + \mathcal{O}(\epsilon) = \pi\left(\sum_{l=1}^{n_{k-1}} \mathrm{rot}_{k_l,k_{l+1}} + \delta_{c^+_{k_l},1}\right) + \mathcal{O}(\epsilon),$$

leaving us on a neighborhood of the strand of Λ lying at the starting point of the chord $r_{k_{n_k}}$ which ends on Λ^0. Each summand in the above formula is the result of adding the contributions of (42) and (43). As in the case $\mathrm{wl}(\kappa) = 1$, the linearized flow up to Λ^0 along $r_{k_{n_k}}$ is trivial in the basis (X, Y). This nearly completes the construction of the section ϕ^G along the chord κ: we must apply one more rotation to ensure that the unoriented Lagrangian line closes up as described in the discussion preceding Definition 3.8.

In the case that our asymptotic indicator is $a_k = 1$, the total rotation along the chord will be

$$\pi\left(-\tfrac{1}{2} + \sum_{l=1}^{n_{k-1}} (\mathrm{rot}_{k_l,k_{l+1}} + \delta_{c^+_{1,k_l}})\right),$$

where the $\frac{1}{2}$ is the contribution of the clockwise correction rotation at the end of the chord. From the above analysis we know that the angle for this rotation is $-\frac{1}{2}\pi + \mathcal{O}(\epsilon)$.

If the asymptotic indicator is -1, we must travel in the opposite direction, from the tip to the tail of the chord, and then apply small the clockwise rotation to obtain a total rotation angle of

$$\pi\left(-\tfrac{1}{2} - \sum_{l=1}^{n_{k-1}} (\mathrm{rot}_{k_l,k_{l+1}} + \delta_{c^+_{1,k_l}})\right).$$

The section ϕ^G appearing in the definition of M_s is determined by the $\theta(\zeta_k)$ as the framing (X, Y) coincides with $(\partial_x - y\partial_z, \partial_y)$ — from which the $\theta(\zeta_k)$ are computed — on the complement of N_ϵ, in which Λ^0 is presumed to be contained. □

8 Diagrammatic index formulas

In this section we compute indices of holomorphic curves in $(\mathbb{R}\times\mathbb{R}^3_{\Lambda^\pm}, d(e^t\alpha_\epsilon))$. We begin by covering the case of curves whose domain is a closed surface with punctures, which is a simple application of (8) to our existing computations of Conley–Zehnder indices and Chern classes. Next we cover the case of a holomorphic disk which is asymptotic to a broken closed string on $\Lambda^0 \subset (\mathbb{R}^3_{\Lambda^\pm}, \xi_{\Lambda^\pm})$ in the sense of Example 3.4. The case $\Lambda^\pm = \varnothing$ recovers a classic index formula appearing in combinatorial versions of LCH and Legendrian *RSFT*. These index formulas are then combined to describe indices associated to holomorphic curves with arbitrary configurations of interior and boundary punctures in Theorem 8.3.

All indices computed will depend only on topological data, so mention of any specific almost-complex structures are ignored.

8.1 Index formulas for closed orbits

Let $\{w_1^+, \dots, w_{m^+}^+\}$ and $\{w_1^+, \dots, w_{m^-}^-\}$ be collections of cyclic words of chords on Λ. By Theorem 7.1, we may choose some $\epsilon_\gamma > 0$ such that for all $\epsilon < \epsilon_\gamma$, the closed orbits $\gamma_j^\pm$ of R_ϵ corresponding to these cyclic words via Theorem 5.8 are all nondegenerate hyperbolic à la Theorem 5.3. Write $\gamma^+ = \{\gamma_1^+, \dots, \gamma_{m^+}^+\}$ and $\gamma^- = \{\gamma_1^-, \dots, \gamma_{m^-}^-\}$ for the corresponding collections of orbits.

Suppose that (Σ, j) is a closed Riemann surface containing a nonempty collection of punctures and that $(t, U)\colon \Sigma' \to \mathbb{R} \times \mathbb{R}^3_{\Lambda^\pm}$ is a holomorphic curve (as in Section 2.7) which is positively asymptotic to the punctures γ^+ and negatively asymptotic to the γ^-.

Theorem 8.1 *Using the framing (X, Y) described in Section 6.2, we can write the expected dimension of the moduli space of curves near (t, U) as*

$$\text{(44)}\quad \operatorname{ind}((t,U)) = \mathrm{CZ}_{X,Y}(\gamma^+) - \mathrm{CZ}_{X,Y}(\gamma^-) - \chi(\Sigma') - 2\sum_1^n c_i \operatorname{rot}(\Lambda_i)(U \cdot T_i^{c_i})$$

for all $\epsilon < \epsilon_\gamma$, where the sum runs over the connected components of $\Lambda^\pm$ and the $\mathrm{CZ}_{X,Y}$ are computed as in Theorem 7.1.

Proof By comparing with (8), we only need to check that

$$c_{X,Y}(U) = -\sum_1^n c_i \operatorname{rot}(\Lambda_i)(U \cdot T_i^{c_i}),$$

where $c_{X,Y}(U)$ is the relative Chern class of the framing (X, Y). Letting $X_U \in U^*(\mathbb{R}^3_{\Lambda^\pm}, \xi_{\Lambda^\pm})$ be a section for which $T_z U(X_U) = X(U(z))$ for $z \in \Sigma'$ to compute $c_{X,Y}(U)$ provides the desired result, as $X^{-1}(0)$ is a union of connected components of $\bigcup T_i^{c_i}$ and the coefficients $-c_i \operatorname{rot}(\Lambda_i)$ account for the multiplicities of the zeros of X_U by the construction of (X, Y) in Section 6. □

8.2 Index formulas for disks with boundary punctures

Now suppose that $\{p_j\}_1^m \subset \partial\mathbb{D}$ is a collection of distinct points on the boundary of a disk. Write $\mathbb{D}' = \mathbb{D} \setminus \{p_j\}$ for the complement of the boundary punctures in $\mathbb{D}$ and write j for the standard complex structure on $\mathbb{D}$. Suppose that $(t, U)\colon \mathbb{D}' \to \mathbb{R} \times \mathbb{R}^3_{\Lambda^\pm}$ is a (j, J)–holomorphic map satisfying

(1) $(t, U)(\partial\mathbb{D}') \subset \mathbb{R} \times \Lambda^0$, and

(2) the punctures $\{p_j\}$ are asymptotic to chords of R_ϵ with boundary on $\Lambda^0 \subset (\mathbb{R}^3_{\Lambda^\pm}, \xi_{\Lambda^\pm})$.

As described in Example 3.4, such a map determines a broken closed string which we will denote by $\operatorname{bcs}(U)$. As in the case of (8), we use $\operatorname{ind}((t, U))$ to denote the expected dimension of the space of holomorphic maps with the same $\operatorname{bcs}(U)$ boundary conditions as (t, U) and in the same relative homotopy class obtained by allowing the locations to vary and then modding out by holomorphic reparametrization in the domain (when $m < 3$).

Theorem 8.2 *The moduli space of holomorphic disks with boundary condition* $\mathrm{bcs}(U)$ *in the homotopy class of* U *has expected dimension*

$$\mathrm{ind}((t,U)) = \mathrm{M}_{X,Y}(\mathrm{bcs}(U)) + m - 1 - 2\sum_{1}^{n} c_i\,\mathrm{rot}(\Lambda_i)(U \cdot T_i^{c_i}) \tag{45}$$

near the point (t,U)*. The sum appearing in the above formula is indexed over the components* Λ_i *of* Λ*.*

Proof We are simply plugging our definition of broken closed strings into formulas appearing in [19; 17].

Assume first that X is nonvanishing over $\mathrm{im}(U)$, so that ∂_t, R_ϵ, X and Y determine a trivialization of $U^*T(\mathbb{R}\times\mathbb{R}^3_{\Lambda^\pm})$ which splits as a pair of complex lines. Using framing deformation-invariance of $\mathrm{M}_{X,Y}$, we may perturb (X,Y) so that it is invariant under the flow of R_ϵ, in which case the geometric setup described in [17, Section 3.1] applies. Our choices of "clockwise rotations" along positive punctures and "counterclockwise rotations" along negative punctures in the definition of the path of symplectic matrices defining M_s coincide with those used to define the Maslov numbers (which are denoted by $\mu(\gamma)$) in that text. The tangent space of our Lagrangian — $\mathbb{R}\times\Lambda^0$ — splits as $\mathbb{R}\partial_t \oplus T\Lambda^0$, so the only contribution to the Maslov number in question comes from the rotation of $T\Lambda^0$ along the boundary of the disk by the direct sum formula for Maslov numbers. Then the moduli space dimension formula of [17, Section 3.1] completes our proof.

Now suppose that X is nonvanishing along $\mathrm{im}(U)$. By the construction of the framing (X,Y), we have that this section must be nonvanishing along Λ^0 and all of its Reeb chords, and so is nonvanishing along $\mathrm{im}(\mathrm{bcs}(U))$. Therefore, the Maslov index can corrected by a relative Chern class term as in (8), which may be computed as signed count of intersections of U with the transverse push-offs of the Λ_i as in the statement of that theorem. □

8.3 Index formulas for curves with interior and boundary punctures

Now we state an index formula for holomorphic curves of general topological type. The geometric setup is as follows.

Let (Σ, j) be a compact, connected Riemann surface with boundary components

$$(\partial\Sigma)_k, \quad k = 1,\dots,\#(\partial\Sigma),$$

marked points $p_i^{\mathrm{int},\pm}$ contained in $\mathrm{int}(\Sigma)$, and marked points $p_i^{\partial,\pm}$ contained in $\partial\Sigma$. We write Σ' for Σ with all of its marked points removed. Consider a holomorphic map $(t,U)\colon \Sigma' \to \mathbb{R}\times(\mathbb{R}^3_{\Lambda^\pm},\xi_{\Lambda^\pm})$ subject to the following conditions:

(1) the $p_i^{\mathrm{int},+}$ are positively asymptotic to some collection γ^+ of closed orbits of R_ϵ,

(2) the $p_i^{\mathrm{int},-}$ are negatively asymptotic to some collection γ^- of closed orbits of R_ϵ,

(3) the $p_i^{\partial,+}$ are positively asymptotic to some collections κ^+ of chords of $\Lambda^0\subset(\mathbb{R}^3_{\Lambda^\pm},\xi_{\Lambda^\pm})$,

(4) the $p_i^{\partial,-}$ are negatively asymptotic to some collections κ^- of chords of $\Lambda^0\subset(\mathbb{R}^3_{\Lambda^\pm},\xi_{\Lambda^\pm})$, and

(5) $(t,U)(\partial\Sigma')\subset\mathbb{R}\times\Lambda^0$.

In this setup, we have a broken closed string bcs_k associated to each component $(\partial\Sigma)_k$ of Σ. We may consider the moduli space of curves subject to the same asymptotics — $\gamma^\pm$ and bcs_k — allowing the complex structure on Σ to vary and taking a quotient by j–holomorphic symmetries on the domain.

Theorem 8.3 *In the above notation, the expected dimension of the moduli space of holomorphic maps is*

$$\begin{aligned}\mathrm{ind}((t,U)) = \mathrm{CZ}_{X,Y}(\gamma^+) - \mathrm{CZ}_{X,Y}(\gamma^-) + \sum_k \mathrm{M}_{X,Y}(\mathrm{bcs}_k)\\ -\chi(\Sigma) + \#(p^{\mathrm{int}}) + \#(p^{\partial}) - 2\sum_{\Lambda_i\subset\Lambda^\pm} c_i\,\mathrm{rot}(\Lambda_i)(U\cdot T_i^{c_i}).\end{aligned}$$

The proof is a simple combination of Theorems 8.1 and 8.2 using index additivity; see [58, Section 3].

9 H_1 computations and push-outs of closed orbits

Here we compute the first homology $H_1(\mathbb{R}^3_{\Lambda^\pm})$ of $\mathbb{R}^3_{\Lambda^\pm}$ and the homology classes of the closed orbits of R_ϵ.

Theorem 9.1 *The first homology $H_1(\mathbb{R}^3_{\Lambda^\pm})$ is presented with generators μ_i and relations*

$$(\mathrm{tb}(\Lambda_i)+c_i)\mu_i + \sum_{j\neq i}\mathrm{lk}(\Lambda_i,\Lambda_j)\mu_j = 0.$$

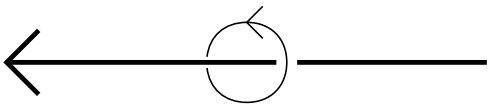

Figure 16: Default orientations for meridians.

Let γ be a Reeb orbit of α_ϵ with $\mathrm{cw}(\gamma) = r_{j_1} \cdots r_{j_n}$. Then its homology class in $H_1(\mathbb{R}^3_{\Lambda\pm})$ with respect to the above basis is

$$[\gamma] = \frac{1}{2} \sum_{k=1}^{n} (\mathrm{cr}_{j_k} + \mathrm{cr}_{j_k, j_{k+1}}),$$

where the k are considered modulo n.

Relative homology classes $[\kappa] \in H_1(\mathbb{R}^3_{\Lambda\pm}, \Lambda^0)$ of chords κ with boundary on $\Lambda^0 \subset (\mathbb{R}^3_{\Lambda\pm}, \xi_{\Lambda\pm})$ can similarly be computed using the technique of the proof of Theorem 9.1 which is carried out in Section 9.3. It will be clear that the method of proof allows the reader to compute $[\gamma]$ as an element of the H_0 of the free loop space of $\mathbb{R}^3_{\Lambda\pm}$. In Section 9.4, we show how the proof can be generalized to provide a general means of homotoping closed orbits of R_ϵ into $\mathbb{R}^3 \setminus N$, a technique we will need for the proof of Theorem 1.2.

9.1 Conventions for meridians and longitudes

Before proving Theorem 9.1, we quickly review some standard notation. Let μ_j denote a meridian of Λ and λ_i a longitude of Λ provided by the Seifert framing and orientation of Λ_i. We note that, with respect to the Seifert framing of Λ_i, the longitude provided by ξ, denoted by $\lambda_{\xi,i}$ is

$$\lambda_{\xi,i} = \lambda_i + \mathrm{tb}(\Lambda_i)\mu_i.$$

Each μ_i is oriented so that

$$(\text{meridian, longitude, outward-pointing normal})$$

is a basis for $T\mathbb{R}^3$ agreeing with the usual orientation over ∂N (after rounding the edges of ∂N in the obvious fashion). See Figure 16.

9.2 First homology of the ambient space

The computation of $H_1(\mathbb{R}^3_{\Lambda\pm})$ easily follows from the fact that contact ± 1 surgery is a form of Dehn surgery. Suppose that $\mathbb{R}^3_L$ is a 3–manifold obtained by Dehn surgery on a smooth link $L = \bigcup L_i$ for which the surgery coefficients with respect to the Seifert

framing are p_i/q_i for relatively prime integers p_i and q_i. Writing μ_j for the oriented meridians of the L_i, we have the following theorem from Kirby calculus — see eg [52, Theorem 2.2.11]:

Theorem 9.2 *Denote by $\mathbb{R}^3_L$ a 3–manifold determined by a surgery diagram where each component L_i of L has Dehn surgery coefficient p_i/q_i for relative prime integers p_i and q_i. Then $H_1(\mathbb{R}^3_L)$ is presented with generators μ_i and relations*

$$p_i\mu_i + q_i \sum_{j\neq i} \operatorname{lk}(L_i, L_j)\mu_j = 0,$$

where $\operatorname{lk}(L_i, L_j)$ is the linking number.

When performing contact surgery on the component Λ_i of Λ, the meridian μ_i bounding a core disk of the surgery handle is sent to

$$\mu_i + c_i\lambda_{\xi,i} = (1 + c_i \operatorname{tb}(L_i))\mu_i + c_i\lambda_i.$$

Thus, for Legendrian knots in $\mathbb{R}^3$, contact ±1 surgery on Λ_i is topologically a $(\operatorname{tb}(\Lambda_i)\pm 1)$ surgery. From this computation, the calculation of $H_1(M)$ in Theorem 9.1 is then immediate.

9.3 Homology classes of Reeb orbits

In this section we describe how to compute homology classes of the Reeb orbits of α_ϵ. Our strategy will be to homotop orbits to the complement of N_ϵ in $\mathbb{R}^3_{\Lambda^\pm}$, after which the following computational tool may be applied:

Theorem 9.3 *Let γ be an oriented link in $\mathbb{R}^3 \setminus L$. Then the homology classes of γ in $H_1(\mathbb{R}^3 \setminus L)$ and $H_1(\mathbb{R}^3_L)$ is given by*

$$[\gamma] = \sum_i \operatorname{lk}(\gamma, L_i)\mu_i.$$

Proof Assume that γ is embedded and let $S \subset \mathbb{R}^3$ be a Seifert surface which transversely intersects the L_i. Punch holes in S near its intersections with the L_i, producing a surface S' which is disjoint from L and whose oriented boundary is a union of γ and a linear combination $\sum a_i\mu_i$. Then S' provides a cobordism from γ to these μ_i, providing an equivalence $[\gamma] = \sum a_i\mu_i$ in homology. By the definition of lk, we have $a_i = \operatorname{lk}(\gamma, L_i)$. □

Warning 9.4 The homotopies which we apply to closed Reeb orbits γ are not guaranteed to preserve the isotopy class of their embedding in $\mathbb{R}^3_{\Lambda^\pm}$ (assuming γ is embedded).

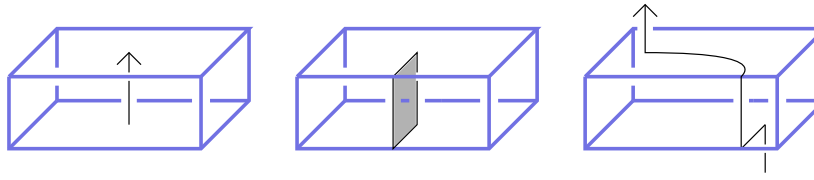

Figure 17: Homotoping a Reeb orbit into $\mathbb{R}^3 \setminus N_\epsilon$ as it passes through a $c = +1$ surgery handle.

Figure 17 demonstrates how to homotop a segment of a Reeb orbit γ into the exterior of the surgery handle N_ϵ as it passes through a component $N_{\epsilon,i}$ for which $c_i = 1$. The boxes represent the surgery handles with ∂_p pointing into the page, ∂_q pointing to the left, and ∂_z pointing up. On the left we have an arc parallel to the Reeb vector field entering the handle as seen from the inside of $N_{\epsilon,i}$. The arc extends in the ∂_z direction through the handle, along which it can be realized as being contained in the boundary of a square of the form $\{p \leq p_0, q = q_0\}$, depicted in gray. On the right, we see intersection of the boundary of this square with ∂N_ϵ as seen from the outside of the surgery handle $\mathbb{R}^3 \setminus N_\epsilon$. By homotoping γ across the gray disk, we obtain this arc shown on the right.

Figure 18 demonstrates the same procedure for orbits as they pass through surgery handles with surgery coefficient -1. In this case we consider squares of the form $\{p \geq p_0, q = q_0\}$ through which we homotop our arcs. Note that our choice of homotopy for both surgery coefficients is such that the homotoped arcs traverse ∂N in the ∂_q direction in which the components of Λ are oriented.

For a Reeb orbit γ, we can perform homotopies as described above at the tips of all chords in $\mathrm{cw}(\gamma)$ to push it to the exterior of N_ϵ. Away from the chords, we may arrange that the homotoped orbit traverses the $p = \mp\epsilon$ side of $N_{\epsilon,i}$ when the surgery coefficient of Λ_i is ± 1. The image of γ after homotopy is shown in the Lagrangian projection in Figure 19.

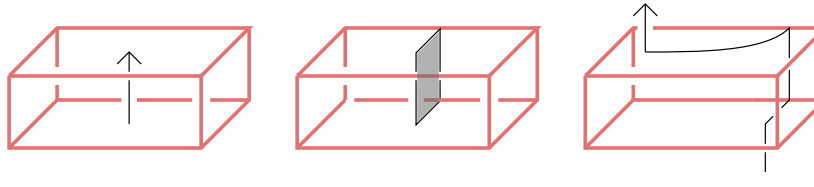

Figure 18: Homotoping a Reeb orbit into $\mathbb{R}^3 \setminus N_\epsilon$ as it passes through a $c = -1$ surgery handle.

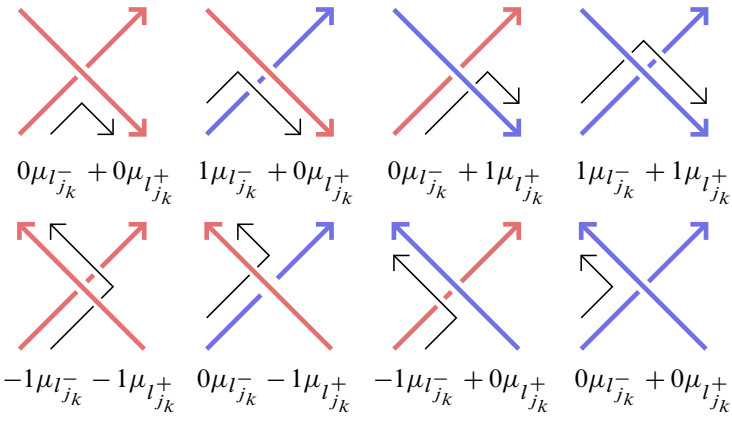

Figure 19: Here the homotopy described in Figures 17 and 18 are depicted in the Lagrangian projection. The top (bottom) row shows positive (negative) crossings of $\Lambda^{\pm}$. Each subfigure may be rotated by π. Local contributions to linking numbers are indicated below each subfigure.

The computation of homology classes of orbits in Theorem 9.1 then amounts to packaging the above observations algebraically:

Proof of Theorem 9.1 We homotop γ to $\mathbb{R}^3 \setminus N_\epsilon$ as described above and then apply Theorem 9.3. We write γ' for the image of γ under the homotopy. The linking number of two knots in $\mathbb{R}^3$ may be computed from a diagram as half of the signed count of crossings in the diagram. Therefore, in order to compute $[\gamma]$, it suffices to show that the signed count of crossings between γ' and each Λ_i is given by the μ_i coefficients in $\sum(\mathrm{cr}_{j_k} + \mathrm{cr}_{j_k, j_{k+1}})$.

In a neighborhood of a crossing, γ' will be as depicted in Figure 19 in the Lagrangian projection, where the contribution to the signed count of crossings between γ and the Λ_i is given by the terms

$$\tfrac{1}{2}((c^-_{j_k} + \mathrm{sgn}_{j_k})\mu_{l^-_{j_k}} + (c^+_{j_k} + \mathrm{sgn}_{j_k})\mu_{l^+_{j_k}}).$$

The formula may be verified on a case-by-case basis for each of the eight components of the figure. This is exactly the definition of cr_{j_k} given in (12).

Away from a crossing, γ' will continue following alongside arc components of the Λ_i, to the right (in the $p > 0$ direction) of Λ when the component of Λ has coefficient -1 and to the left otherwise as it travels from a crossing j_k to j_{k+1}. The contributions to the signed count of crossings with each of the Λ_i are given by the coefficients of μ_i in $\mathrm{cr}_{j_k, j_{k+1}}$ in the formula, as is clear from the definition of the crossing monomial. □

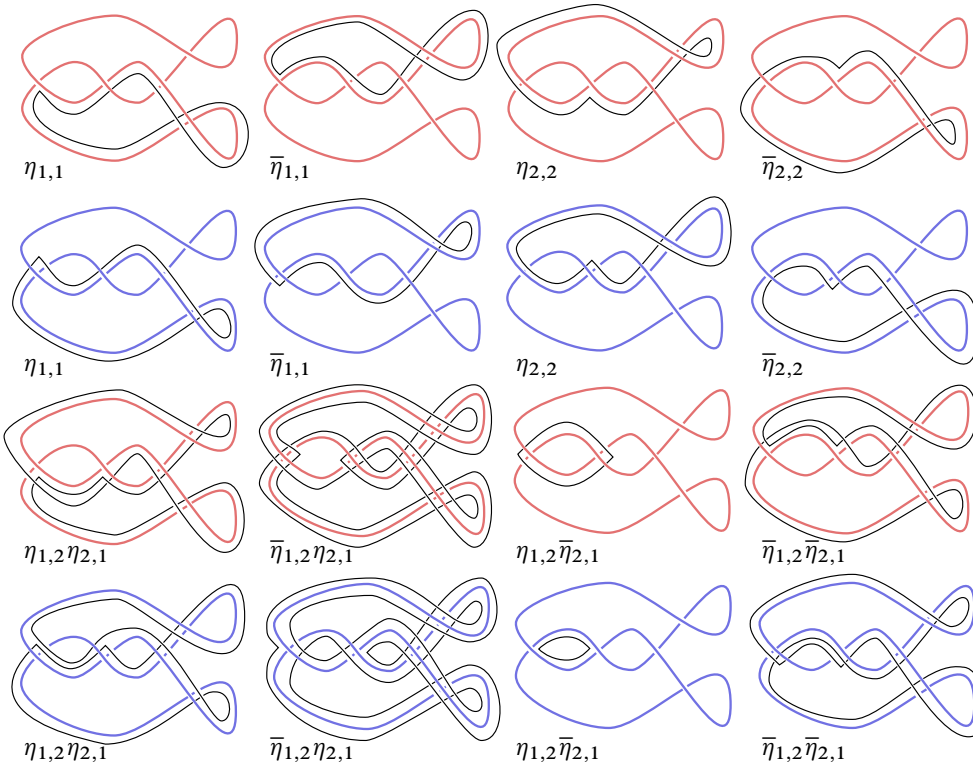

Figure 20: Push-outs of Reeb orbits in $(\mathbb{R}^3_{\Lambda^\pm}, \xi_{\Lambda^\pm})$, where Λ is the trefoil of Figure 6. Default orientations for Λ and hence for capping paths are determined by the arrow on Λ appearing in that figure. Each subfigure is labeled (to its lower-left) with the capping paths which determine the homotopy shown with homotoped Reeb orbits appearing in black.

9.4 Push-outs of Reeb orbits

We've demonstrated how squares of the form $\{p \leq p_0, q = q_0\} \subset N_\epsilon$ in the case of $+1$ surgery and of the form $\{p \geq p_0, q = q_0\}$ in the case of -1 surgery are used to homotop Reeb orbits into $\mathbb{R}^3_{\Lambda^\pm} \setminus N_\epsilon = \mathbb{R}^3 \setminus \epsilon$ so that the homotoped circles ride along some $\eta_{j_1,j_2} \subset \Lambda$ according to its prescribed orientation.

Squares of the form $\{p \geq p_0, q = q_0\}$ inside of a $c_i = +1$ component of Λ and of the form $\{p \leq p_0, q = q_0\}$ inside of a $c_i = -1$ component could also be used. As may be checked with the same local model — Figures 17 and 18 — but with opposite the prescribed orientation for Λ, we may use these squares to homotop an orbit γ to $\mathbb{R}^3 \setminus \epsilon$. Using these squares will result in the homotoped arcs riding along some $\overline{\eta}_{j_1,j_2} \subset \Lambda$.

We then have two choices of homotoping square each time our orbit γ passes through N_ϵ, with each choice corresponding to a choice of either a η_{j_1,j_2} or a $\overline{\eta}_{j_1,j_2}$. Hence, for a Reeb orbit $\gamma = (r_{j_1} \cdots r_{j_n})$, a choice of $\zeta_1, \dots, \zeta_n$ with each $\zeta_j \in \{\eta_{j_k,j_{k+1}}, \overline{\eta}_{j_k,j_{k+1}}\}$ determines a means of homotoping γ into $\mathbb{R}^3 \setminus N_\epsilon$.

Definition 9.5 Provided $\zeta_1, \dots, \zeta_n$ as above, we say that the homotopy class of the map of the circle in $\mathbb{R}^3 \setminus N_\epsilon$ determined by homotoping γ as described above is the *push-out of* $\zeta_1, \dots, \zeta_n$.

In other words, each orbit string — recall Definition 3.7 — determines instructions for homotoping γ into the complement of the surgery locus. Various examples are depicted in Figure 20, displaying all push-outs for orbits (r_1), (r_2) and $(r_1 r_2)$ for $\mathbb{R}^3_{\Lambda^\pm}$, where Λ is the trefoil of Figure 6 for both choices of surgery coefficient.

10 Surgery cobordisms and Lagrangian disks

The purpose of this section is to build symplectic cobordisms between the $(\mathbb{R}^3_{\Lambda^\pm}, \xi_{\Lambda^\pm})$ with specialized properties. We consider the following setup: Take $\Lambda \subset (\mathbb{R}^3, \xi_{\text{std}})$ in good position with $\Lambda^0 \subset \Lambda$ nonempty. After performing surgery on $\Lambda^\pm \subset \Lambda$, we have a contact form α_ϵ on $(\mathbb{R}^3_{\Lambda^\pm}, \xi_{\Lambda^\pm})$ and consider Λ^0 as a Legendrian link in $(\mathbb{R}^3_{\Lambda^\pm}, \xi_{\Lambda^\pm})$. We choose a constant $c = \pm 1$ and denote the contact manifold obtained by performing contact c surgery along $\Lambda^0 \subset (\mathbb{R}^3_{\Lambda^\pm}, \xi_{\Lambda^\pm})$ by $(\mathbb{R}^3_\Lambda, \xi_\Lambda)$; we also denote the contact form on $(\mathbb{R}^3_\Lambda, \xi_\Lambda)$ so obtained by α_ϵ. We write N^0_ϵ for a standard neighborhood of $\Lambda^0 \subset \mathbb{R}^3_{\Lambda^\pm}$, as described in Section 4.4, of size ϵ.

Theorem 10.1 *For any $\epsilon > 0$, there exists a positive constant $C > 0$ and a Liouville cobordism (W_c, λ_c) with the following properties*:

(1) *If $c = +1$, the convex end of the cobordism is $(\mathbb{R}^3_{\Lambda^\pm}, e^C \alpha_\epsilon)$ and the concave end is $(\mathbb{R}^3_\Lambda, e^{-C} \alpha_\epsilon)$.*

(2) *If $c = -1$, the convex end of the cobordism is $(\mathbb{R}^3_\Lambda, e^C \alpha_\epsilon)$ and the concave end is $(\mathbb{R}^3_{\Lambda^\pm}, e^{-C} \alpha_\epsilon)$.*

(3) *(W_c, λ_c) contains a disjoint collection of disks $\mathbb{D}_{c,i}$ along which $\lambda_c = 0$, bounding Λ^0 in the convex end of the cobordism when $c = +1$ and bounding Λ^0 in the concave end of the cobordism when $c = -1$.*

(4) *A finite symplectization*

$$([-C, C] \times (\mathbb{R}^3_{\Lambda^\pm} \setminus N^0_\epsilon), e^t \alpha_\epsilon)$$

of $(\mathbb{R}^3_{\Lambda^\pm}\setminus N^0_\epsilon)$ is contained in (W_c,λ_c), so that the restriction of its inclusion map to $(\partial[-C,C])\times(\mathbb{R}^3_{\Lambda^\pm}\setminus N^0_\epsilon)$ provides the obvious inclusions into $(\mathbb{R}^3_{\Lambda^\pm}, e^{\pm C}\alpha_\epsilon)$ and $(\mathbb{R}^3_{\Lambda}, e^{\pm C}\alpha_\epsilon)$.

We will construct (W_c,λ_c) by attaching 4–dimensional surgery handles to $\mathbb{R}^3_{\Lambda^\pm}$. As mentioned in the above theorem, the key properties of our cobordism are that

(1) we get exactly the contact forms α_ϵ on its boundaries, and

(2) all of the perturbations required to achieve this end happen within a standard neighborhood of Λ^0 whose size shrinks as ϵ tends to zero.

Then the analysis of Sections 4–7 applies to contact forms on the ends of our cobordisms without modification.

We are only slightly modifying known handle-attachment constructions — corresponding to the case $c=-1$ above — such as appear in Weinstein's original work [60] and Ekholm [18].

An outline of this section is as follows:

(1) In Section 10.1 we collect lemmas required to perturb contact forms on contactizations, being particularly interested in standard neighborhoods of Legendrian knots.

(2) In Section 10.2 we describe a square surgery handle sitting inside of $\mathbb{R}^4$ and outline the properties of its ambient geometry.

(3) In Section 10.4 we flatten the corners of the handle to prepare for later attachment.

(4) In Section 10.5 we describe Reeb dynamics on the convex end of this handle, showing that its flow is described as a Dehn twist.

(5) In Section 10.6 we modify the handle so that the Dehn twist determined by the Reeb flow is a linear Dehn twist as described in the gluing construction of Section 4.7.

(6) In Section 10.7 we finalize our construction by attaching our handle to finite symplectizations of $(\mathbb{R}^3_{\Lambda^\pm},\alpha_\epsilon)$.

10.1 Geometry of 1–forms on contactizations and their symplectizations

Let $(I\times W,\alpha=dz+\beta)$ be a contactization of an exact symplectic manifold (W,β) as in Section 2.3.2.

10.1.1 ξ–preserving perturbations We first look at how the Reeb vector field changes if we multiply α by a positive function, thereby preserving the contact structure.

Lemma 10.2 *Given $H \in \mathcal{C}^\infty(I \times W)$, the Reeb vector field R_H of the contact form*

$$\alpha_H = e^H(dz + \beta)$$

on $I \times W$ is

$$R_H = e^{-H}\Big((1 + \beta(X_H))\partial_z - X_H - \frac{\partial H}{\partial z} X_\beta\Big),$$

where X_H is computed with respect to $d\beta$.

This is a straightforward computation. We'll be interested in the following special case:

Lemma 10.3 *Suppose that $H = H(z, p)$ is a smooth function on $I \times I \times S^1$. Then the Reeb vector field of $\alpha_H = e^H(dz + p\,dq)$ is*

$$R_H = e^{-H}\Big(\Big(1 + p\frac{\partial H}{\partial p}\Big)\partial_z - \frac{\partial H}{\partial p}\partial_q - p\frac{\partial H}{\partial z}\partial_p\Big)$$

and the function pe^H is invariant under $\mathrm{Flow}^t_{R_H}$.

For the last item, we see that the projection of R_H onto the (z, p) coordinates is the Hamiltonian vector field associated to $dp \wedge dz$ and the function pe^{-H}.

10.1.2 ξ–modifying perturbations Now we study perturbations of α which modify ξ. Similar modifications of contact forms appear in [4, Definition 3.1.1; 14, Corollary 2.5].

Lemma 10.4 *Given a smooth function $h \in \mathcal{C}^\infty(I \times W, (0, \infty))$, the contact form*

$$\alpha_h = h\,dz + \beta$$

is contact if and only if

$$h\,d\beta + \beta \wedge dh$$

is a symplectic form on each $\{z\} \times W$. If this form is contact, its Reeb vector field R_h is

$$R_h = (h - \beta(X_h))^{-1}(\partial_z - X_h),$$

where X_h is computed with respect to $d\beta$. The contact structure $\xi_h = \ker(\alpha_h)$ is given by

$$\xi_h = \{hV - \beta(V)\partial_z : V \in TW\}.$$

The following technical result will allow us to modify the Reeb vector field on standard neighborhoods of Legendrians so that the flow map from the bottom to the top of the neighborhood realizes a Dehn twist τ_g associated to a function g. For applications to surgery later in this section, it will be important to keep track of the size of our neighborhood.

Proposition 10.5 *For positive constants $\epsilon_p, \epsilon_g > 0$, let $g = g(p)\colon I_{\epsilon_p} \to \mathbb{R}$ be a smooth function which vanishes for all orders on ∂I_{ϵ_p} and satisfies the pointwise bound $|g(p)| \leq \epsilon_g$. Then, for constants ϵ_z and ϵ_t satisfying*

$$\epsilon_p \epsilon_g \leq \tfrac{1}{2}\epsilon_z, \frac{\epsilon_t \epsilon_z}{2(1+\epsilon_t)},$$

there exists a function $h = h(z, p)$ on $I_{\epsilon_z} \times I_{\epsilon_p}$ and an exact symplectic manifold

$$([-\epsilon_t, 0] \times I_{\epsilon_z} \times I_{\epsilon_p} \times S^1, \lambda)$$

such that the following conditions hold:

(1) $\lambda|_{\{-\epsilon_t\}\times I_{\epsilon_z}\times I_{\epsilon_p}\times S^1} = e^{-\epsilon_t}(dz + p\,dq)$.

(2) $\lambda|_{\{0\}\times I_{\epsilon_z}\times I_{\epsilon_p}\times S^1} = \alpha_h$, *where α_h is as in Lemma 10.4 for a positive function h.*

(3) $s\alpha_h + (1-s)(dz + p\,dq)$ *is contact for all* $s \in [0, 1]$.

(4) $\alpha_h - (dz + p\,dq)$ *and all of its derivatives vanish along* $\partial(I_{\epsilon_z} \times I_{\epsilon_p} \times S^1)$.

(5) *The Reeb vector field R_h of α_h satisfies $dz(R_h) > 0$ everywhere.*

(6) *For each point $(p, q) \in I_{\epsilon_p} \times S^1$ a flow-line of R_h passing through $(-\epsilon_z, p, q)$ will pass through $(\epsilon_z, p, q + g(p))$.*

(7) *The Liouville vector field of λ agrees with ∂_t on a collar neighborhood of the boundary of its domain.*

Proof We first outline the contact forms we'll need. Consider functions of the form $h = 1 + F(z)G(p)$ on $I_{\epsilon_z} \times I_{\epsilon_p}$ and 1–forms

$$\alpha_h = h\,dz + p\,dq$$

as studied in Lemma 10.4. We assume $F \geq 0$ and that both F and G and all of their derivatives vanish on collar neighborhoods of the boundary of their domains. By Lemma 10.4, α_h is contact if and only if

$$0 < 1 + FG - pF\frac{\partial G}{\partial p}. \tag{46}$$

Second we outline the construction of Liouville forms which interpolate between $\alpha = dz + p\,dq$ and α_h. Consider functions E on an interval $[-\epsilon_t, 0]$ satisfying $E(-\epsilon_t) = 0$ and $E(0) = 1$ with $\partial^k E/\partial t^k = 0$ for all $k > 0$ at the endpoints of its domain and $\partial E/\partial t \geq 0$ everywhere. Define a 1–form

$$\lambda_{EFG} \in \Omega^1([0, \epsilon_t] \times I_{\epsilon_z} \times I_{\epsilon_p} \times S^1)$$

determined by

$$\lambda_{EFG} = e^t\big((1 + E(t)F(z)G(p))\,dz + p\,dq\big). \tag{47}$$

Then we compute

$$d\lambda_{EFG} \wedge d\lambda_{EFG} = e^{2t}\left(1 + EFG - pEF\frac{\partial G}{\partial p} + \frac{\partial E}{\partial t}FG\right) dt \wedge dz \wedge dp \wedge dq. \tag{48}$$

We seek to specify the E, F and G so that

(1) α_h is contact and its flow determines a Dehn twist by g,

(2) $d\lambda_{EFG}$ is symplectic, and

(3) the sizes of our neighborhood and symplectic cobordism — governed by the constants ϵ_z and ϵ_t — are reasonably small.

First we show that G is determined by g. If α_h is contact, its Reeb vector field is

$$R_h = \left(1 + FG - pF\frac{\partial G}{\partial p}\right)^{-1}\left(\partial_z - F\frac{\partial G}{\partial p}\partial_q\right).$$

This Reeb vector field is particularly friendly in that it preserves p and provides us with a separable ODE. For, provided an initial condition (z_0, p_0, q_0) and some $z > z_0$, we see that, after some time $t > 0$, $\mathrm{Flow}^t_{R_h}$ will pass through the point (z, p_0, q) with

$$q = q_0 - \frac{\partial G}{\partial p}\int_{z_0}^{z} F(Z)\, dZ.$$

In order to realize the flow from $\{-\epsilon_z\}\times\mathbb{R}\times S^1$ to $\{\epsilon_z\}\times\mathbb{R}\times S^1$ as a Dehn twist by g, we need

$$G(p) = -\left(\int_{-\epsilon_z}^{\epsilon_z} F(z)\, dz\right)^{-1}\int_{-\infty}^{p} g(P)\, dP.$$

This quantity is well defined by our presumption that g is compactly supported.

With this choice of G, the contact condition provided by (46) is equivalent to

$$F\cdot\left(\int_{-\infty}^{p} g(P)\, dP - pg(p)\right) \le \int_{-\epsilon_z}^{\epsilon_z} F(z)\, dz \tag{49}$$

for all (z, p, q). The condition that $d\lambda_{EFG}$ is symplectic provided by (48) is equivalent to

$$EF\cdot\left(\int_{-\infty}^{p} g(P)\, dP - pg(p)\right) + \frac{\partial E}{\partial t}F\cdot\left(\int_{-\infty}^{p} g(P)\, dP\right) \le \int_{-\epsilon_z}^{\epsilon_z} F(z)\, dz. \tag{50}$$

Now choose F and a constant ϵ_F so that

$$\epsilon_F = \sup|F(z)|, \quad \epsilon_F\epsilon_z = \int_{-\epsilon_z}^{\epsilon_z} F(z)\, dz.$$

It's easy to see by drawing pictures of bump functions that these choices can be made. Then (49) is satisfied so long as

$$\epsilon_p\epsilon_g \le \tfrac{1}{2}\epsilon_z$$

and, since $0 \leq E \leq 1$, we have that (50) is satisfied so long as

$$\Big(2 + \frac{\partial E}{\partial t}\Big)\epsilon_p \epsilon_g \leq \epsilon_z.$$

Choose E so that $\sup \partial E/\partial t = 2/\epsilon_t$. Then this last inequality, which we seek to satisfy, becomes

$$2(1+\epsilon_t^{-1})\epsilon_p\epsilon_g \leq \epsilon_z \iff \epsilon_p\epsilon_g \leq \frac{\epsilon_t\epsilon_z}{2(1+\epsilon_t)}. \qquad \square$$

10.2 The square handle

Having established the above lemmas, we proceed with the construction of our symplectic handle. Here we construct a square Weinstein handle sitting in $\mathbb{R}^4$.

Consider the Liouville form on $\mathbb{R}^4 = \mathbb{C}^2$,

$$\lambda_0 = \sum_1^2 2x_i\, dy_i + y_i\, dx_i.$$

This is a potential for the standard symplectic form $d\lambda_0 = dx_i \wedge dy_i$ with Liouville vector field

$$X_{\lambda_0} = 2x_i\,\partial_{x_i} - y_i\,\partial_{y_i},$$

whose time t flow is given by

$$\mathrm{Flow}^t_{X_{\lambda_0}}(x,y) = (e^{2t}x, e^{-t}y). \tag{51}$$

For $\rho_0 > 0$, consider also the convex set with corners

$$\mathbb{D}_{\rho_0} \times \mathbb{D} = \{|x| \leq \rho_0,\, |y| \leq 1\} \subset \mathbb{R}^4,$$

whose smooth boundary strata we denote by

$$M^+_{\rho_0} = \partial\mathbb{D}_{\rho_0} \times \mathbb{D}, \quad M^-_{\rho_0} = \mathbb{D}_{\rho_0} \times \partial\mathbb{D}.$$

Then X_{λ_0} is positively transverse to the $M^\pm_{\rho_0}$ if we equip $M^+_{\rho_0}$ with the outward-pointing orientation and equip $M^-_{\rho_0}$ with its inward-pointing orientation. Therefore, $\lambda_0|_{M^\pm}$ is contact. Applying $\mathrm{Flow}^t_{X_{\lambda_0}}$ for $t \in (-\infty, 0]$, we have embeddings of the negative half-infinite symplectizations of the $(M^\pm_{\rho_0}, \lambda_0|_{TS^\pm})$ into $\mathbb{R}^4$,

$$\mathrm{Flow}^t_{X_{\lambda_0}} \circ i^\pm \colon (-\infty, 0] \times M^\pm_{\rho_0} \to \mathbb{R}^4, \tag{52}$$

where $i^\pm \colon M^\pm_{\rho_0} \to \mathbb{R}^4$ denote the inclusion mappings.

10.2.1 Reeb trajectories across the square handle The Reeb vector field R_{ρ_0} along $M^+_{\rho_0}$ is

$$R_{\rho_0} = \frac{1}{2\rho_0^2} x_i\,\partial_{y_i} \implies \mathrm{Flow}^t_{R_{\rho_0}}(x,y) = \Big(x, y + \frac{t}{2\rho_0^2}x\Big).$$

Starting at points $(x_\theta, y_0) = (\rho_0 \cos(\theta), \rho_0 \sin(\theta), 1, 0)$, Reeb trajectories are

$$\mathrm{Flow}^t_{R_{\rho_0}}(x_\theta, y_0) = \left(\rho_0 \cos(\theta), \rho_0 \sin(\theta), 1 + \frac{t}{2\rho_0}\cos(\theta), \frac{t}{2\rho_0}\sin(\theta)\right).$$

In order that such a trajectory does not immediately exit $M^+_{\rho_0}$ (maintaining the condition $|y| \le 1$ for small $t \ge 0$), we must have $\theta \in \left[\frac{1}{2}\pi, \frac{3}{2}\pi\right]$. These trajectories touch $\partial M^+_{\rho_0}$ when

$$1 = \left(1 + \frac{t}{2\rho_0}\cos(\theta)\right)^2 + \left(\frac{t}{2\rho_0}\sin(\theta)\right)^2 \iff -4\rho_0 \cos(\theta) = t,$$

at which point the y coordinate will be

$$\begin{aligned} y_\theta &= (1 - 2\cos^2(\theta), -2\cos(\theta)\sin(\theta)) = (-\cos(2\theta), -\sin(2\theta)) \\ &= (\cos(2\theta - \pi), \sin(2\theta - \pi)). \end{aligned}$$

We can then measure the angle from y_0 to y_θ as $2\theta - \pi \in [0, 2\pi]$.

10.3 Identification of the concave end of the handle as a 1–jet space

We define an embedding of a standard neighborhood of a Legendrian into M_1^- as

$$\Phi_-(z, p, q) = \left(z\cos - \frac{p}{2\pi}\sin, z\sin + \frac{p}{2\pi}\cos, \cos, \sin\right),$$

where the arguments of cos and sin are both $2\pi q$. The map parametrizes M_1^- so that

(1) $2\pi q$ is the angle in the y–plane,

(2) $z = x \cdot y$,

(3) $p = x \cdot \partial y/\partial q$, and

(4) $|x|^2 = z^2 + (p/2\pi)^2$.

The tangent map of Φ_- is

$$T\Phi_- = \begin{pmatrix} \cos & -(1/2\pi)\sin & -2\pi z \sin - p\cos \\ \sin & (1/2\pi)\cos & 2\pi z \cos - p \sin \\ 0 & 0 & -2\pi \sin \\ 0 & 0 & 2\pi \cos \end{pmatrix}$$

with incoming basis $\{\partial_z, \partial_p, \partial_q\}$ and outgoing basis $\{\partial_{x_1}, \partial_{x_2}, \partial_{y_1}, \partial_{y_2}\}$, from which it follows that

$$\Phi_-^* \lambda_0 = dz + p\, dq.$$

We can extend Φ_- to an embedding of the symplectization of the 1–jet space into $\mathbb{R}^4$ by

$$\begin{aligned}(53)\quad \overline{\Phi}_-(t,z,p,q) &= \mathrm{Flow}^t_{X_{\lambda_0}} \circ \Phi_-(z,p,q)\\ &= \Big(e^{2t}\Big(z\cos -\frac{p}{2\pi}\sin\Big), e^{2t}\Big(z\sin +\frac{p}{2\pi}\cos\Big), e^{-t}\cos, e^{-t}\sin\Big).\end{aligned}$$

By (51) and $\mathcal{L}_{X_{\lambda_0}}\lambda_0 = \lambda_0$, we have

$$(54)\qquad \overline{\Phi}_-^*\lambda_0 = e^t(dz + p\,dq).$$

10.4 Shaping the handle

Here we shape our handle so that the manifold obtained by the handle attachment will be smooth. Moreover, we will choose a specific shape which allows us to control Reeb dynamics on the surgered contact manifold.

Pick a positive constant $\rho_1 < \rho_0$ and a smooth function $B = B(\rho)\colon (0,\infty) \to [0,\infty)$ satisfying the conditions

(1) $B(\rho) = \log\sqrt{\rho_0/\rho} = -\frac{1}{2}(\log\rho - \log\rho_0)$ for $\rho \in (0,\rho_1)$,

(2) $B(\rho) = 0$ for $\rho > \rho_0$, and

(3) $0 \le -\partial B/\partial\rho < \rho^{-1}$ everywhere.

Along $\rho \in (0,\rho_1)$, we have $\partial B/\partial\rho = -1/2\rho$, so that our last condition is satisfied. To find such a function B, we can take a smoothing of the piecewise-smooth function

$$(55)\qquad B^{\mathrm{PW}}(\rho) = \begin{cases} \log\sqrt{\rho_0/\rho} & \text{if } \rho \le \rho_0,\\ 0 & \text{if } \rho \ge \rho_0.\end{cases}$$

Let $N = I \times I \times S^1$ be a standard neighborhood of a Legendrian Λ with $\Lambda = \{0\}\times\{0\}\times S^1$. Using the function B, we define an embedding

$$\Phi_H\colon (N\setminus\Lambda) \to \mathbb{R}^4, \quad \Phi_H = \mathrm{Flow}^H_{X_{\lambda_0}} \circ \Phi_-,$$

where

$$H(p,z) = B(\rho(p,z)), \quad \rho(p,z) = \sqrt{z^2 + \Big(\frac{p}{2\pi}\Big)^2}.$$

We outline some important properties of the map Φ_H:

(1) From (54), $\Phi_H^*\lambda_0 = e^H(dz + p\,dq)$.

(2) Along the set $\{z^2 + (p/2\pi)^2 \ge \rho_0\}$, Φ_H is the same as Φ_-.

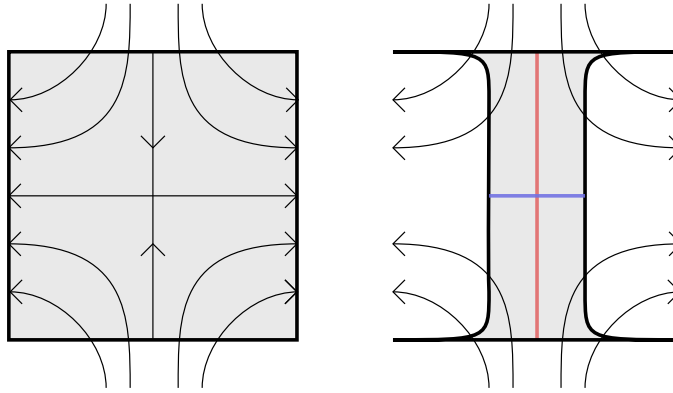

Figure 21: On the left is the square handle $\mathbb{D}_{\rho_0} \times \mathbb{D}$ and on the right is the handle W_H. Flow-lines of X_{λ_0} transversely pass through $M^{\pm}_{\rho_0}$ and M_H. The Lagrangian disks $\{x = 0\}$ and $\{y = 0\}$ are shown in red and blue, respectively.

(3) From the first property characterizing B and (53), we see that, on the set $\{\rho \le \rho_1\}$, the x and y coordinates of the embedding satisfy

$$\begin{aligned} |x \circ \Phi_H(z, p, q)| &= e^{2H}\sqrt{z^2 + \left(\frac{p}{2\pi}\right)^2} = \rho_0, \\ |y \circ \Phi_H(z, p, q)| &= e^{-H} = \sqrt{\frac{\rho}{\rho_0}}. \end{aligned} \tag{56}$$

From the last equation, we have the equivalences

$$\begin{aligned} \Phi_H(\{\rho \le \rho_1\}) &= \left\{|x| = \rho_0, |y| \le \sqrt{\frac{\rho_1}{\rho_0}}\right\} \setminus \{y = 0\}, \\ \overline{\Phi_H(\{\rho \le \rho_1\})} &= \left\{|x| = \rho_0, |y| \le \sqrt{\frac{\rho_1}{\rho_0}}\right\}. \end{aligned}$$

The closure of the image of Φ_H in $\mathbb{R}^4$ is a smooth hypersurface M_H which is positively transverse to X_{λ_0}. We write M_H for this hypersurface and define $W_H \subset \mathbb{R}^4$ to be the set enclosed by M_1^- and M_H. The handle W_H is depicted in Figure 21, right.

10.5 Analysis of R_H over M_H

Here we analyze dynamics on M_H of the Reeb vector field R_H for the contact form $\alpha_H = \lambda_0|_{M_H}$. Because of our use of the imprecisely defined function B, we won't be able to solve for $\mathrm{Flow}^t_{R_H}$ explicitly. However, we'll be able to capture enough information about this flow for the applications to handle attachment.

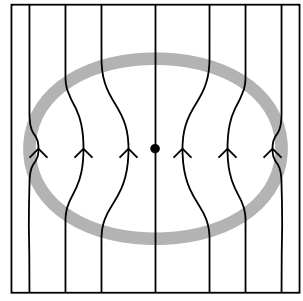

Figure 22: Projections of flow-lines of R_H to the (p,z) coordinates. By Lemma 10.3, these are the level sets of pH. Here p points to the right and z points upward. The dot represents the circle $|x|=0$ along which our flow is not defined in the (z,p,q) coordinate system. The region $\rho\in[\rho_1,\rho_0]$ where the function B^{PW} is smoothed to obtain B is shaded.

On the complement of the set $\{z=p=0\}$, our contact form is $\alpha_H=e^H(dz+p\,dq)$, whose Reeb field will be denoted by R_H. Writing $\rho=\rho(p,z)$, we compute

$$dH=\frac{\partial B}{\partial\rho}\,d\rho,\quad d\rho=\rho^{-1}\Big(z\,dz+\frac{p}{(2\pi)^2}\,dp\Big).$$

Now apply Lemma 10.3 to compute R_H using the coordinates (z,p,q) on $M_H\setminus\{y=0\}$ as

$$R_H=e^{-H}\Big(\Big(1+\frac{\partial B}{\partial\rho}\rho^{-1}\Big(\frac{p}{2\pi}\Big)^2\Big)\partial_z-\frac{p}{\rho}\frac{\partial B}{\partial\rho}\Big(\frac{1}{(2\pi)^2}\partial_q+z\partial_p\Big)\Big). \tag{57}$$

Here is a collection of observations regarding R_H and its flow:

(1) The ∂_z part of R_H is always strictly positive. This is a consequence of the inequalities

$$-\frac{\partial B}{\partial\rho}\rho^{-1}\Big(\frac{p}{2\pi}\Big)^2\le-\frac{\partial B}{\partial\rho}\rho^{-1}\rho^2=-\frac{\partial B}{\partial\rho}\rho<1\implies 1+\frac{\partial B}{\partial\rho}\rho^{-1}\Big(\frac{p}{2\pi}\Big)^2>0$$

following from the definition of ρ and the third defining property of the function B.

(2) For each p and $\epsilon>0$, a flow-line starting at the point $(-\epsilon,p,q)$ will pass through some (ϵ,p,q'). This follows from the facts that $(pe^{-H})(-z,p)=(pe^{-H})(z,p)$ and that the projection of R_H onto the (z,p)–plane is Hamiltonian with respect to $dp\wedge dz$ as per Lemma 10.3. See Figure 22.

(3) The flow-line passing through $(-\epsilon,0,q)$ will pass through the point $\big(\epsilon,0,q+\frac{1}{2}\big)$. To see this, observe that such a flow-line with such an initial condition must flow up into the circle $\{z=p=0\}$ along the line $\{p=0\}$ and compare with the definition of the map Φ_H.

(4) A twist map $f_{H,\rho_0}\colon I_{2\pi\rho_0} \to S^1$ is defined by following the flow-line of R_H passing through $(-\epsilon, p, q)$ to a point $(\epsilon, p, q + f_{H,\rho_0}(p))$. By the properties we've used to specify B, the derivatives of f_{H,ρ_0} are supported on $I_{2\pi\rho_0}$ as R_H coincides with ∂_z outside of this region. Likewise, $R_H = \partial_z$ on $\{|\rho| \geq \rho_0\}$.

(5) The twist map satisfies

$$f_{H,\rho_0}(-p) = -f_{H,\rho_0}(p), \quad f_{H,\rho_0}(-2\pi\rho_0) = f_{H,\rho_0}(2\pi\rho_0) = 0.$$

The first equality follows from the fact that the ∂_z factor of R_H is a function of p^2 while the ∂_p and ∂_q factors are antisymmetric in p. The second equality follows from the previous item.

(6) As $\partial B/\partial p \leq 0$, the ∂_q coefficient of R_H from (57) has sign equal to $\operatorname{sgn}(p)$ where is it nonzero. Hence, f_{H,ρ_0} always twists to the right for $p < 0$ and to the left along $p > 0$. This is the expected behavior of a positive Dehn twist.

Proposition 10.6 *Write $\tilde{f}_{H,\rho_0}\colon I_{2\pi\rho_0} \to \mathbb{R}$ for the lift of the twist map $f_{H,\rho_0}\colon I_{2\pi\rho_0} \to \mathbb{R}$ with initial condition*

$$\tilde{f}_{H,\rho_0}(-2\pi\rho_0) = 0 \quad \Longrightarrow \quad \tilde{f}_{H,\rho_0}(0) = -\tfrac{1}{2}, \quad \tilde{f}_{H,\rho_0}(2\pi_{\rho_0}) = -1$$

by the preceding analysis. Suppose that $\tilde{f}\colon I_{2\pi_{\rho_0}} \to [-1, 0]$ is a decreasing function also satisfying the above equalities. Then, for H constructed using a function B which is sufficiently C^0–close to the function B^{PW}, the estimate

$$|\tilde{f}_{H,\rho_0}(p) - \tilde{f}(p)| \leq \tfrac{1}{2} \tag{58}$$

is satisfied for all $p \in I_{2\pi\rho_0}$.

Proof The analysis of Section 10.2.1 provides a very explicit approximation of the function $\tilde{f}_{H,\rho_0}$. Let's consider the degenerate case when $B = B^{\mathrm{PW}}$ as described in (55), writing H^{PW} for the associated piecewise-smooth function. Then $M_{H^{\mathrm{PW}}}$ will be piecewise smooth as a submanifold of $\mathbb{R}^4$. We have a C^0 flow on $M_{H^{\mathrm{PW}}}$ given by following ∂_z on $M_{H^{\mathrm{PW}}} \setminus M^+_{\rho_0}$ and by following R_{ρ_0} on $M^+_{\rho_0}$. We can view $M_{H^{\mathrm{PW}}}$ as a smooth manifold by viewing its nonsmooth part to be the graph of a C^0 function, and observe that M_H and $M_{H^{\mathrm{PW}}}$ coincide along the sets $|x| \geq \rho_0$.

We look at flow trajectories passing over the $q = 0$ slice of our neighborhood, which corresponds to the $y = y_0$ subset of $M_{H^{\mathrm{PW}}}$. Then $\Phi_{H^{\mathrm{PW}}}$ maps the arc

$$A = \left\{ z = -\sqrt{\rho_0^2 - \left(\frac{p}{2\pi}\right)^2}, q = 0 \;\middle|\; p \in [-2\pi\rho_0, 2\pi\rho_0] \right\}$$

to the semicircle

$$\left\{\left(-\sqrt{\rho_0^2-\left(\frac{p}{2\pi}\right)^2},\frac{p}{2\pi},1,0\right)\;\middle|\;p\in[-2\pi\rho_0,2\pi\rho_0]\right\}\subset M_{H^{\mathrm{PW}}}. \tag{59}$$

In the language of Section 10.2.1, this semicircle is the set

$$\left\{(x_\theta,y_0)\mid\theta\in\left[\tfrac{1}{2}\pi,\tfrac{1}{2}3\pi\right]\right\}\subset\mathbb{R}^4$$

equipped with a clockwise parametrization (determined by the variable p). When a trajectory passes through the handle entering at angle $\theta=\theta(p)\in\left[\frac{1}{2}\pi,\frac{3}{2}\pi\right]$ determined by p in the x–plane, it will come out on the top of our neighborhood at angle $2\theta-\pi$, as described in Section 10.2.1. Therefore, when using the piecewise-smooth handle, the lift $\tilde{f}_{H,\rho_0}$ of our continuous flow map $f_{H^{\mathrm{PW}},\rho_0}$ can be written as

$$\tilde{f}_{H^{\mathrm{PW}},\rho_0}(p)=\begin{cases}0 & \text{if } p<-2\pi\rho_0,\\ (1/2\pi)(2\theta(p)-\pi) & \text{if } p\in[-2\pi\rho_0,2\pi\rho_0],\\ -1 & \text{if } p>2\pi\rho_0,\end{cases}$$

where $\theta(p)$ is the angle in the x–plane given by (59).

As the p coordinate wraps around the semicircle of (59) in a clockwise fashion, we conclude that $\tilde{f}_{H^{\mathrm{PW}},\rho_0}$ is a decreasing function. Moreover, $\tilde{f}_{H,\rho_0}(-2\pi\rho)=0$, $\tilde{f}_{H^{\mathrm{PW}},\rho_0}(0)=-\frac{1}{2}$ and $\tilde{f}_{H^{\mathrm{PW}},\rho_0}(-2\pi\rho)=-1$, just like our test function $\tilde{f}$. Therefore, both $\tilde{g}=\tilde{f}$, $\tilde{f}_{H^{\mathrm{PW}},\rho_0}$ must satisfy

$$\tilde{g}([-2\pi\rho_0,0])=\left[-\tfrac{1}{2},0\right],\quad \tilde{g}([0,2\pi\rho_0])=\left[-\tfrac{1}{2},-1\right]. \tag{60}$$

From this we conclude that (58) holds for $\tilde{f}_{H^{\mathrm{PW}},\rho_0}$ given any function $\tilde{f}$ satisfying the required properties.

Now we suppose that B is smooth and $\mathcal{C}^0$–close to B^{PW}. Then the twist map $\tilde{f}_{H,\rho_0}$ will be $\mathcal{C}^0$–close to $\tilde{f}_{H^{\mathrm{PW}},\rho_0}$. This is because the twist map is entirely determined by the flow of the arc A across the surgery handle. All Reeb trajectories starting at points in A which pass through the $|y|<1$ portion of the handle will intercept the region $\rho\in[\rho_1,\rho_0]$ where B^{PW} is smoothed to obtain B. See Figure 22.

Because of item (6) in the observations preceding this proof, $\tilde{f}_{H,\rho_0}(p)<0$ for $p<0$, we can guarantee to that $\tilde{f}_{H,\rho_0}$ satisfies $\tilde{g}([-2\pi\rho_0,-\delta])\subset\left[-\frac{1}{2},0\right]$ for some arbitrarily small $\delta>0$. Therefore, we have $|\tilde{f}_{H,\rho_0}(p)-\tilde{f}(p)|\leq\frac{1}{2}$ for $p\in[-2\pi\rho_0,-\delta]$. By continuity we can also ensure that the desired inequality holds for $p\in[-\delta,0]$ by making B $\mathcal{C}^0$–close enough to B^{PW}. The same arguments with modified notation apply to ensure that (58) holds over $[0,2\pi\rho_0]$ for B close enough to B^{PW}. □

10.6 Perturbing λ_0

Now that we've shown that the flow from the set $\{z = -\rho_0\}$ to the set $\{z = \rho_0\}$ defined by R_H is determined by a Dehn twist by f_{H,ρ_0}, which is supported on $I_{2\pi\rho_0} \times S^1$. Moreover, equation (58) tells us that we can use Proposition 10.5 to correct λ_0 so that the flow over our handle will be an "approximately linear twist" satisfying Assumptions 5.4. We now carry out the details of this correction.

We construct a new coordinate system (z, p, q) on M_H as follows: On the set

$$\{|y| = 1, |x| > \rho_0\},$$

we have coordinates (p, q, z) on M_H coming from the embedding Φ_- as M_1^- and M_H overlap on this region. To get a standard coordinate system on M_H, apply the map

$$(z, p, q) \mapsto \mathrm{Flow}_{R_H}^{z+\rho_0} \circ \Phi_-(-\rho_0, p, q), \quad z \in I_{\rho_0}. \tag{61}$$

With respect to this coordinate system,

$$\lambda_0|_{M_H} = dz + p\, dq.$$

Due to our identification of the flow from the top to bottom of this region — with respect to the (z, p, q) coordinates on M_- — as being determined by a Dehn twist by $f_{H,\delta}$, the change of coordinates on the overlap

$$(M_H \setminus \{\rho < \rho_0\}) \to M_1^-$$

is given exactly as the gluing map of Section 4.7 with the "height perturbation function" — denoted in that section by $H_{f,\epsilon}$ — uniquely determined by f_{H,ρ_0}.

We seek to modify $f_{H,\epsilon}$ using Proposition 10.5 so that the flow over the convex boundary of our handle satisfies the linear dynamics assumptions described in Assumptions 5.4. To this end, let $g\colon I_{2\pi\rho_0} \to \mathbb{R}$ be a function satisfying the following properties:

(1) A Dehn twist by $f_{\rho_0}(0) = f_{H,\rho_0}(p) + g(p)$ satisfies Assumptions 5.4 with $\partial f_{\rho_0}/\partial p(0) = (2\pi\rho_0)^{-1}$.

(2) $|g(p)| \le \frac{1}{2}$.

(3) g and all of its derivatives vanish along $\partial I_{2\pi\rho_0}$.

Such a choice of g is possible by (58). According to Proposition 10.5, using

$$\epsilon_p = \epsilon_z = 2\pi\rho_0, \quad \epsilon_g = \tfrac{1}{2} \tag{62}$$

and ϵ_t arbitrarily large, we can modify the contact form within the coordinate system on M_H by

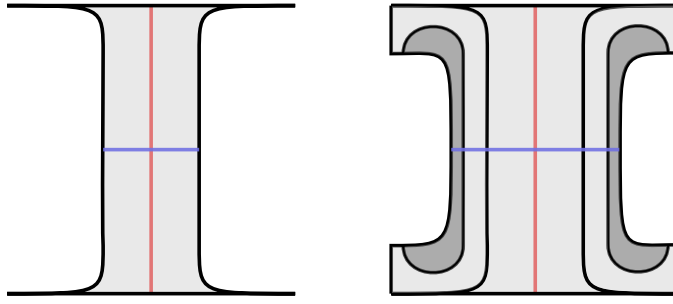

Figure 23: On the left, the rounded handle W_H of Figure 21. On the right, the perturbed handle $W \subset \mathbb{R}^4$. The region along which λ_0 is modified — as in Proposition 10.5 — is shaded in dark gray. The lightly shaded extension of W_H indicates extension by the Liouville flow.

(1) adding a finite symplectization $([0, e^{\epsilon_t}] \times M_H, \lambda_0 = e^t(dz + p\,dq))$ to obtain a handle $W \subset \mathbb{R}^4$ containing W_H, and

(2) perturbing λ_0 within a proper subset of this region to obtain a contact form λ on W,

so that the flow over M_H in the coordinates (z, p, q) is given by a Dehn twist by f_{ρ_0}. A schematic for this extension and perturbation is depicted in Figure 23, right.

Now we rework through (61) and its consequences this time using the new Reeb vector field R. The map

$$(z, p, q) \mapsto \mathrm{Flow}_R^{z+\rho_0} \circ \Phi_-(-\rho_0, p, q) \tag{63}$$

will provide us with a coordinate system (z, p, q) on the convex boundary of W. Now our attaching map is determined by the composition of the Dehn twists

$$(p, q) \mapsto (p, q + g(p)), \quad (p, q) \mapsto (p, q + f_{H,\rho_0}),$$

yielding a Dehn twist by f_{ρ_0}, as desired.

10.7 Attaching the handle to finite symplectizations

To finish our construction, we attach the handle (W, λ) to a finite symplectization of $(\mathbb{R}^3_{\Lambda^\pm}, \alpha_\epsilon)$. In doing so, we will omit the specific choices of ρ_0 required provided that they are determined by ϵ as described in Definition 4.10. Likewise, we assume that Λ^0 consists of a single connected component to simplify notation.

We first consider the case $c = -1$; the map Φ_- provides us with an identification of standard neighborhood N^0_ϵ of Λ^0. The map Φ_- provides us with an identification

of this neighborhood with the convex end of the handle W. By considering $\mathbb{R}^3_{\Lambda^\pm}$ as being contained in the top of a finite symplectization $[-C,0]\times\mathbb{R}^3_{\Lambda^\pm}$, we may attach the handle W via this identification to obtain a 4–manifold along which we set

$$\lambda_{-1}|_W=\lambda,\quad \lambda_{-1}|_{[-C,0]\times\mathbb{R}^3_{\Lambda^\pm}}=e^t\alpha_\epsilon.$$

Outside of a neighborhood of the form $\{\rho(p,z)<\text{const}\}\subsetneq\{0\}\times N^0_\epsilon$, we may extend by some $[0,C]\times\mathbb{R}^3_{\Lambda^\pm}\setminus\{|z|+|p|<\text{const}\}$, over which we take

$$\lambda_{-1}|_{[0,C]\times\mathbb{R}^3_{\Lambda^\pm}\setminus\{\rho(p,z)<\text{const}\}}=e^t\alpha_\epsilon.$$

The constant C may be chosen so that the top of this region coincides with the convex end of the handle W. By the fact that the perturbation of λ described in the previous subsection occurs away from the attaching locus, W_{-1} is smooth with λ_{-1} determining a smooth form, as desired. The disk $\mathbb{D}_{-1}$ is obtained by taking the intersection of the plane $\{|x|=0\}\subset\mathbb{R}^4$ with the handle $W_H\subset W$, depicted as the red line in Figures 21 and 23, and then extending through $[-C,0]\times\mathbb{R}^3_{\Lambda^\pm}$ by a Lagrangian cylinder $[-C,0]\times\Lambda^0$.

Now set $c=+1$. In this case our disk $\mathbb{D}_{+1}$ is taken to be the intersection of the plane $\{|y|=0\}$ with the handle W. According to (47), $\lambda|_{\mathbb{D}_{+1}}=0$. Using the coordinates (p,q,z) on (63), we may identify a neighborhood of the boundary of this disk with a standard neighborhood of Λ^0, which we may consider as being contained in the bottom of a finite symplectization $[0,C]\times\mathbb{R}^3_{\Lambda^\pm}$. We extend the disk by a Lagrangian cylinder over Λ^0 within $[0,C]\times\mathbb{R}^3_{\Lambda^\pm}$ so that its boundary lies in $\{C\}\times\mathbb{R}^3_{\Lambda^\pm}$. To complete the construction of our Liouville cobordism (W_{+1},λ_{+1}), we layer on $[-C,0]\times\mathbb{R}^3_{\Lambda^\pm}\setminus\{|z|+|p|<\text{const}\}$ so that the concave end of the cobordism is smooth and coincides with $(\mathbb{R}^3_\Lambda,\alpha_\epsilon)$.

11 Holomorphic foliations, intersection numbers and the Λ quiver

In this section we describe some tools which allow us to frame geometric questions regarding holomorphic curves in the 4–manifolds relevant to this article — symplectizations and surgery cobordisms — as algebraic problems. We will largely be relying on intersection positivity for holomorphic curves in 4–manifolds [47, Appendix E] and basic algebraic topology.

These tools serve to establish some properties of holomorphic curves in $\mathbb{R}\times\mathbb{R}^3_{\Lambda^\pm}$ and surgery cobordisms which we believe to be true intuitively but which are more difficult to articulate precisely: curves with "high energy" should look like Legendrian *RSFT*

disks as they pass through the complement of the surgery locus N_ϵ while "low energy" curves should be trapped inside of the union of N_ϵ with a neighborhood of the chords of Λ and have constrained asymptotics. This will be formalized in Section 11.7 as the *exposed/hidden alternative*.

The first three subsections deal with geometry: In Section 11.1, we describe special almost-complex structures on contactizations and how combinatorial *LRSFT* disks can be "lifted" to holomorphic disks. Section 11.2 described how these complex structures J can be used on large open subsets of symplectizations and surgery cobordisms. Next, in Section 11.3, we show that such J endow open subsets of our 4–manifolds with a foliation by J–holomorphic planes. This is another area of analysis which is considerably simplified by working with $(\mathbb{R}^3_{\Lambda^\pm}, \xi_{\Lambda^\pm})$ rather than $(S^3_{\Lambda^\pm}, \xi_{\Lambda^\pm})$.

The remainder of the section is concerned with algebra: Section 11.4 describes some properties of intersections between these planes and finite-energy holomorphic curves asymptotic to chords and orbits of the R_ϵ. These intersection numbers are essentially homological invariants of curves. In the event that the intersection numbers all vanish, an alternative bookkeeping device can be used to keep track of holomorphic curves — an object we call the Λ *quiver*, Q_Λ. This quiver can be used as an algebraic tool to encode $\mathrm{LCH}^{\mathrm{cyc}}$ chain complexes — see Remark 4.1 of [7] — but we will be most interested in the fact that it is a quotient of a space homotopy equivalent to the complement of the $\mathbb{C}$–foliated region of our 4–manifold.

11.1 Model almost-complex structures on symplectizations of contactizations of Stein manifolds

Here we review some generalities regarding holomorphic curves in symplectizations of contactizations of Stein manifolds. For the purposes of this paper, we're really only interested in the cotangent bundles of the real line — for $(\mathbb{R}^3, \xi_{\mathrm{std}})$ is the 1–jet space of $\mathbb{R}$ — though the results are no harder to state or prove in fuller generality. The results here are known; for example, they are implicit in the convexity arguments of [14] and definitions of LCH moduli spaces in [19].

Let W be a manifold of dimension $2n$ with complex structure J and suppose that $F \in C^\infty(\Sigma)$ is such that

$$\beta = -dF \circ J$$

is a Liouville form on W. In other words, (W, J, F) is a *Stein manifold* except that we have omitted any requirements regarding transversality between X_β and ∂W. Define a

contact 1–form $\alpha = dz + \beta$ on $\mathbb{R} \times W$ so that

$$\xi = \{V - \beta(V)\partial_z : V \in TW\}$$

for $V \in TW$. We can define a J' adapted to the symplectization of $(\mathbb{R} \times W, \alpha)$ by

$$J'\partial_t = \partial_z, \quad J'(V - \beta(V)\partial_z) = JV - \beta(JV)\partial_z.$$

As previously mentioned, we're primarily concerned with the cases $W = \mathbb{R} \times I$ for a 1–manifold I with $\beta = p\,dq = -\frac{1}{2}d(p^2) \circ j$. We get $(\mathbb{R}^2, -y\,dx)$ by a change of coordinates.

Lemma 11.1 *If a map $(t, z, u)\colon \Sigma' \to \mathbb{R} \times \mathbb{R} \times W$ is (J', j)–holomorphic, then*

(1) *z is harmonic, and*

(2) *u is (J, j)–holomorphic.*

Moreover, if Σ' is simply connected and we have (z, u) for which z is harmonic and u is (J, j)–holomorphic, then there exists $t\colon \Sigma' \to \mathbb{R}$ for which (t, z, u) is (J', j)–holomorphic. Such t is unique up to addition by a constant.

Proof This is a local calculation: Take coordinates x and y on $\mathbb{D}$, which we may consider being contained in Σ' with j denoting the standard complex structure on $T\mathbb{D}$. We will be studying (7).

Write $\overline{\partial}_{J',j}(t, z, u) = \frac{1}{2}(T(t, z, u) + J'T(t, z, u) \circ j)$ for the usual Cauchy–Riemann operator. For $V \in TW$, we calculate

$$\pi_\alpha(a\partial_z + V) = V - \beta(V)\partial_z,$$

so that the ξ–valued part $\frac{1}{2}(\pi_\alpha + J' \circ \pi_\alpha \circ j)$ of $\overline{\partial}_{J',j}(s, t, u)$ depends only on u. Then

$$(\pi_\alpha + J' \circ \pi_\alpha \circ j)(s, t, u) = \overline{\partial}_{J,j}u - \beta \circ (\overline{\partial}_{J,j}u)\partial_z,$$

where $\overline{\partial}_{J,j}$ is the Cauchy–Riemann operator for u. The TW part of this expression vanishes if and only if u is (J, j)–holomorphic, which would imply that the ∂_z part of the expression vanishes as well.

Assuming that (t, z, u) is (J', j)–holomorphic, then u is (J, j)–holomorphic and $dt = ((z, u)^*\alpha) \circ j$, implying

$$\begin{aligned} u^*\beta = -u^*(dF \circ J) &= -d(F \circ u) \circ j, \\ (z, u)^*\alpha \circ j &= dz \circ j + d(F \circ u), \\ d^2t = d((z, u)^*\alpha \circ j) &= d(dz \circ j) = -\Delta(z) = 0, \end{aligned}$$

where Δ is the Laplacian. Therefore, z is harmonic.

Now, provided harmonic z and (J, j)–holomorphic u for simply connected Σ', the above expression tells us that $(z,u)^*\alpha \circ j$ is closed, and so is exact. Therefore, we have a function t — determined uniquely up to addition by scalars — satisfying $dt = (z,u)^*\alpha \circ j$. Then, by the above formula and (7), (t,z,u) is (J', j)–holomorphic. □

Corollary 11.2 (drawing-to-disk correspondence) *Suppose that (W, J, F) is a Stein manifold of complex dimension 1 and that Λ is a chord-generic Legendrian link in $(I \times W, dz - dF \circ J)$. Suppose that*

$$u : \mathbb{D} \setminus \{p_j\} \to W$$

is an orientation-preserving immersion of the disk with a finite set of boundary punctures $\{p_k\}$ removed such that $u(\partial\mathbb{D} \setminus \{p_k\}) \subset \pi_W(\Lambda)$. Then there exists a set $\{p'_k\}$ of boundary punctures on the disk, a diffeomorphism $\phi : \mathbb{D} \setminus \{p'_k\} \to \mathbb{D} \setminus \{p_k\}$ and functions $t, z : \to \mathbb{R}$ such that

$$(t, z, u \circ \phi) : \mathbb{D} \setminus \{p'_k\} \to \mathbb{R} \times \mathbb{R} \times W$$

is (J', j)–holomorphic with $(z, u \circ \phi)(\partial\mathbb{D} \setminus \{p_k\}) \subset \Lambda$. Provided ϕ, z is uniquely determined and t is uniquely determined up to addition by a positive constant.

Proof Because u is an immersion, we can force it to be (J, j')–holomorphic for some almost-complex structure j' on $\mathbb{D}$ by defining $j'\partial_x = (Tu)^{-1} J(Tu)\partial_x$. We can then find a diffeomorphism ϕ which is (j', j)–holomorphic by the uniformization theorem.

By the chord-genericity and smoothness of Λ, there exists a unique, bounded, smooth function z_∂ on $\partial\mathbb{D} \setminus \{p'_k\}$ for which

$$(z_\partial, u \circ \phi) \in \Lambda.$$

Applying [1, Chapter 6, Section 4.2], there is a function $z : \mathbb{D} \setminus \{p'_k\} \to \mathbb{R}$ solving the Dirichlet problem

$$\Delta(f) = 0, \quad z|_{\partial\mathbb{D}\setminus\{p'_k\}} = z_\partial,$$

which is unique by the maximum principle. By Lemma 11.1, we can find t for which $(t, z, u \circ \phi)$ is (J', j)–holomorphic, as desired. □

11.2 N–standard almost-complex structures

As always, let N_ϵ be a tubular neighborhood of Λ, whose complement we may consider to be a codimension-0 submanifold of either $\mathbb{R}^3$ or $\mathbb{R}^3_{\Lambda^\pm}$. Define

$$\widetilde{N}_\epsilon = \pi_{xy}^{-1}(\pi_{xy}(N_\epsilon)),$$

which we may view as an open set in either $\mathbb{R}^3$ or $\mathbb{R}^3_{\Lambda^\pm}$. Denote its complement by $\widetilde{N}_\epsilon^{\complement}$.

Definition 11.3 We say that an almost-complex structure J on $\mathbb{R}\times\mathbb{R}^3_{\Lambda^\pm}$ is *N–standard* if its restriction to $\xi_{\Lambda^\pm}$ agrees with the standard almost-complex structure J_0 on $\xi_{\Lambda^\pm}$ described by (14) on $\widetilde{N}^{\complement}_{\epsilon}$ as well as on a neighborhood

$$N_{C,\infty} = \{x^2 + y^2 + z^2 > C\}$$

of the puncture of our 3–manifold for some $\epsilon, C > 0$. In order that J be adapted to the symplectization, we require $J\partial_t = \partial_z$ on $\mathbb{R}\times\widetilde{N}^{\complement}_{\epsilon}$.

We may define N–standard for almost-complex structures on completions of surgery cobordisms (W_c, λ_c) of Section 10 analogously as the cobordisms contain the symplectizations of $(\mathbb{R}^3_{\Lambda^\pm}\setminus N_\epsilon, \alpha_{\text{std}})$.

For an N–standard almost-complex structure J and a (J, j)–holomorphic curve

$$U : \Sigma' \to \mathbb{R}\times\mathbb{R}^3_{\Lambda^\pm},$$

along $U^{-1}(\mathbb{R}\times N_{C,\infty})$ we can write $U = (t, z, u)$. By Lemma 11.1, z is harmonic and u is holomorphic, so that $x\circ u$ and $y\circ u$ are harmonic as well. It follows that $-d(d(z^2+|u|^2)\circ j)$ is nonnegative as an area form on Σ'. Hence, for $C' > C$, finite-energy curves with punctures asymptotic to chords and orbits of R_ϵ cannot touch spheres of radius C' by the maximum principle.

11.2.1 Compatibility with perturbation schemes and adaption to symplectizations

Note that perturbations of almost-complex structures required to achieve the transversality required to define SFT curve counts in $\mathbb{R}\times\mathbb{R}^3_{\Lambda^\pm}$ or $(\overline{W}_c, \overline{\lambda}_c)$ may be defined in arbitrarily small neighborhoods of the orbits of R_ϵ [4, Section 5] and these orbits are properly contained in open sets unconstrained by the N–standard condition. Hence, these perturbations may be carried out for N–standard almost-complex structures while maintaining their defining properties.

Similarly, the cobordisms (W_c, λ_c) of Section 10 are designed to support N–standard almost-complex structures which are adapted to their cylindrical ends. For such cobordisms, we'll be additionally interested in studying somewhere-injective curves positively asymptotic to chords of the Legendrian boundaries of the disks $\mathbb{D}_{c,i}\subset W_c$ with Lagrangian boundary. See Section 12.2. In this context, the perturbation scheme of [18, Section 2] may be applied, which likewise only deforms Cauchy–Riemann equations in arbitrarily small neighborhoods of chords and orbits. Again, there is no lack of compatibility with the N–standard condition.

Assumptions 11.4 Throughout the remainder of this section, we assume that any almost-complex structure J on a symplectization or surgery cobordisms is N–standard and that all somewhere-injective curves under consideration are regular. When discussing surgery cobordisms, we assume that J is adapted to the cylindrical ends of its completion and that almost-complex structures on symplectizations are adapted.

11.3 Semiglobal foliation by holomorphic planes

Here we describe holomorphic foliations by infinite-energy planes in symplectizations and surgery cobordisms.

11.3.1 $\mathbb{C}$ foliations in symplectizations Observe that $\widetilde{N}_\epsilon^{\mathbb{C}}$ is foliated by embedded, $\mathbb{R}$–parametrized Reeb orbits of the form $t \to (t, x_0, y_0)$. Then $\mathbb{R} \times \widetilde{N}_\epsilon^{\mathbb{C}}$ is foliated by holomorphic planes parametrized

$$(s,t) \mapsto (s,t,x,y)$$

for $(x,y) \in \mathbb{R}^2 \setminus \pi_{x,y}(N_\epsilon)$. We denote each such unparametrized plane by $\mathbb{C}_{x,y}$.

11.3.2 $\mathbb{C}$ foliations in surgery cobordisms For the following, we require that Λ^0 be nonempty. The link $\Lambda^\pm$ is allowed to be empty, in which case we would have $(\mathbb{R}^3_{\Lambda^\pm}, \xi_{\Lambda^\pm}) = (\mathbb{R}^3, \xi_{\text{std}})$ and set $\alpha_\epsilon = dz - y\,dx$. Let (W_c, λ_c) be a surgery cobordism associated to the pair

$$\Lambda^0 \subset (\mathbb{R}^3_{\Lambda^\pm}, \xi_{\Lambda^\pm}), \quad c \in \{\pm 1\}$$

as described in the introduction of Section 10, with completion $(\overline{W}_c, \overline{\lambda}_c)$. Because the handles are attached along a neighborhood of Λ^0, we can view $\mathbb{R} \times \widetilde{N}^{\mathbb{C}}$ as a subset of $\overline{W}_c$ which is also foliated by infinite-energy planes $\mathbb{C}_{x,y}$.

11.4 Intersection numbers

For the following, let (Σ, j) be a compact Riemann surface, possibly with boundary, with fixed collections of interior points p_k^{int} and boundary points p_k^{∂}. As usual, we write Σ' for Σ with all of its marked points removed. When discussing completions $(\overline{W}_c, \overline{\lambda}_c)$, we write

$$\overline{\mathbb{D}}_{c,i} \subset \overline{W}_c$$

for the Lagrangian planes obtained by extending the disks $\mathbb{D}_{c,i}$ of Theorem 10.1 by the positive (resp. negative) half-infinite Lagrangian cylinders over their Legendrian boundaries when $c = 1$ (resp. $c = -1$).

Definition 11.5 We say that a holomorphic map $U\colon \Sigma' \to \overline{W}_c$ is a $\overline{W}_c$ *curve* if it its boundary is mapped to the $\overline{\mathbb{D}}_{c,i}$, its boundary punctures are asymptotic to chords of their Legendrian boundaries, and all interior punctures are asymptotic to closed Reeb orbits at the convex and concave ends of $\overline{W}_c$.

We say that a holomorphic map $U\colon \Sigma' \to \mathbb{R}\times\mathbb{R}^3_{\Lambda^\pm}$ is an $\mathbb{R}\times\mathbb{R}^3_{\Lambda^\pm}$ *curve* if the boundary of Σ' is mapped to the Lagrangian cylinder over Λ^0, its boundary punctures are asymptotic to chords of Λ^0, and its interior punctures are asymptotic to closed orbits of R_ϵ.

We recall — see [47, Definition E.2.1] — that, provided a pair of maps $u_i\colon \Sigma_i' \to W$ from surfaces Σ_i' for $i=1,2$ into a 4–manifold W whose images are disjoint outside of some open sets $S_i \subset \Sigma_i$ with compact closures outside of which the Σ_i are disjoint, then we can define a *intersection number* $u_1\cdot u_2 \in \mathbb{Z}$ by perturbing the u_i along the S_i so that the maps are transverse and counting their intersections with signs.[15]

Theorem 11.6 *Suppose that U is a $\overline{W}_c$ curve or an $\mathbb{R}\times\mathbb{R}^3_{\Lambda^\pm}$ curve. Then, for $(x,y)\in\mathbb{R}^2\setminus\pi_{x,y}(N_\epsilon)$, the intersection number $\mathbb{C}_{x,y}\cdot U_s \in \mathbb{Z}$ is well defined and nonnegative. Furthermore, they are homological invariants in the following sense*:

(1) ***Boundaryless curves in symplectizations*** *Suppose that U is an $\mathbb{R}\times\mathbb{R}^3_{\Lambda^\pm}$ curve positively asymptotic to a collection γ^+ of Reeb orbits and negatively asymptotic to some γ^-. Then the intersection number $\mathbb{C}_{x,y}\cdot U$ depends only on the relative homology class*

$$[\pi_{\mathbb{R}^3_{\Lambda^\pm}}(U)] \in H_2(\mathbb{R}^3_{\Lambda^\pm}, \gamma^+\cup\gamma^-).$$

(2) ***Curves in symplectizations with Lagrangian boundary*** *Suppose that U is an $\mathbb{R}\times\mathbb{R}^3_{\Lambda^\pm}$ curve asymptotic to collections $\gamma^\pm$ of Reeb orbits and collections of chords $\kappa^\pm$ of Λ^0. Then the intersection number $\mathbb{C}_{x,y}\cdot U$ depends only on the relative homology class*

$$[\pi_{\mathbb{R}^3_{\Lambda^\pm}}(U)] \in H_2(\mathbb{R}^3_{\Lambda^\pm}, \gamma^+\cup\gamma^-\cup\kappa^+\cup\kappa^-\cup\Lambda^0).$$

(3) ***Boundaryless curves in surgery cobordisms*** *Suppose that U is a $\overline{W}_c$ curve positively asymptotic to a collection of closed Reeb orbits γ^+ in ∂^+W and*

[15] We're taking a slight modification of [47, Definition E.2.1] by defining the intersection number to be the sum of the *local intersection numbers* over all points of intersection. This is feasible for holomorphic curves in 4–manifolds with our hypotheses as distinct curves have isolated intersections [47, Proposition E.2.2].

negatively asymptotic to some collection of closed Reeb orbits γ^- in $\partial^- W$. Then the intersection number $\mathbb{C}_{x,y} \cdot U$ depends only on the relative homology class

$$[U] \in H_2(W_c, \gamma^+ \cup \gamma^-).$$

Here we view U as a cobordism in the compact manifold W_c bounding the orbit collections $\gamma^\pm$ in its boundary.

(4) ***Curves in surgery cobordisms with Lagrangian boundary*** *Suppose that U is a $\overline{W}_c$ curve positively asymptotic collection of closed Reeb orbits $\gamma^\pm$ in $\partial^+ W$ with boundary punctures asymptotic to some collection $\kappa^\pm$ of chords of the Legendrian boundaries of disks $\mathbb{D}_k$. Then the intersection number $\mathbb{C}_{x,y} \cdot U$ depends only on the relative homology class*

$$[U] \in H_2\Big(W_c, \gamma^+ \cup \gamma^- \cup \kappa^+ \cup \kappa^- \cup \bigcup \overline{\mathbb{D}}_{c,i}\Big).$$

Proof To check well-definedness, we need to ensure that any intersections between $\mathbb{C}_{x,y}$ and $U(\Sigma')$ occur away from the boundary and punctures of Σ', so that intersection numbers are independent of the perturbation required in their definition. By our boundary conditions, U must be such that there exists some open neighborhood $S \subset \Sigma'$ of the punctures and boundary of Σ which maps into the complement of $\mathbb{R} \times (\mathbb{R}^3_{\Lambda^\pm} \setminus N_\epsilon)$. The images of the complements of the S_s must be contained in some compact set of the form $[-C_1, C_1] \times (\mathbb{R}^3_{\Lambda^\pm} \setminus N_\epsilon)$. Likewise, the images of the complements of the S_s must be bounded in the z coordinate on $\mathbb{R}^3$. Hence, all intersections occur within a subset of the form $[-C_1, C_1] \times [-C_2, C_2] \times \{(x, y)\} \subset \mathbb{C}_{x,y}$, implying that the $\mathbb{C}_{x,y} \cdot U_s \in \mathbb{Z}$ are well defined.

Intersection nonnegativity follows from positivity of intersections of holomorphic curves in 4–manifolds. See for example [47, Section E.2]. For homological invariance, we will work out the details in the case of boundaryless curves in symplectizations. The other cases follow similar reasoning.

As in the statement of the theorem, we can slightly perturb U near its asymptotic ends to obtain a 2–cycle in $[-C, C] \times \mathbb{R}^3_{\Lambda^\pm}$ bounding $\{C\} \times \gamma^+ - \{-C\} \times \gamma^-$ for some large $C > 0$. Using the coordinates on $\mathbb{R} \times \mathbb{R}^3$ in which we may consider $\mathbb{C}_{x,y}$ to be contained, each intersection between U and $\mathbb{C}_{x,y}$ occurs at some (t, z, x, y). Possibly perturbing U near each such intersection to achieve transversality and isolation of intersections, the sign of each intersection is given by the sign of $T\mathbb{C}_{x,y} \wedge TU$ considered as an oriented ray in the orientation line bundle $\mathbb{R}\partial_t \wedge \partial_z \wedge \partial_x \wedge \partial_y$ for

$T_{(t,z,x,y)}W$. As $T\mathbb{C}_{x,y} = \mathrm{span}_{\mathbb{R}}(\partial_t, \partial_z)$, this sign only depends on the ∂_x and ∂_y parts of the tangent map TU of U. Hence, the intersection number $\mathbb{C}_{x,y} \cdot U$ only depends on (x, y) and $\pi_{\mathbb{R}^3_{\Lambda\pm}} \circ U$. □

The ending of the above proof also immediately implies the following:

Lemma 11.7 *Suppose that $U : \mathbb{D} \setminus \{p_k\} \to \mathbb{R} \times \mathbb{R}^3$ is a holomorphic disk determined by an immersion $u : \mathbb{D} \setminus \{p_k\} \to \mathbb{R}^2$ as in Corollary 11.2. Given a point $(x, y) \in \mathbb{R}^2 \setminus \pi_{x,y}(N_\epsilon)$, the intersection number is*

$$\mathbb{C}_{x,y} \cdot U = \#u^{-1}((x, y)).$$

11.5 Bases and energy bounds

Here we'll reduce the information of the $\mathbb{C}_{x,y}$ down to that of a finite collection of planes. Write $\mathcal{R}_k$ for the connected components of $\mathbb{R}^2 \setminus \pi_{x,y}(N_\epsilon)$ of finite area and write

$$\mathcal{E}_k = \int_{\mathcal{R}_k} dx \wedge dy$$

for their areas. There is also a single connected component $\mathbb{R}^2 \setminus \pi_{x,y}(N_\epsilon)$ of infinite area, which we will denote by $\mathcal{R}_\infty$.

Pick a point (x_k, y_k) within the interior of each $\mathcal{R}_k$ as well as a point $(x_\infty, y_\infty) \in \mathcal{R}_\infty$. We'll call such a choice of indices and points a *point basis* for Λ. Provided a point basis, we may abbreviate

$$\mathbb{C}_k = \mathbb{C}_{(x_k,y_k)}.$$

Such a choice allows us to package a simple-to-state energy estimate:

Proposition 11.8 *Let U be a finite-energy $\mathbb{R} \times \mathbb{R}^3_{\Lambda\pm}$ curve with interior punctures asymptotic to some collections of orbits of R_ϵ and boundary punctures asymptotic to chords of $\Lambda^0 \subset \mathbb{R}^3_{\Lambda\pm}$. Then*

$$\mathcal{E}(U) > \sum_k \mathcal{E}_k \mathbb{C}_k \cdot U.$$

Proof For each $k \neq \infty$ for which

$$\Sigma'_k = U^{-1}(\mathbb{R} \times \mathbb{R} \times \mathcal{R}_k)$$

is not empty,

$$\pi_{x,y} \circ \pi_{\mathbb{R}^3_{\Lambda\pm}} \circ U : \Sigma'_k \to \mathcal{R}_k$$

is a nonconstant holomorphic map. By our boundary conditions, each Σ'_k is disjoint from some neighborhood of the boundary and punctures of Σ' and so must be a branched

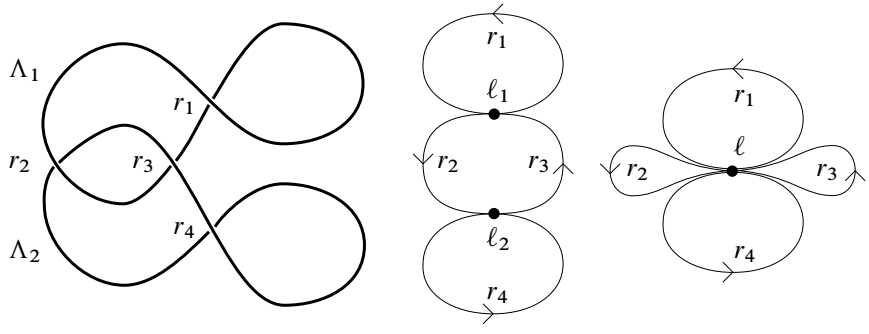

Figure 24: From left to right: a Legendrian Hopf link Λ in the Lagrangian projection, the associated quiver Q_Λ and the quiver Q_Λ/ℓ.

covering. The degree of the associated map

$$(\overline{\Sigma}'_k, \partial\overline{\Sigma}'_k) \to (\overline{\mathcal{R}}_k, \partial\overline{\mathcal{R}}_k)$$

is equal to $\mathbb{C}_k \cdot U$, so that our requirement that α_ϵ coincides with $\alpha_{\text{std}} = dz - y\,dx$ on the compliment of $N^\pm$ implies

$$\mathcal{E}(U) > \sum_k \int_{\Sigma'_k} d\alpha_\epsilon = \sum_k \int_{\Sigma'_k} dx \wedge dy = \sum_k \mathcal{E}_k \mathbb{C}_k \cdot U. \qquad \square$$

11.6 The Λ quiver

In the event that all intersection numbers $\mathbb{C}_k \cdot U$ are zero for a given curve U, we can employ another device to keep track of holomorphic curves and their boundary conditions.

Definition 11.9 The Λ *quiver*, denoted by Q_Λ, is the directed graph with

(1) one vertex ℓ_i for each connected component Λ_i of Λ, and

(2) one directed edge for each chord r_j of $\Lambda \subset \mathbb{R}^3$ starting at the vertex $\ell_{l_j^-}$ and ending at $\ell_{l_j^+}$.[16]

Also define a graph Q_Λ/ℓ which is the quotient of Q_Λ obtained by identifying all of its vertices. We write

$$\pi_\ell \colon Q_\Lambda \to Q_\Lambda/\ell$$

for the quotient map.

An example is provided in Figure 24.

[16] We recall the $l_j^\pm$ are defined in Section 3.

11.6.1 Algebraic aspects of Q_Λ and Q_Λ/ℓ The primary utility of the space Q_Λ/ℓ is that its homology has a particularly nice presentation, with H_1 freely generated by the chords of $\Lambda \subset (\mathbb{R}^3, \xi_{\text{std}})$,

$$H_1(Q_\Lambda/\ell) = \oplus \mathbb{Z} r_j,$$

while its fundamental group — based at its unique vertex, ℓ — is a free group on the chords of Λ,

$$\pi_1(Q_\Lambda/\ell, \ell) = \langle r_j \rangle.$$

In applications, we'll make use of the following definitions and lemma:

Definition 11.10 For an edge e of a directed graph G we define the *collapse map at* e, denoted by $\pi_e \colon G \to S^1$, as the map which takes the quotient by $G \setminus \text{int}(e)$. The target is naturally pointed and oriented by the direction of e. A continuous map $\Phi \colon S^1 \to G$ from an oriented circle is *nonnegative* if, for every edge e of g, the composition

$$S^1 \xrightarrow{\Phi} G \xrightarrow{\pi_e} S^1$$

with the collapse map has nonnegative degree. We say that the map is *positive* if it is nonnegative and there exists at least one $e \subset G$ for which $\pi_e \circ \Phi$ has positive degree.

Definition 11.11 Let $\mathcal{S}$ be a set with associated free group $\langle \mathcal{S} \rangle$. We say that an element $x \in \langle \mathcal{S} \rangle$ is *positive* if it can be described as a word

$$x = x_1 \cdots x_n, \quad x_k \in \mathcal{S}.$$

Alternatively, the set of positive elements in $\langle \mathcal{S} \rangle$ is equivalent to the image of the natural monoid homomorphism from the free monoid on $\mathcal{S}$ into $\langle \mathcal{S} \rangle$.

If x is positive then the above factorization is necessarily unique. We say that two positive elements x and y of $\langle \mathcal{S} \rangle$ are *cyclically equivalent* if their positive factorizations differ by a cyclic rotation. That is, provided a factorization of x as above, there exists k for which

$$y = x_k \cdots x_n x_1 \cdots x_{k-1}.$$

We say that $x \in \langle \mathcal{S} \rangle$ is *negative* if x^{-1} is positive. Two negative elements x and y are *cyclically equivalent* if x^{-1} and y^{-1} are cyclically equivalent.

Cyclic equivalence is no stronger than conjugacy equivalence.

Lemma 11.12 *Suppose that $x, y \in \langle \mathcal{S} \rangle$ are positive and conjugate in $\langle \mathcal{S} \rangle$. Then they are cyclically equivalent.*

Proof Suppose there exists some z for which $zx = yz$ and write $z = z_1 \cdots z_n$ with the z_k being elements of $\mathcal{S}$ or inverses of such letters. We can assume that at least one of z_1 or z_n is positive. Otherwise we can write $z^{-1}y = xz^{-1}$ to obtain the desired hypothesis by a change of notation.

Suppose that z_1 is positive. Then the positive factorization of y must start with z_1. Then $y' = z_1^{-1} y z_1$ is positive, so we can write $z'x = y'z'$ with $z' = z_2 \cdots z_n$. We have reduced the problem to finding a cyclic equivalence between two positive elements x and y' which are conjugate by a word z' of length $n-1$. A similar argument may be applying in the case that z_n is positive.

To complete the proof, loop through this argument n times. □

11.6.2 Geometric aspects of Q_Λ and Q_Λ/ℓ The primary utility of the space Q_Λ in relation to the present discussion is given by the following result:

Proposition 11.13 *There exist surjective maps*

$$\mathbb{R}^3_{\Lambda^\pm} \setminus \widetilde{N}^{\complement}_\epsilon \to Q_\Lambda, \quad \overline{W}_c \setminus \mathbb{R} \times \widetilde{N}^{\complement}_\epsilon \to Q_\Lambda,$$

both of which we will denote by π_Q, such that, for each chord r_j of Λ and each line segment I directed by ∂_z connecting $\mathcal{D}^{\mathrm{ex}}_j$ to $\mathcal{D}^{\mathrm{en}}_j$, the submanifold $\mathbb{R} \times I$ is mapped onto the edge r_j of Q_Λ in a way such that, for each t in $\mathbb{R}$, $\{t\} \times I \to e_j$ is a homeomorphism.[17]

Proof We start with the case in which the domain of π_Q is $\mathbb{R}^3_{\Lambda^\pm} \setminus \widetilde{N}^{\complement}_\epsilon$. We have that $\mathbb{R}^3_{\Lambda^\pm} \setminus \widetilde{N}^{\complement}_\epsilon$ is homotopy equivalent the union of N_ϵ with all of the chords r_j of Λ. We can perform this homotopy so that the intervals connecting the $\mathcal{D}^{\mathrm{en}}_j$ and $\mathcal{D}^{\mathrm{ex}}_j$ (forming a neighborhood of r_j) collapse onto r_j as a fibration. Note that N_ϵ is a collection of solid tori, so that $N_\epsilon \cup \{r_j\}$ is homotopy equivalent to a 1–dimensional CW complex. If we collapse each connected component $N_{\epsilon,i}$ of N_ϵ to a point ℓ_i, the graph Q_Λ is obtained.

The proof for $\overline{W}_c \setminus \mathbb{R} \times \widetilde{N}^{\complement}_\epsilon$ is nearly identical except at the last step; the addition of the surgery handles already provides the effect of attaching 2–cells along the circles in our 1–complex corresponding to components of $\Lambda^\pm$. We then collapse these 2 cells to points, which has the same effect — in the homotopy category — as collapsing the circles corresponding to the components of Λ to points. □

[17] We recall that the $\mathcal{D}^*_j$ are defined in Section 5.1.

Proposition 11.14 *Suppose that $\gamma(t)$ parametrizes a Reeb orbit in $\mathbb{R}^3_{\Lambda\pm}$ or ∂W_c. Then $\pi_Q \circ \gamma$ is positive in the sense of Definition 11.10.*

The open string version of this assertion is as follows: Let U be a $\overline{W}_c$ or $\mathbb{R}\times\mathbb{R}^3_{\Lambda\pm}$ curve with domain Σ' having a boundary component $\partial_i\Sigma \subset \partial\Sigma$ for which all punctures along $\partial_i\Sigma$ have positive asymptotics. Then $\pi_Q \circ U|_{\partial_i\Sigma}$ is a positive loop. If all punctures along $\partial_i\Sigma$ have negative asymptotics, then this loop is negative.

This is clear from the construction of the map π_Q. For a parametrization γ of a Reeb orbit with cyclic word $r_{j_1}\cdots r_{j_n}$, we have

$$[\pi_\ell \circ \pi_Q \circ \gamma] = \sum_1^n [r_{j_k}] \in H_1(Q_\Lambda/\ell).$$

Intuitively, the map $\pi_\ell \circ \pi_Q$ induces a map on homology which abelianizes boundary conditions for holomorphic curves. We can also view $[\pi_\ell \circ \pi_Q \circ \gamma]$ as an element of the H_0 of the free loop space of Q_Λ/ℓ which records the word map of γ.

For a single chord κ with boundary on some $\Lambda^0 \subset (\mathbb{R}^3_{\Lambda\pm}, \xi_{\Lambda\pm})$, we can view $\pi_\ell\circ\pi_Q\circ\kappa$ as a pointed map

$$(\kappa, \partial\kappa) \to (Q_\Lambda/\ell, \ell)$$

as Λ is mapped to ℓ by $\pi_\ell \circ \pi_Q$. In this way, κ determines a positive element of $\pi_1(Q_\Lambda/\ell)$ as well as a relative homology class

$$[\pi_\ell \circ \pi_Q \circ \kappa] \in H_1(Q_\Lambda/\ell, \ell).$$

Both the π_1 and H_1 classes record the word map of κ.

11.7 The exposed/hidden alternative

Assume that Λ is equipped with a basis of points $(x_k, y_k) \in \mathbb{R}^2 \setminus \pi_{x,y}(N_\epsilon)$ as described in Section 11.5.

Definition 11.15 (exposed/hidden alternative) We say that an $\mathbb{R}\times\mathbb{R}^3_{\Lambda\pm}$ or $\overline{W}_c$ curve U is *exposed* if there exists at least one k for which $\mathbb{C}_k \cdot U > 0$. Otherwise we say that U is *hidden*.

If a curve U is exposed, then we can use the intersection numbers to keep track of the location of its image within the target manifold. If the curve is hidden, then, by intersection positivity, its image must be entirely contained in the complement of $\mathbb{R}\times\widetilde{N}^{\mathbb{C}}_\epsilon$, whence we can apply the map $\pi_\ell \circ \pi_Q$. We state some simple applications, the first few of which tell us that the homology of Q_Λ/ℓ dictates whether a curve is exposed or hidden.

Proposition 11.16 (homological mismatches are exposed) *Suppose that U is an $\mathbb{R}\times\mathbb{R}^3_{\Lambda\pm}$ or $\overline{W}_c$ curve without boundary components positively asymptotic to some collection $\gamma^+=\{\gamma_k^+\}$ of closed orbits and negatively asymptotic to some collection $\gamma^-=\{\gamma_k^-\}$ of Reeb orbits. If the 1–cycle*

$$\sum[\pi_\ell\circ\pi_Q\circ\gamma_k^+]-\sum[\pi_\ell\circ\pi_Q\circ\gamma_k^-]\neq 0\in H_1(Q_\Lambda/\ell),$$

then U is exposed.

Proof If the curve was hidden, then we could apply the map $\pi_\ell\circ\pi_Q$ to the image of U. Our hypotheses on asymptotics imply that we would get a 2–cycle in $\mathbb{R}^3_{\Lambda\pm}\setminus\widetilde{N}_\epsilon^{\complement}$ or $W_c\setminus\mathbb{R}\times\widetilde{N}_\epsilon^{\complement}$ bounding a homologically nontrivial 1–cycle, providing a contradiction. □

A slight modification applies to chords as well.

Proposition 11.17 (exposure of filling curves) *Suppose that U is an $\mathbb{R}\times\mathbb{R}^3_{\Lambda\pm}$ or $\overline{W}_c$ curve for which all asymptotic chords and orbits are positive. Then U must be exposed.*

Proposition 11.18 (homological matches are hidden) *Let $h\in H_1(Q_\Lambda/\ell)$ be a positive homology class.*[18] *Then there exists ϵ_h such that, for each $\epsilon<\epsilon_h$, given a holomorphic curve in $\mathbb{R}\times\mathbb{R}^3_{\Lambda\pm}$ positively asymptotic to a collection of orbits γ^+ and negatively asymptotic to a collection γ^- of R_ϵ orbits with*

$$[\pi_\ell\circ\pi_Q\circ\gamma^+]=[\pi_\ell\circ\pi_Q\circ\gamma^-]=h\in H_1(Q_\Lambda/\ell),$$

then U is hidden.

Proof By the action estimates of Section 5.5, we have

$$\mathcal{E}(U)=\mathcal{O}\Big(3\epsilon\sum\mathrm{wl}(\gamma_k^+)\Big).$$

For ϵ sufficiently small, we could guarantee that this quantity is less than the energies $\mathcal{E}_k$ of the regions $\mathcal{R}_k$ (which grow slightly as ϵ tends to 0 with N_ϵ shrinking). Therefore, the energy bound of Proposition 11.8 would imply that U must be hidden. □

Proposition 11.19 (cyclic order preservation of open–closed interpolations) *Suppose that U is a hidden $\overline{W}_c$ curve whose domain is a disk with a single interior puncture and any number of boundary punctures. We require that*:

(1) *If $c=+1$, the boundary punctures are positively asymptotic to chords of Λ^0 with words $w_1,\dots,w_n$.*

[18] That is, h may be represented as a sum of positive cycles.

(2) *If $c = -1$, the boundary punctures are negatively asymptotic to chords of Λ^0 with words $w_1, \dots, w_n$.*

Here indices follow the counterclockwise cyclic ordering of the punctures around $\partial\mathbb{D}$. Then interior puncture of U asymptotic to the orbit $(w_1 \cdots w_n)$.

The $c = -1$ curves described are those used to determine homomorphisms from linearized contact homology to a cyclic version of Legendrian contact homology when performing a contact -1 surgery in [7; 18; 20].[19] We'll see some of the $c = 1$ curves shortly in Theorem 12.2.

Proof Consider the map $\pi_\ell \circ \pi_Q \circ U$ from the punctured disk to the graph Q_Λ/ℓ. Then $\partial\mathbb{D}$ — compactified appropriately — will give us an element of the free loop space of Q_Λ/ℓ. It is clear from the construction of the map π_Q that the connected component of the free loop space of Q_Λ/ℓ containing this loop is indexed by $w_1 \cdots w_n$. Looking at circles of varying radii in $\mathbb{D}$ provides a homotopy between this loop and the one provided by the interior puncture. Again by the construction of π_Q, observe that, if the orbit to which the puncture is asymptotic has cyclic word $r_{j_1} \cdots r_{j_n}$, then this word must also index the component of the free loop space of Q_Λ/ℓ to which the puncture is associated. The connected components of the free loop space of Q_Λ/ℓ are in bijective correspondence with conjugacy classes on $\langle r_j \rangle$, so that the expressions $r_{j_1} \cdots r_{j_n}$ and $w_1 \cdots w_n$ are conjugate by the existence of the aforementioned homotopy. They are also both positive in the sense of Definition 11.11 and so differ by a cyclic permutation of their letters by Lemma 11.12. □

Proposition 11.20 (triviality of hidden cylinders and strips) *Suppose that U is a hidden holomorphic cylinder in $\mathbb{R} \times \mathbb{R}^3_{\Lambda^\pm}$. Then U is a trivial cylinder.*

If U has domain $\mathbb{R} \times I_C$ for some $C > 0$, is hidden, with boundary on the Lagrangian cylinder over $\Lambda^0 \subset (\mathbb{R}^3_{\Lambda^\pm}, \xi_{\Lambda^\pm})$, and with punctures asymptotic to chords of Λ^0, then U is a trivial strip.

Proof If U is positively asymptotic to some orbit $(r_{j_1} \cdots r_{j_n})$, then we can follow the proof of Proposition 11.19 verbatim to conclude that U is negatively asymptotic to $(r_{j_1} \cdots r_{j_n})$. Hence, the energy of U is zero and it must be a trivial cylinder.

The case of a holomorphic strip is even easier. Suppose the strip is parametrized by $s \in \mathbb{R}$ and $t \in I_C$, and consider the family of paths $\gamma_s(t) = \pi_{\mathbb{R}^3_{\Lambda^\pm}} \circ U(s,t)$ with boundary on $\Lambda^0 \subset \mathbb{R}^3_{\Lambda^\pm}$. Then we may consider the $\pi_\ell \circ \pi_Q \circ \gamma_s$ as an $\mathbb{R}$ family of based

[19] We're ignoring anchors, which can be avoided in some settings, such as [20].

loops in Q_Λ/ℓ. As $s \to \infty$, the $\pi_1(Q_\Lambda/\ell)$ element recorded by this based loop is the word map of the chord to which U is positively asymptotic. As $s \to -\infty$, the element recorded is the word map of the chord to which U is negatively asymptotic. Hence, the asymptotics are equivalent by our chord-to-chord correspondence (Theorem 5.10), the energy of U is zero, and U is a trivial strip. □

12 Applications

In this section we apply our computational tools to study the contact homology of various contact manifolds. A summary of the results are as follows:

(1) In Section 12.1, we compute the contact homology of contact ± 1 surgeries on the $\mathrm{tb} = -1$, $\mathrm{rot} = 0$ unknot in $\mathbb{R}^3$.

(2) In Section 12.2, we use the results of Section 11 to prove a general existence result for holomorphic planes in $\mathbb{R} \times \mathbb{R}^3_{\Lambda^\pm}$ when $\Lambda^+ \neq \varnothing$.

(3) In Section 12.3, we use the existence of these holomorphic planes to provide a new proof of the vanishing of CH for overtwisted contact structures.

(4) In Section 12.4, we state how the intersection numbers of Section 11 can be used to define a grading $\mathcal{I}_\Lambda$ on the CH chain complex for α_ϵ.

(5) In Section 12.5, we compute the homology classes and Conley–Zehnder indices of R_ϵ orbits appearing after application of contact surgeries to the $\mathrm{tb} = 1$, right-handed trefoil.

(6) In Section 12.6, we combine computations of Section 12.5 with the results of Sections 12.2 and 12.4 to prove Theorem 1.2.

For notational simplicity, we will ignore mention of specific contact forms α_ϵ, assuming that each contact manifold $(\mathbb{R}^3_{\Lambda^\pm}, \xi_{\Lambda^\pm})$ is equipped with such a contact form with ϵ small enough to guarantee that all orbits under consideration are hyperbolic and that Theorem 7.1 may be applied. Assumptions 11.4 are also in effect. When working with symplectizations of $(\mathbb{R}^3, \xi_{\mathrm{std}})$, we assume that we're using the standard almost-complex structure J_0.

12.1 Surgeries on the standard unknot

Let Λ be the Legendrian unknot with $\mathrm{tb} = -1$ and $\mathrm{rot} = 0$, depicted as a figure 8 in the Lagrangian projection in Figure 25. Performing contact -1 surgery will produce the standard contact lens space $L(2,1)$ — the unit cotangent bundle of S^2, or alternatively

Figure 25: Contact surgeries on the $\mathrm{tb} = -1$ unknot with push-outs of their unique embedded Reeb orbits. A -1 $(+1)$ surgery is applied on the left (right) subfigure.

the unit circle bundle associated to the line bundle $\mathcal{O}(-2) \to \mathbb{P}^1$. We'll denote this contact lens space by $(L(2,1), \xi_{\mathrm{std}})$. Performing contact $+1$ surgery produced the standard contact $S^1 \times S^2$ — see Theorem 2.8 — denoted by $(S^1 \times S^2, \xi_{\mathrm{std}})$.

We can arrange that the Lagrangian projection of Λ has a single crossing corresponding to a Reeb chord we denote by r, so that after performing a contact ± 1 surgery there is only a single embedded orbit (r) with cyclic word r. Push-outs of (r) using a choice of capping path are shown in Figure 25. As $\mathrm{rot}(\Lambda) = 0$, the framing (X, Y) described in Section 6 is nowhere-vanishing. For either choice of surgery coefficient, the first homology H_1 is generated by a meridian μ of Λ with

$$H_1(L(2,1)) = (\mathbb{Z}/2\mathbb{Z})\mu, \quad H_1(S^1 \times S^2) = \mathbb{Z}\mu.$$

Theorem 12.1 *The Conley–Zehnder gradings $|*|_{X,Y}$ on*

$$\widehat{\mathrm{CH}}(L(2,1), \xi_{\mathrm{std}}) \quad \text{and} \quad \widehat{\mathrm{CH}}(S^1 \times S^2, \xi_{\mathrm{std}})$$

are canonical in the sense of Proposition 2.5. We compute

$$\widehat{\mathrm{CH}}(L(2,1), \xi_{\mathrm{std}}) = \mathbb{Q}[z_0, z_2, \dots, z_{2k}, \dots], \quad |z_{2k}|_{X,Y} = 2k, \quad [z_{2k}] = \mu \in H_1,$$

for the lens space and

$$\widehat{\mathrm{CH}}(S^1 \times S^2, \xi_{\mathrm{std}}) = \textstyle\bigwedge_{k=1}^{\infty} \mathbb{Q} z_{2k-1}, \quad |z_{2k-1}|_{X,Y} = 2k-1, \quad [z_{2k-1}] = 0 \in H_1,$$

for $S^1 \times S^2$.

Proof For either choice of surgery coefficient $c = \pm 1$, we may compute Conley–Zehnder indices of (r) using a capping path η. We see that the rotation angle of η is $\frac{3}{2}\pi$, so that its rotation number 1. We conclude that

$$\mathrm{CZ}_{X,Y}((r^k)) = \begin{cases} k & \text{if } c = -1, \\ 2k & \text{if } c = +1. \end{cases}$$

Here and throughout the remainder of the proof, $(r^k) = (r \cdots r)$ is the k–fold cover of the embedded orbit (r) for $k > 0$. To sanity check our index computations against known results, we may:

(1) Compare the case $c = -1$ with [7, Section 7.1], in which contact -1 surgery is applied to Λ.

(2) Compare the case $c = +1$ with [20, Lemma 4.2], in which a contact 1–handle is attached to $(\mathbb{R}^3, \xi_{\text{std}})$ to obtain $\widehat{(S^1 \times S^2, \xi_{\text{std}})}$.

In each case a single closed, embedded orbit is produced with Conley–Zehnder index as described in the present scenario.

For the homology classes of orbits, we may apply Theorem 9.1, or simply look at the push-outs depicted in Figure 25 to compute

$$[(r)] = \begin{cases} \mu & \text{if } c = -1, \\ 0 & \text{if } c = +1. \end{cases}$$

As the framing (X, Y) is nonvanishing, we conclude that $\widehat{\text{CH}}$ is canonically $\mathbb{Z}$–graded for either choice of surgery coefficient, for, when $c = -1$, we have a $\mathbb{Q}$–homology sphere and, when $c = +1$, all orbits are homologically trivial.

When $c = -1$, an orbit (r^k) is bad exactly when $k \mod 2 = 0$. Write z_{2k} for the orbit (r^{2k-1}). Then the $\widehat{\text{CH}}$ chain algebra is freely generated by the z_{2k} with gradings as described in the statement of the theorem. As the $\text{CZ}_{X,Y}$ grading is even, ∂_{CH} must vanish. The theorem is now complete in the case $c = -1$.

When $c = +1$, all of the (r^k) are good orbits, which we will denote by z_{2k-1}. These are graded as described in the statement of the theorem. As (r) is the unique orbit of index 1, $\partial_{\text{CH}}(r)$ must be a count of holomorphic planes. If this count was nonzero, then the unit in $\widehat{\text{CH}}$ would be exact. This is impossible, as $(S^1 \times S^2, \xi_{\text{std}})$ bounds the Liouville domain

$$(S^1 \times \mathbb{D}^3, x\, dy - y\, dx + z\, d\theta),$$

implying that $\text{CH}(S^1 \times S^2, \xi_{\text{std}}) \neq 0$ and so $\widehat{\text{CH}}(S^1 \times S^2, \xi_{\text{std}}) \neq 0$ by Theorem 2.6. We conclude $\partial_{\text{CH}}(r) = 0$.

For $c = +1$ and $k > 1$, the contact homology differential of (r^k) is determined by counts of pairs of pants $\mathbb{P}^1 \setminus \{0, 1, \infty\}$ with

(1) ∞ positively asymptotic to (r^k),

(2) 0 negatively asymptotic to some (r^{k_0}),

(3) 1 negatively asymptotic to some (r^{k_1}), and

(4) $k = k_0 + k_1$, as required by the index formula, equation (8).

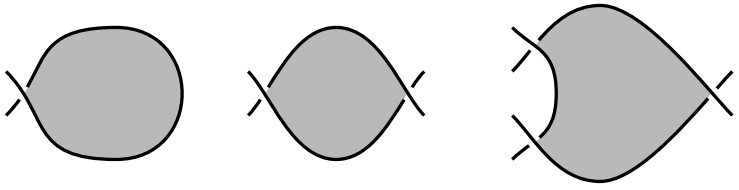

Figure 26: Some *RSFT* disks with only positive punctures.

The energies of any such curves must be 0, indicating that these curves must be branched covers of the trivial cylinder over (r). According to calculations of Fabert [28], the contact homology differential must be strictly action-decreasing, implying that the counts of such curves are 0. We conclude $\partial_{\mathrm{CH}}(r^k) = 0$, completing the proof. □

12.2 Bubbling planes in surgery diagrams

In this section we use the results of Section 11 to count holomorphic curves in completed surgery cobordisms $(\overline{W}_{+1}, \overline{\lambda}_{+1})$ determined by certain *LRSFT* disks on Legendrian links in $(\mathbb{R}^3, \xi_{\mathrm{std}})$ with only positive punctures. The arguments can be generalized to Legendrians Λ^0 in arbitrary punctured contact manifolds $(\mathbb{R}^3_{\Lambda^\pm}, \xi_{\Lambda^\pm})$, with additional notation and hypothesis. We consider *LRSFT* disks with arbitrary numbers of positive punctures, although in the applications of Sections 12.3 and 12.5 we'll only need to look at disks with a single positive puncture.

As mentioned in the introduction, the inspiration for our construction is Hofer's bubbling argument [35], used to prove the Weinstein conjecture — that every Reeb vector field on a given contact manifold has a closed orbit — for certain contact 3–manifolds. We also have in mind the holomorphic curves in contact -1 surgery cobordisms of [7; 18] positively asymptotic to closed orbits and negatively asymptotic to chords of a Legendrian link. In the case of $+1$ surgery, we will see some curves for which these boundary conditions have been flipped upside-down, allowing us to interpolate between chords of Legendrian links and Reeb orbits appearing after contact $+1$ surgery.

Suppose that $\Lambda^0 \subset (\mathbb{R}^3, \xi_{\mathrm{std}})$ has an immersed *LRSFT* disk $u\colon \mathbb{D} \setminus \{p_k\} \to \mathbb{R}^2$ for some boundary punctures $\{p_k\}$ as in Figure 26. Specifically, we assume that u is an embedding with only positive punctures, completely covering a connected component of $\mathbb{R}^2 \setminus \pi_{x,y}(\Lambda_0)$. Write $r_{j_1}, \dots, r_{j_n}$ for the chords associated to the punctures of the disk indexed in a counterclockwise fashion along its boundary and write

$$U : \mathbb{D} \setminus \{p_k\} \to \mathbb{R} \times (\mathbb{R}^3, \xi_{\mathrm{std}})$$

for the associated holomorphic curve with boundary mapping to $\mathbb{R}\times\Lambda^0$ determined by the drawing-to-disk correspondence, Corollary 11.2.

Let (x_k, y_k) be a basis of points for Λ^0, indexed so that (x_1, y_1) lies in the interior of the image of u. Then, by our hypothesis on u,

$$\mathbb{C}_k \cdot U = \begin{cases} 1 & \text{if } k = 1, \\ 0 & \text{if } k \neq 1. \end{cases} \tag{64}$$

Consider the completed cobordism $(\overline{W}_{+1}, \overline{\lambda}_{+1})$ obtained by performing contact $+1$ surgery on Λ^0 as described by Theorem 10.1. Then we may consider U as having $\overline{W}_{+1}$ as its target with boundary on an embedded union of Lagrangian planes $\overline{\mathbb{D}}_{+1,i}$ — as described in Section 10 — whose intersection with the positive end of $\overline{W}_{+1}$ is $[0,\infty)\times\Lambda^0$. We simply write $\overline{\mathbb{D}}_{+1}$ for this union of planes. We may consider the planes $\mathbb{C}_k$ as being contained in any of $\mathbb{R}\times\mathbb{R}^3$, $\overline{W}_{+1}$ or $\mathbb{R}\times\mathbb{R}^3_\Lambda$.

We consider the following moduli spaces:

(1) $\mathcal{M}_{\mathbb{R}^3}$ is the moduli space of holomorphic disks in $\mathbb{R}\times\mathbb{R}^3$ with positive punctures asymptotic to the $r_1,\dots,r_n$ and boundary on $\mathbb{R}\times\Lambda^0$ satisfying (64).

(2) $\mathcal{M}_{\overline{W}_{+1}}$ is the moduli space of holomorphic disks in $\overline{W}_{+1}$ with positive punctures asymptotic to the $r_1,\dots,r_n$ and boundary on $\overline{\mathbb{D}}_{+1}$ satisfying (64).

(3) $\mathcal{M}_{\mathbb{R}^3_\Lambda}$ is the moduli space of holomorphic planes in $\mathbb{R}\times\mathbb{R}^3_\Lambda$ positively asymptotic to the closed orbit $(r_{j_1}\cdots r_{j_n})$ and satisfying (64).

Within the positive end of the completed cobordism, we can translate U positively in the $\mathbb{R}$ direction, determining a half-infinite ray $[0,\infty)\subset\mathcal{M}_{\overline{W}_{+1}}$. The index of U is equal to 1, so that these curves are regular. Following the analogy with [35], these disks will serve as our Bishop family.

Theorem 12.2 *The boundary of the* SFT *compactification $\overline{\mathcal{M}}_{\overline{W}_{+1}}$ of the moduli space $\mathcal{M}_{\overline{W}_{+1}}$ consists of two points (when curves in symplectizations are considered equivalent modulo $\mathbb{R}$–translation). One point is given by $\mathbb{R}$–translations of the curve U, considered as living in $\mathbb{R}\times\mathbb{R}^3$. The other point is given by a height* 3 SFT *building consisting of*:

(1) *A collection of trivial strips over the r_{j_k} in $\mathbb{R}\times\mathbb{R}^3$.*

(2) *A hidden curve U_c^o in $\overline{W}_{+1}$ from a disk with n boundary punctures positively asymptotic to the r_{j_k} — preserving the cyclic ordering of the r_{j_k} — and a single interior puncture negatively asymptotic to the closed Reeb orbit $(r_{j_1}\cdots r_{j_n})$.*

(3) *A curve $U_\varnothing^c\in\mathcal{M}_{\mathbb{R}^3_\Lambda}$.*

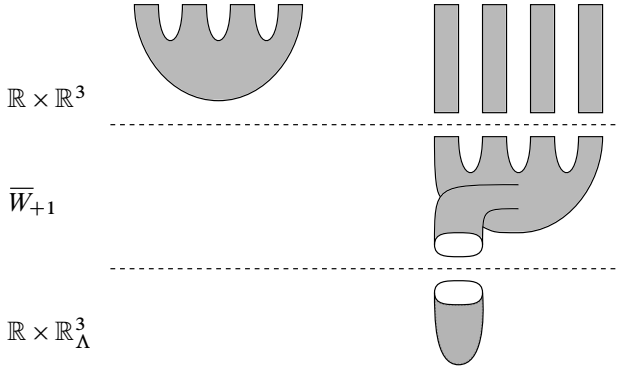

Figure 27: Elements of $\partial\overline{\mathcal{M}}_{\overline{W}_{+1}}$.

The algebraic count of such U_c^o is ±1 and the algebraic count of points in $\mathcal{M}_{\mathbb{R}^3_\Lambda}$ is also ±1.

The two buildings in $\partial\overline{\mathcal{M}}_{\overline{W}_{+1}}$ are shown in Figure 27. The notation U_c^o indicates that the curves interpolates between open and closed strings — that is, between chords and orbits — and this curve is shown in the center-right of Figure 27. The curve $U_\varnothing^c$ is shown in the bottom-right of the figure.

Proof The space $\partial\overline{\mathcal{M}}_{\overline{W}_{+1}}$ consists of multilevel SFT buildings such that, when their levels are glued together, an index 1 curve obeying the topological hypotheses on $\mathcal{M}_{\overline{W}_{+1}}$ is obtained. Subject to these conditions, such buildings may be of any of the following configurations:

(1) **Case $(1,\varnothing,\varnothing)$** A 3–level building consisting of an index 1 curve in $\mathbb{R}\times\mathbb{R}^3$, an empty curve in $\overline{W}_{+1}$, and an empty curve in the symplectization of the surgered manifold $\mathbb{R}\times\mathbb{R}^3_\Lambda$.

(2) **Case $(1,0,\varnothing)$** A 3–level building consisting of an index 1 curve in $\mathbb{R}\times(\mathbb{R}^3,\xi_{\text{std}})$, a collection of index 0 curves in $\overline{W}_{+1}$, and an empty curve in $\mathbb{R}\times\mathbb{R}^3_{\Lambda^\pm}$.

(3) **Case $(0,0,1)$** A 3–level building consisting of a collection of index 0 curves in $\mathbb{R}\times\mathbb{R}^3$, a collection of index 0 curves in $\overline{W}_{+1}$, and an index 1 curve in $\mathbb{R}\times\mathbb{R}^3_{\Lambda^\pm}$.

The buildings are required to recover the boundary conditions of U when glued in the obvious way. Buildings of height greater than 3 are ruled out by presumption of transversality for somewhere-injective curves in Assumptions 11.4, index additivity and the fact that all closed orbits of R_ϵ at the negative end of $\overline{W}_{+1}$ are assumed hyperbolic,

so that there cannot be levels consisting of branched covers of trivial cylinders with ind ≤ 0 as described in [41, Section 1].

We will show, using the intersections with the $\mathbb{C}_k$, that

(1) U is the only possibility for the case $(1, 0, \varnothing)$,

(2) there are no curves in the case $(1, 0, \varnothing)$, and

(3) the second configuration described in the statement of the proposition — appearing in Figure 27, right — is the only possibility for the case $(0, 0, 1)$.

Case (1, ∅, ∅) For the case $(1, \varnothing, \varnothing)$, our assumptions on the immersion u indicate that U is the only disk in $\mathbb{R} \times \mathbb{R}^3$ satisfying (64). We conclude that U is then the only possibility in this case.

Case (1, 0, ∅) Next, suppose we have a holomorphic building satisfying the conditions of the case $(1, 0, \varnothing)$ and note that the middle level — a union of curves in $\overline{W}_{+1}$ we'll denote by $U_{\overline{W}_{+1}}$ — must be positively asymptotic to some number of chords and have no negative asymptotics. Hence, each connected component of $U_{\overline{W}_{+1}}$ must be exposed by Proposition 11.17.[20] The conditions on intersection numbers of (64) then indicate that $U_{\overline{W}_{+1}}$ must consist of a single component and that the upper level of this building $U_{\mathbb{R}\times\mathbb{R}^3}$ must be hidden.

For each component of $U_{\mathbb{R}\times\mathbb{R}^3}$, the number of positive punctures must match the number of negative punctures, as otherwise Proposition 11.16 would indicate that this component is exposed. If any component had more than a single negative puncture, then $U_{\overline{W}_{+1}}$ would have more than a single connected component in violation of the above arguments. We conclude that $U_{\mathbb{R}\times\mathbb{R}^3}$ must be a union of hidden strips, which are then trivial by Proposition 11.20.

Since $U_{\mathbb{R}\times\mathbb{R}^3}$ is a collection of trivial strips, it must then have ind $= 0$, in violation of our hypothesis. We conclude that no buildings of type $(1, 0, \varnothing)$ can exist.

Case (0, 0, 1) Finally, we address configurations of type $(0, 0, 1)$. Suppose that we have such a height 3 building whose levels — going from top to bottom — will be denoted by $U_{\mathbb{R}\times\mathbb{R}^3}$, $U_{\overline{W}_{+1}}$ and $U_{\mathbb{R}\times\mathbb{R}^3_\Lambda}$. By Proposition 11.17, $U_{\mathbb{R}\times\mathbb{R}^3_\Lambda}$ must be exposed and so, by (64), both $U_{\mathbb{R}\times\mathbb{R}^3}$ and $U_{\overline{W}_{+1}}$ must be hidden. Then $U_{\mathbb{R}\times\mathbb{R}^3_\Lambda}$ must consist of a holomorphic plane positively asymptotic to some orbit γ. The curve $U_{\overline{W}_{+1}}$

[20] By connected component we intend that nodal configurations, such as those appearing in the appendix of [12], are broken up into their irreducible pieces, with any removable boundary singularities filled in. We maintain this convention throughout the remainder of the proof.

must then consist of a single connected component negatively asymptotic to γ, as any additional components would necessarily have trivial negative asymptotics and therefore be exposed by Proposition 11.17. As its index is zero, $U_{\mathbb{R}\times\mathbb{R}^3}$ must be a collection of trivial strips. We conclude that $U_{\overline{W}_{+1}}$ must consist of a punctured disk exactly as described in the statement of the proposition. We know that the negative puncture of $U_{\overline{W}_{+1}}$ must be asymptotic to $(r_{j_1}\cdots r_{j_n})$ by Proposition 11.19.

Apart from the statement regarding algebraic counts, our proof is complete. To prove this last statement, observe that $\partial\overline{\mathcal{M}}_{\overline{W}_{+1}}$ has a count of 0 points when taking into account some choice of orientation as it is the boundary of a 1–manifold. We can also write

$$\#\partial\overline{\mathcal{M}}_{x_0,y_0} = \#((1,\varnothing,\varnothing)\text{ buildings}) + \#((1,0,\varnothing)\text{ buildings}) + \#((0,0,1)\text{ buildings}),$$

where the $\#(\cdots)$ are counted with signs. We know that the set of $(1,\varnothing,\varnothing)$ buildings consists of a single element yielding a count of ±1 and that the set of $(1,0,\varnothing)$ buildings must be empty by our previous arguments providing a count of 0. Hence, the number of $(0,0,1)$ buildings must be ∓1. But this number is equal to $\#(U_{\overline{W}_{+1}})\cdot\#(U_{\mathbb{R}\times\mathbb{R}^3_\Lambda})$, so that both numbers must have absolute value 1. Observing that $\#(U_{\mathbb{R}\times\mathbb{R}^3_\Lambda})$ coincides with a count of points in the moduli space $\mathcal{M}_{\mathbb{R}\times\mathbb{R}^3_\Lambda}$, the proof is complete. □

12.3 Vanishing invariants of overtwisted contact manifolds

Here we use the holomorphic planes of Section 12.2 to prove that the contact homologies of overtwisted contact 3–manifolds are 0. Throughout, we write $(M_{\mathrm{OT}},\xi_{\mathrm{OT}})$ for a closed, overtwisted contact 3–manifold.

Theorem 12.3 [65] $\widehat{\mathrm{CH}}(M_{\mathrm{OT}},\xi_{\mathrm{OT}}) = \mathrm{CH}(M_{\mathrm{OT}},\xi_{\mathrm{OT}}) = 0$.

Proof Applying Eliashberg's theorem [21; 39], which asserts that isotopy classes of overtwisted contact structures on a given contact 3–manifold are classified by the homotopy classes of their underlying oriented 2–plane fields, we know that, for each $n\in\mathbb{Z}$, there exists a unique overtwisted contact structure ξ_n on S^3 whose d_3 invariant is $n-\frac{1}{2}$. For the tight contact structure (S^3,ξ_{std}) on S^3, we have $d_3(\xi_{\mathrm{std}}) = -\frac{1}{2}$.[21] Denoting contact-connected sum by $\#$ and isotopic contact structures by $\simeq$,

$$(M_{\mathrm{OT}},\xi_{\mathrm{OT}}) \simeq (M_{\mathrm{OT}},\xi_{\mathrm{OT}})\#(S^3,\xi_{\mathrm{std}}) \simeq (M_{\mathrm{OT}},\xi_{\mathrm{OT}})\#(S^3,\xi_{-1})\#(S^3,\xi_1).$$

By the connected-sum formula of Theorem 2.6, then, we only need to show that $\widehat{\mathrm{CH}}(S^3,\xi_1)=0$.

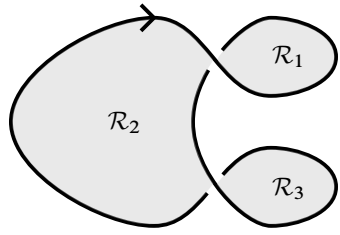

Figure 28: A basis for the $\mathrm{tb} = -2$, $\mathrm{rot} = 1$ unknot.

A contact surgery diagram for (S^3, ξ_1) is provided by a contact $+1$ surgery on a $\mathrm{tb} = -1$, $\mathrm{rot} = 1$ unknot. See [52, Lemma 11.3.10]. A Lagrangian resolution of this knot Λ — shown in Figure 28 — has two chords, say r_1 and r_2. Perturbing Λ as necessary, we may assume that the actions of the chords are distinct and that r_1 has the least action of the two chords with r_1 corresponding to the positive puncture of the disk determined by the region $\mathcal{R}_1$ of Figure 28. Applying the Conley–Zehnder index calculations of Theorem 7.1 to the figure, we see that the Reeb orbit (r_1) has $\mathrm{CZ}_{X,Y} = 2$. Moreover, the orbit is contractible as can be seen by considering a push-out by the orbit string $\eta_{1,1}$.

As the action of (r_1) is the least among all orbits R_ϵ according to our chord-to-orbit correspondence (Theorem 5.1) and the action estimates of Proposition 5.13, $\partial_{\mathrm{CH}}(r_1)$ and $\partial_{\mathrm{SFT}}(r_1)$ are counts of planes bounding (r_1). Using the notation of Section 11.5, write $\mathcal{E}_i$ for the areas of the regions $\mathcal{R}_i \subset \mathbb{R}^2 \setminus \pi_{xy}(N_\epsilon)$ shown in Figure 28. By taking the ϵ parameter in α_ϵ to be sufficiently small, we may assume that $\mathcal{E}_2, \mathcal{E}_3 > \mathcal{A}((r_1))$. Likewise, by Stokes' theorem, $\mathcal{A}((r_1)) - \mathcal{E}_1$ is positive. and may be assumed arbitrarily small by taking ϵ to be arbitrarily small. Then, by the action-energy bound of Proposition 11.8 and the exposure of filling curves (Proposition 11.17), any plane $U : \mathbb{C} \to \mathbb{R} \times \mathbb{R}^3_\Lambda$ bounding (r_1) must satisfy

$$\mathbb{C}_k \cdot U = \begin{cases} 1 & \text{if } k = 1, \\ 0 & \text{if } k \neq 1. \end{cases}$$

We can view $\mathcal{R}_1$ as determining a disk with a positive puncture at the chord r_1, apply Theorem 12.2 to obtain a holomorphic plane bounding (r_1), and conclude that the count of such planes is ± 1. Hence,

$$\partial_{\mathrm{CH}}(r_1) = \pm 1 \in \mathbb{Q},$$

so that the unit in $\widehat{\mathrm{CH}}$ is zero. This implies that $\mathrm{CH}(M_{\mathrm{OT}}, \xi_{\mathrm{OT}})$ must also be zero by Theorem 2.6. □

[21] See [52, Section 11.3] for an overview of d_3 invariants (which we will be following in this proof) as defined by Gompf [31, Section 4].

12.4 Intersection gradings on $\widehat{\mathrm{CH}}$ chain complexes

Here we describe how the intersections of finite-energy curves with the planes $\mathbb{C}_k$ of Section 11.4 can define gradings on the $\mathrm{CC}_{*,0}(\alpha_\epsilon)$ chain complexes of punctured $\mathbb{Q}$–homology spheres which take values in a free $\mathbb{Z}$–module. As described in the introduction, this is simply a variation of the transverse knot filtrations of [14, Section 7.2].

It will be clear from their construction that analogous gradings — which depend on a surgery presentation of our punctures contact manifold — can be constructed for holomorphic curve invariants of $\mathbb{Q}$–homology spheres $(\mathbb{R}^3_{\Lambda^\pm}, \xi_{\Lambda^\pm})$ such as $\widehat{\mathrm{ECH}}$ and the $\widehat{SFT}$. It will also be clear that the assumption that $H_2(M) = 0$ may be dropped by considering $\mathbb{Q}[H_2(M)]$ coefficient systems as described in [6]. Likewise, such gradings can be extended to all of $\mathrm{CC}_{*,*}$ using $\mathbb{Q}[H_2(M)]$ coefficients and spanning surfaces bounding unions of closed orbits and fixed representatives of homology classes as in [6]. In Section 12.6 we will use this grading to prove Theorem 1.2, in which case we will only need the $\mathrm{CC}_{*,0}$ version of this construction for $\mathbb{Q}$–homology spheres.

Let $(\mathbb{R}^3_{\Lambda^\pm}, \xi_{\Lambda^\pm})$ be a contact manifold determined by a contact surgery diagram $\Lambda^\pm$ with $\mathbb{R}^3_{\Lambda^\pm}$ a $\mathbb{Q}$–homology sphere. Let (x_k, y_k) for $k = 1, \dots, K$ be a point basis for the surgery diagram determining a finite collection of infinite-energy holomorphic planes $\mathbb{C}_k$ as described in Section 11.5.

Suppose $\gamma = \{\gamma_k\}$ is a collection of Reeb orbits for which $[\gamma] = 0 \in H_1(\mathbb{R}^3_{\Lambda^\pm})$ and let S_γ be a surface in $\mathbb{R}^3_{\Lambda^\pm}$ with $\partial S_\gamma = \gamma$. To the surface S_γ and each point (x_k, y_k), we define

$$I_k(\gamma) = \big(\{(x_k, y_k)\} \times \mathbb{R}\big) \cdot S_\gamma \in \mathbb{Z}.$$

By Theorem 11.6 and the fact that $H_2(\mathbb{R}^3_{\Lambda^\pm}) = 0$, the numbers $I_k(\gamma)$ are independent of choice of spanning surface S_γ for γ. We collect all of these numbers as monomials

$$\mathcal{I}_\Lambda(\gamma) = \sum_1^K I_k(\gamma)\iota_k \in \mathbb{Z}^K$$

for formal variables ι_k for $k = 1, \dots, K$. It follows from this definition that, provided two homologically trivial collections γ_1, γ_2 of closed Reeb orbits, we have

$$\mathcal{I}_\Lambda(\gamma_1 \cup \gamma_2) = \mathcal{I}_\Lambda(\gamma_1) + \mathcal{I}_\Lambda(\gamma_2).$$

We set $\mathcal{I}_\Lambda(\varnothing) = 0 \in \mathbb{Z}^K$. Then $\mathcal{I}_\Lambda$ determines a $\mathbb{Z}^K$–valued grading on the $H_1 = 0$ subalgebra $\mathrm{CC}_{*,0}$ of the chain algebra CC for the contact homology associated to the contact form α_ϵ of $\mathbb{R}^3_{\Lambda^\pm}$.

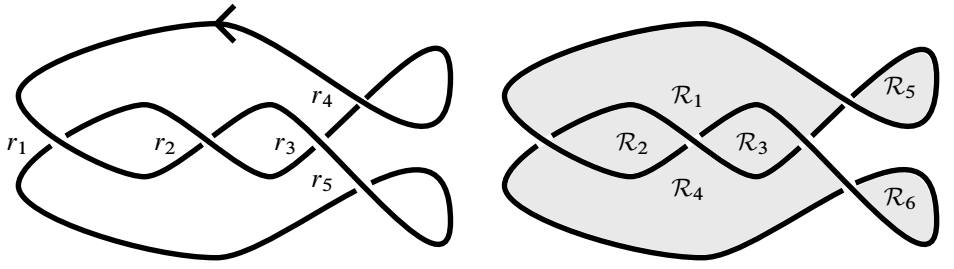

Figure 29: A Legendrian trefoil with $\mathrm{tb} = -1$ and $\mathrm{rot} = 0$ in the Lagrangian projection together with a basis for $\mathbb{R}^2 \setminus N$.

Now suppose that γ^+ and γ^- are two homologically trivial collections of closed orbits and that U is a map from a surface with boundary into $\mathbb{R}^3_{\Lambda^\pm}$ for which $\partial U = \gamma^+ - \gamma^-$. Then, relative to its boundary, we have

$$\big(\{(x_k, y_k)\} \times \mathbb{R}\big) \cdot U = I_k(\gamma^+) - I_k(\gamma^-) \in \mathbb{Z}.$$

In particular, if $(t, U) \colon \Sigma' \to \mathbb{R} \times \mathbb{R}^3_{\Lambda^\pm}$ is a holomorphic curve positively asymptotic to the γ^+ and negatively asymptotic to the γ^-, then

$$\mathcal{I}_\Lambda(\gamma^+) - \mathcal{I}_\Lambda(\gamma^-) = \sum \big(\big(\{(x_k, y_k)\} \times \mathbb{R}\big) \cdot U\big)\iota_k = \sum (\mathbb{C}_k \cdot (t, U))\iota_k \in \mathbb{Z}^K_{\geq 0}. \tag{65}$$

In summary, the $\mathcal{I}_\Lambda$ allows us to make a priori computations of intersection numbers between holomorphic curves asymptotic to orbits with leaves of the foliation as described in Section 11. In particular, if

$$\mathcal{I}_\Lambda(\gamma^+) - \mathcal{I}_\Lambda(\gamma^-) \notin \mathbb{Z}^K_{\geq 0}, \tag{66}$$

then the coefficient of γ^- in $\partial_{\mathrm{CH}}(\gamma^+)$ must be zero.[22]

12.5 Surgery on a trefoil

Take Λ to be the trefoil depicted in Figure 29 with chords $r_1, \ldots, r_5$. This is a reproduction of Figure 6 with a point basis shown in the right-hand side of the figure. This trefoil is the unique nondestabilizable $m(3_1)$ by [25].

[22] Here it is implicit that, if the collection γ^+ contains more than a single orbit, then a holomorphic map (t, U) as above contributing to ∂_{CH} will consist of a connected index 1 holomorphic curve positively asymptotic to some orbit in γ^+ together with a union of trivial cylinders over the remaining orbits in the collection. This deviation from convention allows us to associate cobordisms to differentials of monomials consisting of γ^+ containing more than one orbit.

12.5.1 Ambient geometry According to Theorem 9.1, the first homology of $\mathbb{R}^3_{\Lambda^\pm}$ is generated by the meridian μ with

$$H_1(\mathbb{R}^3_{\Lambda^\pm}) = \begin{cases} \mathbb{Z}/2\mathbb{Z}\mu & \text{if } c = 1, \\ \mathbb{Z}\mu & \text{if } c = -1. \end{cases}$$

Since Λ is smoothly fibered, with fiber a punctured torus, the closed manifold obtained by contact -1 surgery — a topological 0 surgery with respect to the Seifert framing — is a torus bundle over S^1. This manifold is Liouville fillable, and hence tight, and so is a torus bundle covered by the classification in [36, Section 2].

Performing $+1$ contact surgery produces a tight but nonfillable contact manifold studied in [43] — see also [52, Theorem 1.3.4] — which is a Brieskorn sphere with reversed orientation, $-\Sigma(2,3,4)$. Nonfillability may also be viewed as a consequence of the fact that the trefoil is not slice by [15], as mentioned in Theorem 2.8.

12.5.2 Rotation numbers and crossing monomials Here we compute rotation numbers and crossing monomials for the trefoil, which will allow us to compute Conley–Zehnder indices and homology classes of the orbits in the surgered manifolds by applying Theorems 7.1 and 9.1, respectively.

To compute the rotation numbers, we first find the rotation angles θ_{j_1,j_2}, which we see are all either $\frac{1}{2}\pi$, $\frac{3}{2}\pi$ or $\frac{5}{2}\pi$, producing the following table:

chord	$\mathrm{rot}_{j,1}$	$\mathrm{rot}_{j,2}$	$\mathrm{rot}_{j,3}$	$\mathrm{rot}_{j,4}$	$\mathrm{rot}_{j,5}$
r_1	0	0	0	0	1
r_2	0	0	0	0	1
r_3	0	0	0	0	1
r_4	1	1	1	1	2
r_5	0	0	0	0	1

For the computation of the crossing monomials, there is only a single μ_i, so that Remark 3.2 is applicable. The μ coefficients of the relevant crossing monomials are:

chord	sgn	$\mathrm{cr}_j : c = 1$	$\mathrm{cr}_j : c = -1$	$\mathrm{cr}_{j,1}$	$\mathrm{cr}_{j,2}$	$\mathrm{cr}_{j,3}$	$\mathrm{cr}_{j,4}$	$\mathrm{cr}_{j,5}$
r_1	1	2	0	0	0	2	3	1
r_2	1	2	0	0	0	0	1	1
r_3	1	2	0	-2	0	0	1	-1
r_4	-1	0	-2	1	1	3	4	2
r_5	-1	0	-2	-1	1	1	2	0

$\mathrm{cw}(\gamma)$	$\mu : c = 1$	$\mathrm{CZ}_{X,Y} : c = 1$	$\mu : c = -1$	$\mathrm{CZ}_{X,Y} : c = -1$
r_1	1	1	0	0
r_2	1	1	0	0
r_3	1	1	0	0
r_4	0	2	1	1
r_5	0	2	-1	1
r_1r_2	0	2	0	0
r_1r_3	0	2	0	0
r_1r_4	1	3	1	1
r_1r_5	1	3	-1	1
r_2r_3	0	2	0	0
r_2r_4	0	3	0	1
r_2r_5	0	3	0	1
r_3r_4	1	3	1	1
r_3r_5	1	3	-1	1
r_4r_5	0	4	0	2

Table 1

12.5.3 Homology classes and indices of orbits after surgery Using the above computations, we can produce in Table 1 the homology classes and Conley–Zehnder indices of Reeb orbits with word length ≤ 2 using Theorems 9.3 and 7.1. Multiply covered orbits have been omitted. Coefficients for μ in the case $c = 1$ are taken modulo 2.

12.6 Proof of Theorem 1.2

In this section, we prove Theorem 1.2 by computing $\partial_{\mathrm{CH}}(r_4)$.

12.6.1 The subalgebra $C_{0,0}$ and intersection gradings As the rotation numbers of capping paths on Λ are bounded below by 0, Theorem 7.1 tells us that the Conley–Zehnder indices of all orbits of are bounded below by their word lengths. We conclude

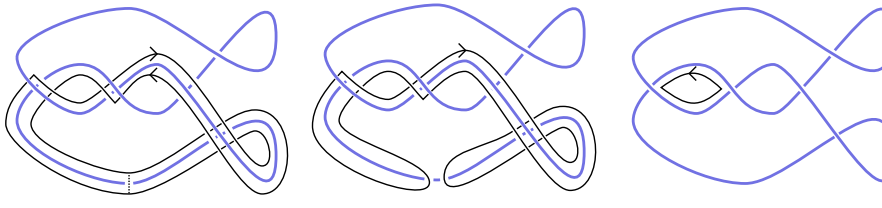

Figure 30: An annulus bounding $(r_1) \cup (r_2)$.

that $\partial_{\mathrm{CH}}(r_4)$ must be an element of $\mathrm{CC}_{0,0}$ which is a commutative algebra on generators

$$1, \quad (r_1)^2, \quad (r_2)^2, \quad (r_3)^2, (r_1)(r_2), \quad (r_1)(r_3), \quad (r_2)(r_3).$$

We'll compute the $\mathcal{I}_\Lambda$ gradings on $\mathrm{CC}_{0,0}$ using points (x_k, y_k) appearing in the centers of the regions $\mathcal{R}_k$ of Figure 29:

$\mathrm{CC}_{*,0}$ monomial	I_1	I_2	I_3	I_4	I_5	I_6
(r_4)	0	0	0	0	1	0
$(r_1)^2$	−1	−1	−2	−1	1	1
$(r_2)^2$	1	2	2	1	−1	−1
$(r_3)^2$	−1	−2	−1	−1	1	1
$(r_1)(r_2)$	0	1	0	0	0	0
$(r_1)(r_3)$	−1	−1	−1	−1	1	1
$(r_2)(r_3)$	0	0	1	0	0	0

To establish the calculations appearing in the above table, we construct surfaces bounding $(r_1)(r_2)$, $(r_2)(r_3)$ and $(r_2)(r_2)$, filling in the remainder of the table using arithmetic. Such surfaces will be constructed out of simple cobordisms built out of homotopies and skein operations. For (r_4), we have an obvious disk bounding a push-out along $\overline{\eta}_4$, obtained by perturbing $\mathcal{R}_5$.

In Figure 30, we construct a spanning surface for the union of the orbits $(r_1) \cup (r_2)$. We begin by homotoping the union of orbits into the complement of N_ϵ, as described in Section 9.4. The result — associated to capping paths η_1 and $\overline{\eta}_2$ — is shown on the left-most subfigure. To get from the left column of the figure to the center, we apply a skein cobordism along the dashed arc, resulting in a pair-of-pants cobordism. The resulting knot can be homotoped to the Reeb orbit $(r_1 r_2)$ as shown in the right-hand side of the figure. So far our surface has avoided passing through any of the lines $\{(x, y) = (x_k, y_k)\} \subset \mathbb{R}^3_{\Lambda^\pm}$. To complete our cobordism, we fill in the knot shown in the right-most subfigure using the obvious disk which is a perturbation of the disk $\mathcal{R}_2$. The union of our pair of pants with this disk provides us with an annular filling of $(r_1) \cup (r_2)$ which intersects the link $\{(x, y) = (x_2, y_2)\}$ exactly once with positive sign. We conclude that

$$\mathcal{I}_\Lambda((r_1)(r_2)) = \iota_2.$$

A similar construction can be carried out to find an annular filling of $(r_2) \cup (r_3)$: we start with a push-out corresponding to capping paths $\overline{\eta}_2$ and η_3, apply a skein cobordism giving us a pair of pants with boundary $(r_2) \cup (r_3) - (r_2 r_3)$, and then fill in $(r_2 r_3)$ with

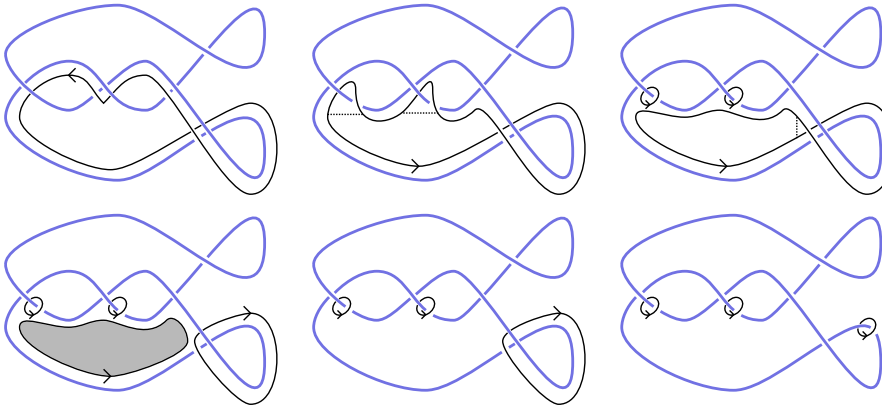

Figure 31: A cobordism with boundary $(r_2)+\mu$.

a perturbation of the disk $\mathbb{D}_3$. We conclude that

$$\mathcal{I}_\Lambda((r_2)(r_3)) = \iota_3.$$

Now we construct a spanning surface for $(r_2)\cup(r_2)$. The construction is more complicated in this case: we construct two cobordisms from (r_2) from a positive and negative meridian of Λ, which can then be patched together to give us a surface with boundary $(r_2)\cup(r_2)$.

We break down the construction of one such cobordism whose boundary is $(r_2)+\mu$ into a sequence of elementary cobordisms, as shown in Figure 31:

(1) We start with a push-out of (r_2) using the capping path $\overline{\eta}_2$, as shown in the top-left subfigure.

(2) Going from the top-left to top-center, we homotop our knot across the disks $\mathcal{R}_2$ and $\mathcal{R}_3$. Along the way, we pick up two intersections with the lines associated to the points (x_2, y_2) and (x_3, y_3) with positive signs.

(3) Going from the top-center to the top-right, we apply skein cobordisms along the dashed arcs appearing in the top-center.

(4) Going from the top-right to the bottom-left, we apply another skein cobordism along the dashed arc appearing in the top-right yielding a 4–component link.

Figure 32: A tube bounding $\mu-\mu$.

(5) Going from the bottom-left to the bottom-center, we fill in one of the components of our link with a disk which is a perturbation of the disk $\mathcal{R}_4$. In doing so, we pick up a positive intersection with the line over the point (x_4, y_4).

(6) Going from the bottom-center to the bottom-right, we homotop one component of our knot over $-\mathcal{R}_6$ to a $-\mu$

Combining all of the above steps, we've constructed a homotopy from (r_2) to a collection of meridians. We can cancel a pair of them with a tube as shown in Figure 32. The end result is a cobordism with boundary $(r_2)+\mu$ passing through the lines associated to the points (x_2, y_2), (x_3, y_3) and (x_4, y_4) once each with positive intersection number and passing through the line over (x_6, y_6) with negative intersection number.

We can also construct a cobordism with boundary $(r_2)-\mu$ by flipping Figure 31 about a horizontal line, starting with a push-out of η_2. The resulting cobordism passes through the lines associated to the points (x_1, y_1), (x_2, y_2) and (x_3, y_3) once each with positive intersection number and passing through the line over (x_5, y_5) with negative intersection number.

We can connect the two cobordisms with another tube bounding $\mu-\mu$ to obtain a spanning surface for $(r_2)\cup(r_2)$. By the above counts of intersections, we have

$$\mathcal{I}_\Lambda((r_2)^2) = \iota_1 + 2\iota_2 + 2\iota_3 + \iota_4 - \iota_5 - \iota_6.$$

Using our calculations of $\mathcal{I}_\Lambda((r_1)(r_2))$, $\mathcal{I}_\Lambda((r_2)(r_3))$ and $\mathcal{I}_\Lambda((r_2)^2)$, we can fill out the remainder of the above table by computing

$$\begin{aligned}
\mathcal{I}_\Lambda((r_1)^2) &= 2\mathcal{I}_\Lambda((r_1)(r_2)) - \mathcal{I}_\Lambda((r_2)^2),\\
\mathcal{I}_\Lambda((r_3)^2) &= 2\mathcal{I}_\Lambda((r_2)(r_3)) - \mathcal{I}_\Lambda((r_2)^2),\\
\mathcal{I}_\Lambda((r_1)(r_3)) &= \mathcal{I}_\Lambda((r_1)(r_2)) + \mathcal{I}_\Lambda((r_2)(r_3)) - \mathcal{I}_\Lambda((r_2)^2).
\end{aligned}$$

12.6.2 Intersection numbers of curves positively asymptotic to (r_4) Now suppose that we have a holomorphic curve U positively asymptotic to (r_4) and negatively asymptotic to a collection of generators γ^- from $C_{0,0}$. Writing γ^- as a monomial in $C_{0,0}$, there are nonnegative constants $C_{i,j}$ for which

$$\gamma^- = (r_1)^{2C_{1,1}}(r_2)^{2C_{2,2}}(r_3)^{2C_{3,3}}((r_1)(r_2))^{C_{1,2}}((r_1)(r_3))^{C_{1,3}}((r_2)(r_3))^{C_{2,3}}.$$

We'll use the intersection grading to show that all of the $C_{i,j}$ must be zero, so that U cannot have any negative asymptotics. We can count the intersection of U with the planes $\mathbb{C}_k$ as the coefficients of the ι_k in the expression $\mathcal{I}_\Lambda((r_4)) - \mathcal{I}_\Lambda(\gamma^-)$ as

described in (65). Using the table above, we compute

$$\begin{aligned}\mathcal{I}_\Lambda((r_4))-\mathcal{I}_\Lambda(\gamma^-) = {}& (C_{1,1}-C_{2,2}+C_{3,3}+C_{1,3})\iota_1\\ &+(C_{1,1}-2C_{2,2}+2C_{3,3}-C_{1,2}+C_{1,3})\iota_2\\ &+(2C_{1,1}-2C_{2,2}+C_{3,3}+C_{1,3}-C_{2,3})\iota_3\\ &+(C_{1,1}-C_{2,2}+C_{3,3}+C_{1,3})\iota_4\\ &+(1-C_{1,1}+C_{2,2}-C_{3,3}-C_{1,3})\iota_5\\ &+(-C_{1,1}+C_{2,2}-C_{3,3}-C_{1,3})\iota_6.\end{aligned}$$

All of the ι_k coefficients above must be nonnegative by intersection positivity.

As the ι_4 and ι_6 coefficients are the same with opposite sign, both must be zero so that

$$C_{2,2}=C_{1,1}+C_{3,3}+C_{1,3}.$$

Therefore, we must have

$$\mathcal{I}_\Lambda((r_4))-\mathcal{I}_\Lambda(\gamma^-)=(-C_{1,1}-C_{1,2}-C_{1,3})\iota_2+(-C_{3,3}-C_{1,3}-C_{2,3})\iota_3+\iota_5,$$

implying that the remaining $C_{i,j}$ are all zero.

12.6.3 Completion of the proof The above analysis implies that, if U is an index 1 holomorphic curve contributing to $\partial_{\mathrm{CH}}(r_4)$, then it cannot have any negative asymptotics and must satisfy

$$\mathbb{C}_k\cdot U=\begin{cases}1 & \text{if } k=5,\\ 0 & \text{if } k\neq 5.\end{cases} \tag{67}$$

Such a curve must be parametrized by $\mathbb{C}$ as per the definition of ∂_{CH}. To complete our proof, we analyze the moduli space of finite-energy curves

$$\mathcal{M}_{4,5}=\{\mathbb{C}\xrightarrow{U}\mathbb{R}\times\mathbb{R}^3_{\Lambda^\pm}: U \text{ asymptotic to } (r_4), \text{ satisfying (67)}\}/\text{reparametrization}.$$

By the above analysis, $\partial_{\mathrm{CH}}((r_4))=\#(\mathcal{M}_{4,5})1$, counting points algebraically. This moduli space exactly describes the lowest levels $U^c_\varnothing$ of the height 3 SFT buildings studied in Theorem 12.2, which when applied to the disk $\mathcal{R}_5$ tell us that $\#(\mathcal{M}_{4,5})=\pm 1$.

The proof of Theorem 1.2 is then complete in the case of the tb $=1$ trefoil shown in Figure 29. By the classification torus knots in $(\mathbb{R}^3,\xi_{\mathrm{std}})$ [25], all other right-handed trefoils are stabilizations of this one — contact $+1$ surgeries on these stabilized knots will be overtwisted and so will have $\mathrm{CH}=0$. The proof is now complete in the case that Λ^+ consists of a single component. In the case that $\Lambda^+=\bigcup_i^n\Lambda_i^+$ has multiple components, we have — as described in Section 10 — a Liouville cobordism (W,λ) whose convex end $(M^+,\xi^+)=(\partial^+W,\ker(\lambda)|_{\partial^+W})$ is given by contact $+1$ surgery

on Λ_1^+ and whose concave end $(M^-, \xi^+) = (\partial^- W, \ker(\lambda)|_{\partial^- W})$ is given by contact surgery on Λ^+. If we index the components of Λ^+ so that Λ_1^+ is a right-handed trefoil, then $\mathrm{CH}(M^+, \xi^+) = 0$, and so, by Liouville functoriality, $\mathrm{CH}(M^-, \xi^-) = 0$ as well. The proof is now complete for all right-handed trefoils and all contact surgery coefficients $1/k$ with $k > 0$.

References

[1] **L V Ahlfors**, *Complex analysis: an introduction to the theory of analytic functions of one complex variable*, 3rd edition, McGraw-Hill, New York (1978) MR Zbl

[2] **R Avdek**, *Contact surgery and supporting open books*, Algebr. Geom. Topol. 13 (2013) 1613–1660 MR Zbl

[3] **E Bao**, **K Honda**, *Definition of cylindrical contact homology in dimension three*, J. Topol. 11 (2018) 1002–1053 MR Zbl

[4] **E Bao**, **K Honda**, *Semi-global Kuranishi charts and the definition of contact homology*, Adv. Math. 414 (2023) art. id. 108864 MR Zbl

[5] **F Bourgeois**, *A Morse–Bott approach to contact homology*, PhD thesis, Stanford University (2002) MR https://www.proquest.com/docview/305591502

[6] **F Bourgeois**, *Introduction to contact homology*, lecture notes (2003) https://www.imo.universite-paris-saclay.fr/~bourgeois/papers/Berder.pdf

[7] **F Bourgeois**, **T Ekholm**, **Y Eliashberg**, *Effect of Legendrian surgery*, Geom. Topol. 16 (2012) 301–389 MR Zbl

[8] **F Bourgeois**, **Y Eliashberg**, **H Hofer**, **K Wysocki**, **E Zehnder**, *Compactness results in symplectic field theory*, Geom. Topol. 7 (2003) 799–888 MR Zbl

[9] **F Bourgeois**, **K Niederkrüger**, *Towards a good definition of algebraically overtwisted*, Expo. Math. 28 (2010) 85–100 MR Zbl

[10] **Y Chekanov**, *Differential algebra of Legendrian links*, Invent. Math. 150 (2002) 441–483 MR Zbl

[11] **K Cieliebak**, **Y Eliashberg**, *From Stein to Weinstein and back: symplectic geometry of affine complex manifolds*, American Mathematical Society Colloquium Publications 59, Amer. Math. Soc., Providence, RI (2012) MR Zbl

[12] **K Cieliebak**, **J Latschev**, *The role of string topology in symplectic field theory*, from "New perspectives and challenges in symplectic field theory" (M Abreu, F Lalonde, L Polterovich, editors), CRM Proc. Lecture Notes 49, Amer. Math. Soc., Providence, RI (2009) 113–146 MR Zbl

[13] **V Colin**, **P Ghiggini**, **K Honda**, *Equivalence of Heegaard Floer homology and embedded contact homology via open book decompositions*, Proc. Natl. Acad. Sci. USA 108 (2011) 8100–8105 MR Zbl

[14] **V Colin**, **P Ghiggini**, **K Honda**, **M Hutchings**, *Sutures and contact homology I*, Geom. Topol. 15 (2011) 1749–1842 MR Zbl

[15] **J Conway**, **J B Etnyre**, **B Tosun**, *Symplectic fillings, contact surgeries, and Lagrangian disks*, Int. Math. Res. Not. 2021 (2021) 6020–6050 MR Zbl

[16] **F Ding**, **H Geiges**, *A Legendrian surgery presentation of contact 3–manifolds*, Math. Proc. Cambridge Philos. Soc. 136 (2004) 583–598 MR Zbl

[17] **T Ekholm**, *Rational symplectic field theory over $\mathbb{Z}_2$ for exact Lagrangian cobordisms*, J. Eur. Math. Soc. 10 (2008) 641–704 MR Zbl

[18] **T Ekholm**, *Holomorphic curves for Legendrian surgery*, preprint (2019) arXiv

[19] **T Ekholm**, **J Etnyre**, **M Sullivan**, *The contact homology of Legendrian submanifolds in $\mathbb{R}^{2n+1}$*, J. Differential Geom. 71 (2005) 177–305 MR Zbl

[20] **T Ekholm**, **L Ng**, *Legendrian contact homology in the boundary of a subcritical Weinstein 4–manifold*, J. Differential Geom. 101 (2015) 67–157 MR Zbl

[21] **Y Eliashberg**, *Classification of overtwisted contact structures on 3–manifolds*, Invent. Math. 98 (1989) 623–637 MR Zbl

[22] **Y Eliashberg**, *On symplectic manifolds with some contact properties*, J. Differential Geom. 33 (1991) 233–238 MR Zbl

[23] **Y Eliashberg**, **A Givental**, **H Hofer**, *Introduction to symplectic field theory*, from "Visions in mathematics" (N Alon, J Bourgain, A Connes, M Gromov, V Milman, editors), volume 2, Birkhäuser (= GAFA special volume), Boston, MA (2000) 560–673 MR Zbl

[24] **J B Etnyre**, *Legendrian and transversal knots*, from "Handbook of knot theory" (W Menasco, M Thistlethwaite, editors), Elsevier, Amsterdam (2005) 105–185 MR Zbl

[25] **J B Etnyre**, **K Honda**, *Knots and contact geometry, I: Torus knots and the figure eight knot*, J. Symplectic Geom. 1 (2001) 63–120 MR Zbl

[26] **J B Etnyre**, **L L Ng**, *Legendrian contact homology in $\mathbb{R}^3$*, from "Surveys in differential geometry 2020: surveys in 3–manifold topology and geometry" (I Agol, D Gabai, editors), Surv. Differ. Geom. 25, International, Boston, MA (2022) 103–161 MR Zbl

[27] **J B Etnyre**, **B Ozbagci**, *Invariants of contact structures from open books*, Trans. Amer. Math. Soc. 360 (2008) 3133–3151 MR Zbl

[28] **O Fabert**, *Obstruction bundles over moduli spaces with boundary and the action filtration in symplectic field theory*, Math. Z. 269 (2011) 325–372 MR Zbl

[29] **P Foulon**, **B Hasselblatt**, *Contact Anosov flows on hyperbolic 3–manifolds*, Geom. Topol. 17 (2013) 1225–1252 MR Zbl

[30] **H Geiges**, **K Zehmisch**, *How to recognize a 4–ball when you see one*, Münster J. Math. 6 (2013) 525–554 MR Zbl

[31] **R E Gompf**, *Handlebody construction of Stein surfaces*, Ann. of Math. 148 (1998) 619–693 MR Zbl

[32] **M Gromov**, *Pseudo holomorphic curves in symplectic manifolds*, Invent. Math. 82 (1985) 307–347 MR Zbl

[33] **A Hatcher**, *Algebraic topology*, Cambridge Univ. Press (2002) MR Zbl

[34] **R Hind**, *Stein fillings of lens spaces*, Commun. Contemp. Math. 5 (2003) 967–982 MR Zbl

[35] **H Hofer**, *Pseudoholomorphic curves in symplectizations with applications to the Weinstein conjecture in dimension three*, Invent. Math. 114 (1993) 515–563 MR Zbl

[36] **K Honda**, *On the classification of tight contact structures, II*, J. Differential Geom. 55 (2000) 83–143 MR Zbl

[37] **K Honda**, *Gluing tight contact structures*, Duke Math. J. 115 (2002) 435–478 MR Zbl

[38] **K Honda**, **W H Kazez**, **G Matić**, *On the contact class in Heegaard Floer homology*, J. Differential Geom. 83 (2009) 289–311 MR Zbl

[39] **Y Huang**, *A proof of the classification theorem of overtwisted contact structures via convex surface theory*, J. Symplectic Geom. 11 (2013) 563–601 MR Zbl

[40] **M Hutchings**, *Lecture notes on embedded contact homology*, from "Contact and symplectic topology" (F Bourgeois, V Colin, A Stipsicz, editors), Bolyai Soc. Math. Stud. 26, János Bolyai Math. Soc., Budapest (2014) 389–484 MR Zbl

[41] **M Hutchings**, **C H Taubes**, *Gluing pseudoholomorphic curves along branched covered cylinders, I*, J. Symplectic Geom. 5 (2007) 43–137 MR Zbl

[42] **Ç Kutluhan**, **Y-J Lee**, **C H Taubes**, HF = HM*, I: Heegaard Floer homology and Seiberg–Witten Floer homology*, Geom. Topol. 24 (2020) 2829–2854 MR Zbl

[43] **P Lisca**, **A I Stipsicz**, *Ozsváth–Szabó invariants and tight contact three-manifolds, I*, Geom. Topol. 8 (2004) 925–945 MR Zbl

[44] **D McDuff**, *The structure of rational and ruled symplectic 4–manifolds*, J. Amer. Math. Soc. 3 (1990) 679–712 MR Zbl

[45] **D McDuff**, *Symplectic manifolds with contact type boundaries*, Invent. Math. 103 (1991) 651–671 MR Zbl

[46] **D McDuff**, **D Salamon**, *Introduction to symplectic topology*, 2nd edition, Oxford Univ. Press (1998) MR Zbl

[47] **D McDuff**, **D Salamon**, *J–holomorphic curves and symplectic topology*, American Mathematical Society Colloquium Publications 52, Amer. Math. Soc., Providence, RI (2004) MR Zbl

[48] **A Moreno**, **Z Zhou**, *A landscape of contact manifolds via rational SFT*, preprint (2020) arXiv

[49] **L L Ng**, *Computable Legendrian invariants*, Topology 42 (2003) 55–82 MR Zbl

[50] **L Ng**, *Rational symplectic field theory for Legendrian knots*, Invent. Math. 182 (2010) 451–512 MR Zbl

[51] **B Ozbagci**, *A note on contact surgery diagrams*, Internat. J. Math. 16 (2005) 87–99 MR Zbl

[52] **B Ozbagci**, **A I Stipsicz**, *Surgery on contact 3–manifolds and Stein surfaces*, Bolyai Society Mathematical Studies 13, Springer (2004) MR Zbl

[53] **P Ozsváth**, **Z Szabó**, *Heegaard Floer homology and contact structures*, Duke Math. J. 129 (2005) 39–61 MR Zbl

[54] **J Pardon**, *Contact homology and virtual fundamental cycles*, J. Amer. Math. Soc. 32 (2019) 825–919 MR Zbl

[55] **J Robbin**, **D Salamon**, *The Maslov index for paths*, Topology 32 (1993) 827–844 MR Zbl

[56] **J Rooney**, *Cobordism maps in embedded contact homology*, preprint (2019) arXiv

[57] **L Rudolph**, *The slice genus and the Thurston–Bennequin invariant of a knot*, Proc. Amer. Math. Soc. 125 (1997) 3049–3050 MR Zbl

[58] **M Schwarz**, *Cohomology operations from S^1 cobordisms in Floer homology*, PhD thesis, ETH Zurich (1995) https://doi.org/10.3929/ethz-a-001475365

[59] **P Seidel**, *A biased view of symplectic cohomology*, from "Current developments in mathematics, 2006" (B Mazur, T Mrowka, W Schmid, R Stanley, S-T Yau, editors), International, Somerville, MA (2008) 211–253 MR Zbl

[60] **A Weinstein**, *Contact surgery and symplectic handlebodies*, Hokkaido Math. J. 20 (1991) 241–251 MR Zbl

[61] **C Wendl**, *Strongly fillable contact manifolds and J–holomorphic foliations*, Duke Math. J. 151 (2010) 337–384 MR Zbl

[62] **C Wendl**, *Non-exact symplectic cobordisms between contact 3–manifolds*, J. Differential Geom. 95 (2013) 121–182 MR Zbl

[63] **C Wendl**, *Signs (or how to annoy a symplectic topologist)*, blog post (2015) https://tinyurl.com/Wendl-annoy

[64] **C Wendl**, *Lectures on symplectic field theory*, preprint (2016) arXiv

[65] **M-L Yau**, *Vanishing of the contact homology of overtwisted contact 3–manifolds*, Bull. Inst. Math. Acad. Sin. 1 (2006) 211–229 MR Zbl With an appendix by Yakov Eliashberg

Department of Mathematics, Uppsala University
Uppsala, Sweden

russell.avdek@math.uu.se

https://russellavdek.com

Proposed: András I Stipsicz
Seconded: Leonid Polterovich, Yakov Eliashberg

Received: 8 July 2020
Revised: 11 October 2021

GEOMETRY & TOPOLOGY

msp.org/gt

See inside back cover or msp.org/gt for submission instructions.

The subscription price for 2023 is US $740/year for the electronic version, and $1030/year (+$70, if shipping outside the US) for print and electronic. Subscriptions, requests for back issues and changes of subscriber address should be sent to MSP. Geometry & Topology is indexed by Mathematical Reviews, Zentralblatt MATH, Current Mathematical Publications and the Science Citation Index.

Geometry & Topology (ISSN 1465-3060 printed, 1364-0380 electronic) is published 9 times per year and continuously online, by Mathematical Sciences Publishers, c/o Department of Mathematics, University of California, 798 Evans Hall #3840, Berkeley, CA 94720-3840. Periodical rate postage paid at Oakland, CA 94615-9651, and additional mailing offices. POSTMASTER: send address changes to Mathematical Sciences Publishers, c/o Department of Mathematics, University of California, 798 Evans Hall #3840, Berkeley, CA 94720-3840.

GT peer review and production are managed by EditFLOW® from MSP.

PUBLISHED BY

mathematical sciences publishers

nonprofit scientific publishing

http://msp.org/

GEOMETRY & TOPOLOGY
Volume 27 Issue 3 (pages 823–1272) 2023